

December 2016

Pendulum Based Impact Testing of Athletic Helmets Using the NOCSAE Headform

Bradley Thorne

University of Nevada, Las Vegas, thorneb2@unlv.nevada.edu

Follow this and additional works at: <https://digitalscholarship.unlv.edu/thesesdissertations>

 Part of the [Mechanical Engineering Commons](#)

Repository Citation

Thorne, Bradley, "Pendulum Based Impact Testing of Athletic Helmets Using the NOCSAE Headform" (2016). *UNLV Theses, Dissertations, Professional Papers, and Capstones*. 2907.

<https://digitalscholarship.unlv.edu/thesesdissertations/2907>

This Thesis is brought to you for free and open access by Digital Scholarship@UNLV. It has been accepted for inclusion in UNLV Theses, Dissertations, Professional Papers, and Capstones by an authorized administrator of Digital Scholarship@UNLV. For more information, please contact digitalscholarship@unlv.edu.

PENDULUM BASED IMPACT TESTING OF ATHLETIC
HELMETS USING THE NOCSAE HEADFORM

By

Bradley Thorne

Bachelors of Science in Mechanical Engineering

University of Nevada, Las Vegas

2013

A thesis submitted in partial fulfillment

of the requirements for the

Master of Science in Engineering – Mechanical Engineering

Department of Mechanical Engineering

Howard R. Hughes College of Engineering

The Graduate College

University of Nevada, Las Vegas

December 2016



Thesis Approval

The Graduate College
The University of Nevada, Las Vegas

September 14, 2016

This thesis prepared by

Bradley Thorne

entitled

Pendulum Based Impact Testing of Athletic Helmets Using the NOCSAE Headform

is approved in partial fulfillment of the requirements for the degree of

Master of Science in Engineering – Mechanical Engineering
Department of Mechanical Engineering

Douglas Reynolds, Ph.D.
Examination Committee Chair

Kathryn Hausbeck Korgan, Ph.D.
Graduate College Interim Dean

Brendan O'Toole, Ph.D.
Examination Committee Member

William Culbreth, Ph.D.
Examination Committee Member

Samaan Ladkany, Ph.D.
Graduate College Faculty Representative

ABSTRACT

Concussions in organized sports can have detrimental short-term and long-term effects on player's health. The focus of this research is the development of a new state of the art test and certification standard for protective headgear. Baseball helmets and soccer soft headgear were used in these tests, but the ultimate goal is to create a universal set of test guidelines for all types of protective headgear. Modifications to current test standards outlined by the National Operating Committee on Standards for Athletic Equipment (NOCSAE) employed the use of a pendulum impactor, which facilitated additional measurements during head impact tests using a NOCSAE headform. This additional data will allow researchers to more accurately characterize the effects of head impacts from sports related objects. This will not only serve to better characterize the effectiveness of currently available protective headgear but will also serve as a means to justify and standardize test protocols for evaluating the effectiveness of protective headgear used in sports where none is currently mandated.

TABLE OF CONTENTS

ABSTRACT iii

TABLE OF CONTENTS iv

LIST OF TABLES vii

LIST OF FIGURES ix

CHAPTER 1 – INTRODUCTION 1

 1.1. Head Impact Health Risk Metrics 1

 1.2. Motivation for Modifying the Current Test Standards 2

CHAPTER 2 – SPORTS TESTING STANDARDS AND LITERATURE REVIEW 6

 2.1. NOCSAE Standards 6

 2.2. SI 9

 2.3. TBI’s in Soccer 10

CHAPTER 3 – PENDULUM BASED IMPACT TESTING DEVELOPED BY DARREN BENN
..... 14

 3.1. Hardware Used in the Development of Benn’s Apparatus 14

 3.2. The Pendulum 20

 3.3. Rigid Pedestal Mount 21

CHAPTER 4 - MODIFICATIONS MADE TO THE PENDULUM IMPACT TEST 23

 4.1. Addition of a Mechanical Release and Pendulum Angle Measurement 23

 4.1.1. Mechanical Release 24

| | |
|---|----|
| 4.1.2. Potentiometer | 26 |
| 4.2. Improved LBT | 28 |
| 4.3. Equipment Setup for Baseball Helmet Testing..... | 31 |
| 4.4. Adapting the Test to Soccer | 32 |
| CHAPTER 5 - ANALYSIS OF THE BASEBALL AND SOCCER HELMET IMPACT TESTS | 34 |
| 5.1. LBT Analysis | 36 |
| 5.2. Rigid Pedestal Analysis | 38 |
| 5.3. Test's Performed in this Experiment | 40 |
| CHAPTER 6 – RESULTS AND DISCUSSION | 42 |
| 6.1. LBT Headform Test Results | 42 |
| 6.2. Pedestal Headform Test Results | 46 |
| 6.3. LBT and Pedestal Comparison | 49 |
| 6.4. Baseball Helmet Results | 57 |
| 6.4.1. Pedestal Tests..... | 57 |
| 6.4.2. LBT Tests..... | 62 |
| 6.4.3. SI Comparisons between LBT and Pedestal Helmet Tests..... | 66 |
| 6.5. Soccer Helmet Results | 67 |
| CHAPTER 7 – CONCLUSIONS | 74 |
| APPENDIX | 77 |

| | |
|--|----|
| A-1. Baseball Pedestal Test Plots (12-32 Inch) | 77 |
| A-2. Baseball LBT Test Plots (12-32 Inch) | 80 |
| A-3. Soccer Pedestal Test Plots (15-65 Inch) | 85 |
| A-4. Sample MATLAB Code | 91 |
| REFERENCES | 95 |
| CURRICULUM VITAE..... | 97 |

LIST OF TABLES

Table 1: Boys’ Soccer Injury Rates by Type of Exposure, High School Sports-Related Injury Surveillance Study, US, 2014-2015 School Year [2] 11

Table 2: Activity Resulting in Boys’ Soccer Injuries by Injury Diagnosis, High School Sports-Related Injury Surveillance Study, US, 2014-15 School Year [2] 12

Table 3: Girls’ Soccer Injury Rates by Type of Exposure, High School Sports-Related Injury Surveillance Study, US, 2014-15 School Year [2] 12

Table 4: Activity Resulting in Girls’ Soccer Injuries by Injury Diagnosis, High School Sports-Related Injury Surveillance Study, US, 2014-15 School Year [2] 13

Table 5: Specifications of Data Acquisition Hardware Components 19

Table 6: Weights of the Pendulum, Balls and Carriage/Headform Used in These Tests 42

Table 7: Theoretical and Measured Velocities in LBT Tests 43

Table 8: Theoretical and Measured Velocities in Pedestal Tests 47

Table 9: SI Values for LBT and Pedestal Tests 49

Table 10: Corrected SI Values for LBT and Pedestal Tests 54

Table 11: Baseball Pedestal Test Velocities 58

Table 12: Rigid pedestal baseball helmet tests SI values. 60

Table 13: Baseball LBT test velocities. 62

| | |
|--|----|
| Table 14: LBT baseball helmet tests SI values. | 64 |
| Table 15: SI Comparison of Baseball Helmet Tests | 67 |
| Table 16: Soccer Pedestal Test Velocities | 69 |
| Table 17: Rigid pedestal soccer helmet tests SI values. | 71 |

LIST OF FIGURES

| | |
|---|----|
| Figure 1: Coup-Contrecoup Injury resulting from an Impact from a Baseball..... | 4 |
| Figure 2: Drawing of NOCSAE Specified Air Cannon [6] | 8 |
| Figure 3: Drawing of NOCSAE Specified LBT [6] | 8 |
| Figure 4: Helmet Positioning for Projectile Impact Testing [7] | 9 |
| Figure 5: Diagnosis of Boys’ Soccer Injuries by Type of Exposure, High School Sports-Related Injury Surveillance Study, US, 2014-15 School Year [2] | 11 |
| Figure 6:Diagnosis of Girls’ Soccer Injuries by Type of Exposure, High School Sports-Related Injury Surveillance Study, US, 2014-15 School Year [2] | 12 |
| Figure 7: Southern Impact Research NOCSAE Headform Size Medium | 14 |
| Figure 8: SolidWorks® Model of the Test Frame in Drop Tower Configuration [1] | 16 |
| Figure 9: Test Frame in Drop Tower Configuration [1]..... | 17 |
| Figure 10: Test Frame with LBT Mounted to the Base [1] | 18 |
| Figure 11: SolidWorks® of the Pendulum [1]..... | 20 |
| Figure 12: Headform on LBT Mounted to the Test Frame and Pendulum Impactor Held in Ready Position [1]..... | 21 |
| Figure 13: SolidWorks® Model of the Pedestal Mount [1] | 22 |

| | |
|---|----|
| Figure 14: Pedestal Mount Attached to Test Frame Base [1]..... | 22 |
| Figure 15: SolidWorks® Model of Test Frame with Pendulum Impactor | 24 |
| Figure 16: NOCSAE Headform Pedestal mounted to the Test Frame with Pendulum Impactor in the Ready Position | 25 |
| Figure 17: Winch Used to Raise and Lower the Pendulum..... | 25 |
| Figure 18: Pendulum Held in Ready Test Position by Mechanical Release..... | 26 |
| Figure 19: Potentiometer Mounted to the Pendulum Axle Shaft..... | 27 |
| Figure 20: Pendulum Angle and Height Measured from the Potentiometer, Starting from a Drop Height of 75 Inches..... | 28 |
| Figure 21: SolidWorks® Model of the Improved LBT | 30 |
| Figure 22: The LBT Mounted to the Test Frame with Headform in Ready Test Position | 30 |
| Figure 23: Baseball Helmet Set Up for Right Side Impact Testing..... | 32 |
| Figure 24: SolidWorks® Soccer Ball Adapter for Pendulum Mounting..... | 33 |
| Figure 25: Soccer Soft Helmet Set Up for Adapted NOCSAE Right Side Impact Test | 33 |
| Figure 26: (A) Rawlings® S100 Pro Comp Helmet and New Era® isoBLOX® protective pitcher's cap | 41 |
| Figure 27: Gamebreaker® Helmets Soft Padded Soccer Headgear | 41 |

| | |
|--|----|
| Figure 28: LBT Tests Pendulum Acceleration | 44 |
| Figure 29: LBT Tests Headform Acceleration after Impact | 44 |
| Figure 30: LBT Tests Carriage Acceleration After Impact | 45 |
| Figure 31: LBT Tests SI Values | 45 |
| Figure 32: Pedestal Tests Pendulum Acceleration..... | 47 |
| Figure 33: Pedestal Test Headform Accelerations After Impact | 48 |
| Figure 34: Pedestal Tests SI Values..... | 48 |
| Figure 35: Comparison of SI from the Initial Acceleration and the Deceleration in LBT and Pedestal Tests..... | 50 |
| Figure 36: Impact Energy Transferred into the Headform During LBT and Pedestal Testing. ... | 50 |
| Figure 37: Response of the Headform to LBT and Pedestal Tests | 51 |
| Figure 38: LBT Headform Response from Times: 0 to a) Initial Acceleration (TBI Phase 1), Velocity Peaks. a to b) Deceleration (TBI Phase 2), Velocity Approaches Zero. b to c) Velocity and Displacement Increase. Carriage/Headform Travels Up the LBT. | 52 |
| Figure 39: Pedestal Headform Response from Times: 0 to a) Initial Acceleration (TBI Phase 1), Velocity Peaks, a to b) Deceleration (TBI Phase 2), Velocity Goes to Zero, Max Displacement Before Rebound. b to c) Velocity Changes Direction and Increases, Displacement Goes to Zero (TBI Phase 2 if Rebound is Considered in SI/HIC Calculation). | 52 |

| | |
|--|----|
| Figure 40: Comparison of Corrected SI from the Initial Acceleration and the Deceleration in LBT and Pedestal Tests | 54 |
| Figure 41: Work done on the headform using force measurement versus Drop-Rebound energy balance and LBT Energy. | 56 |
| Figure 42: Rigid pedestal baseball helmet testing, 45 inch drop height, pendulum acceleration. 59 | |
| Figure 43: Rigid pedestal baseball helmet testing, 45 inch drop height, headform acceleration. . 59 | |
| Figure 44: SI values for baseball pedestal helmet testing, initial acceleration. | 60 |
| Figure 45: SI values for baseball pedestal helmet testing, deceleration. | 61 |
| Figure 46: SI values for baseball pedestal helmet testing, acceleration and deceleration combined..... | 61 |
| Figure 47: LBT baseball helmet testing, 45 inch drop height, pendulum acceleration. | 63 |
| Figure 48: LBT baseball helmet testing, 45 inch drop height, headform acceleration. | 63 |
| Figure 49: LBT baseball helmet testing, 45 inch drop height, carriage acceleration. | 64 |
| Figure 50: SI values for baseball LBT helmet testing, initial acceleration..... | 65 |
| Figure 51: SI values for baseball LBT helmet testing, initial deceleration. | 65 |
| Figure 52: SI values for baseball LBT helmet testing, acceleration and deceleration combined. 66 | |
| Figure 53: Rigid pedestal soccer helmet testing, 75 inch drop height, pendulum acceleration.... | 70 |

| | |
|---|----|
| Figure 54: Rigid pedestal soccer helmet testing, 75 inch drop height, headform acceleration. ... | 70 |
| Figure 55: SI values for soccer pedestal helmet testing, initial acceleration. | 72 |
| Figure 56: SI values for soccer pedestal helmet testing, deceleration. | 72 |
| Figure 57: SI values for soccer pedestal helmet testing, acceleration and deceleration combined. | 73 |
| Figure 58: Rigid pedestal baseball helmet testing, 12 inch drop height, pendulum acceleration. | 77 |
| Figure 59: Rigid pedestal baseball helmet testing, 26 inch drop height, pendulum acceleration. | 78 |
| Figure 60: Rigid pedestal baseball helmet testing, 32 inch drop height, pendulum acceleration. | 78 |
| Figure 61: Rigid pedestal baseball helmet testing, 12 inch drop height, headform acceleration. | 79 |
| Figure 62: Rigid pedestal baseball helmet testing, 26 inch drop height, headform acceleration. | 79 |
| Figure 63: Rigid pedestal baseball helmet testing, 32 inch drop height, headform acceleration. | 80 |
| Figure 64: LBT baseball helmet testing, 12 inch drop height, pendulum acceleration. | 80 |
| Figure 65: LBT baseball helmet testing, 26 inch drop height, pendulum acceleration. | 81 |
| Figure 66: LBT baseball helmet testing, 32 inch drop height, pendulum acceleration. | 81 |
| Figure 67: LBT baseball helmet testing, 12 inch drop height, headform acceleration. | 82 |
| Figure 68: LBT baseball helmet testing, 26 inch drop height, headform acceleration. | 82 |
| Figure 69: LBT baseball helmet testing, 32 inch drop height, headform acceleration. | 83 |

| | |
|--|----|
| Figure 70: LBT baseball helmet testing, 12 inch drop height, carriage acceleration. | 83 |
| Figure 71: LBT baseball helmet testing, 26 inch drop height, carriage acceleration. | 84 |
| Figure 72: LBT baseball helmet testing, 32 inch drop height, carriage acceleration. | 84 |
| Figure 73: Rigid pedestal soccer helmet testing, 15 inch drop height, pendulum acceleration.... | 85 |
| Figure 74: Rigid pedestal soccer helmet testing, 25 inch drop height, pendulum acceleration.... | 85 |
| Figure 75: Rigid pedestal soccer helmet testing, 35 inch drop height, pendulum acceleration.... | 86 |
| Figure 76: Rigid pedestal soccer helmet testing, 45 inch drop height, pendulum acceleration.... | 86 |
| Figure 77: Rigid pedestal soccer helmet testing, 55 inch drop height, pendulum acceleration.... | 87 |
| Figure 78: Rigid pedestal soccer helmet testing, 65 inch drop height, pendulum acceleration.... | 87 |
| Figure 79: Rigid pedestal soccer helmet testing, 15 inch drop height, headform acceleration. ... | 88 |
| Figure 80: Rigid pedestal soccer helmet testing, 25 inch drop height, headform acceleration. ... | 88 |
| Figure 81: Rigid pedestal soccer helmet testing, 35 inch drop height, headform acceleration. ... | 89 |
| Figure 82: Rigid pedestal soccer helmet testing, 45 inch drop height, headform acceleration. ... | 89 |
| Figure 83: Rigid pedestal soccer helmet testing, 55 inch drop height, headform acceleration. ... | 90 |
| Figure 84: Rigid pedestal soccer helmet testing, 65 inch drop height, headform acceleration. ... | 90 |

CHAPTER 1 – INTRODUCTION

Sports related head injuries and the associated traumatic brain injuries (TBI) known as concussions have generated significant media attention in recent years. The sport in which these types of injuries are most prevalent is American football, but they are also a concern in other sports such as baseball and soccer. In the case of football and baseball, players are required to wear protective helmets to help mitigate head injuries. These helmets are tested based on criteria outlined by organizations like the National Operating Committee on Standards for Athletic Equipment (NOCSAE).

Protective headgear is not required in soccer however, because of growing concern over sports related head injuries among soccer players; the use of protective headgear in soccer has become an area of concern.

The objective of this research is to develop reliable and repeatable test procedures based on modifications of current NOCSAE test standards (ND-001, ND-021, ND-022 and ND-023). These modifications are designed to include additional sensors in order to acquire more information about the protective properties of sports headgear and to develop a universal test protocol for a variety of injury scenarios. This will allow for a greater understanding of the nature of head impacts, the evaluation of helmets currently available, and the introduction of a methodology for testing head protection for soccer. A standard for testing soccer headgear currently does not exist.

1.1. Head Impact Health Risk Metrics

The NOCSAE test standard ND-001 uses the severity index (SI) as a pass/fail measure of the protective capabilities of helmets and headgear. The SI value quantifies the severity of an

impact based on the acceleration measured at the center of mass of the NOCSAE headform. SI is defined as:

$$SI = \int_{t_1}^{t_2} a(t)^{2.5} dt \quad (1-1)$$

where $a(t)$ is the instantaneous acceleration expressed in g's measured at the centroid of the NOCSAE headform, t_1 is the time the impact begins, and t_2 is the time the impact ends.

SI was developed for automotive industry and the maximum acceptable SI of 1200 adopted by NOCSAE as a pass/fail criterion. It should be noted however that the SI used here is not a direct measure of the likelihood of TBI but rather based on experimental data for impact skull fracture. In the instances of skull fracture there is a high likelihood of TBI but in sports many of the TBI's also occur below the threshold of skull fracture.

1.2. Motivation for Modifying the Current Test Standards

The standards currently outlined by NOCSAE for testing baseball helmets use a simulated human headform mounted to a linear bearing track (LBT). The helmet to be tested is placed on the instrumented headform and then it is impacted with a baseball propelled out of an air cannon. The acceleration of the head resulting from this initial impact can then be measured then the acceleration signal damps out as the headform travels along the LBT after the collision. This may be a fair approximation of the acceleration of the head from the initial impact of the ball.

However, there is ongoing research including the results of these experiments that suggest the acceleration resulting from the initial impact is not the only part of the collision that need consideration in a potential TBI event. In an actual ball to head collision the head does not float away like on a LBT because it is attached to the neck. So the impact causes the head to

accelerate as the neck flexes then it decelerates as the neck muscles pull the head and stop the motion. In article ‘Heading in Soccer: Dangerous Play?’ Spiotta, Bartsch and Benzel described the impact acceleration response as “biphasic, with an initial spike caused by the head acceleration and a second spike...reflecting head deceleration caused by neck contraction.” [11] In a Highway Safety Research Institute Report, the SI is described as “calculated on the basis of the entire event, including the initial deceleration as the occupant is stopped and the subsequent acceleration as he rebounds against the seat back.” [4] The result of this biphasic acceleration is brain “slosh” described by Smith, Bailes, Fisher et al. as follows:

“The skull and spinal canal contains only nervous tissue, connective tissue, and fat cells and their interstitium, blood, and cerebrospinal fluid. These fluid contents do not completely fill the rigid container delimited by the skull and bony spinal canal, leaving a “reserve volume.” ...In the presence of reserve volume, as seen in a normal physiological state, acceleration to the skull can result in a differential acceleration between the skull and its contents. As a consequence, the brain and fluids collide with the inside of the skull. Considering the semisolid properties of the mammalian brain, we refer to this effect as slosh. [10]”

In the article ‘Biomechanics of Traumatic Brain Injury’, injuries resulting from this biphasic acceleration are referred to as coup-contrecoup injuries where “Coup contusions are produced by the slapping effect of the skull hitting the brain; contrecoup lesions follow from the bouncing of the brain against the inner posterior surface of the skull [3]. Figure 1 shows an illustration to visualize what a coup-contrecoup injury might look like as a result of a baseball impacting the head.

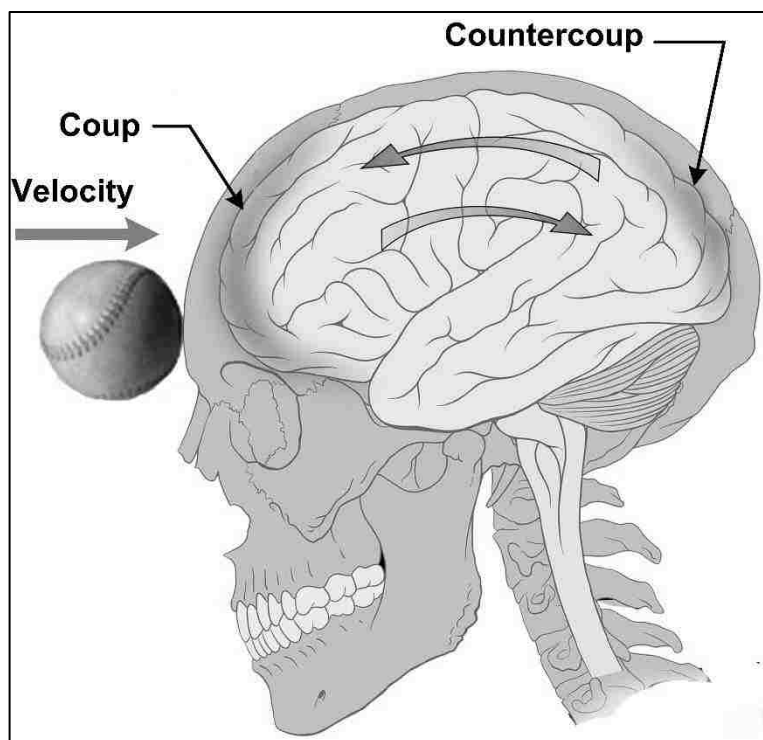


Figure 1: Coup-Contrecoup Injury resulting from an Impact from a Baseball.

In some cases, the head deceleration may rival or even exceed the acceleration of the initial impact. Since the test employing the LBT essential neglects the heads deceleration by allowing the headform to continue traveling in one direction which damps out the deceleration pulse, this test is likely to be an underestimate of the potential for injury. The test and measurement procedure should consider the initial acceleration and the rebound decelerations as a single event and include both in the calculation of the SI values.

In addition to modifying this test procedure making it more representative of actual impacts, the secondary goal of this project was to use the baseball procedure for testing in other sports like soccer. The growing concern over concussions in sports, particularly youth sports, has now included soccer where hitting the ball with the head or “heading” as a normal part of play is

being scrutinized for safety. Sports equipment companies already have soccer head gear available on the market but there is no test standard in place for that head gear. Since the nature of the impact event is similar, ball to head, a modified version of the baseball test was applied to testing soccer soft helmets.

CHAPTER 2 – SPORTS TESTING STANDARDS AND LITERATURE REVIEW

The following sections is a review of testing procedures for sports helmets along with current work on identifying and mitigating potential TBI's. First, the guidelines and standards put in place by NOCSAE is outlined to elucidate the current testing procedure. Then the history of the SI value as metric for measuring the severity of head injuries is explained. Finally, more current research into sports related head injuries is discussed to express the need to revisit the NOCSAE standards and show the potential for expanding sports helmet testing into non-traditional helmet sports.

2.1. NOCSAE Standards

The conditions and methodologies used by NOCSAE for testing baseball helmets is outlined in the standards ND-001, ND-021, ND-022 and ND-023.

The standard ND-001 “Standard Test Method and Equipment Used in Evaluating the Performance Characteristics of Headgear/Equipment” covers laboratory equipment, environmental conditions, test samples and failure criteria for drop testing athletic helmets. It is also used as a base standard for all types of NOCSAE athletic helmet testing including the test of interest here, ball impacts. ND-001 section 3.44 defines the SI as well as the times over which to carry the integration, more specifically “the integration as called for in this formula must begin after the system triggers but before the initial signal rises above 4 g's. The integration must then end when the signal falls below 4 g's, after it has peaked.” [5] This means the SI as stated by NOCSAE only accounts for the acceleration of the initial impact pulse and neglects any successive accelerations associated with head rebound.

ND-001 Section 4.1 states that the purpose of this standard is measurement of the effectiveness of helmets and the establishment of a pass/fail criteria based on the SI. In sections 7-8 the standard goes on to specify helmet material and construction such that: the helmet will remain affixed to the wearer's head during the impact, the equipment will survive all tests protocols intact and ready for use and that no feature of the helmet should increase the likelihood of injury during use. Then in section 13 the dimensions of the headforms used in the testing are specified for the small, medium and large headform sizes. The remainder of the standard specifies measurement equipment and lab procedure. All ball impact testing specific standards refer back to ND-001 for environmental, sampling, data recording and helmet certification guidelines. [5]

Next ND-021 "Standard Projectile Impact Test Method and Equipment Used in Evaluating the Performance Characteristics of Protective Headgear, Faceguards of Projectiles" outlines the specific equipment and procedure used to conduct projectile impact testing. Section 12 Of the standard specifies an apparatus that can propel a projectile, i.e. baseball, at a speed of up to 60 mph at the headform and suggests an air cannon as a possible solution. In between the air cannon and the headform must be some means to measure the velocity of the ball such as a chronograph. Then the headform must be mounted in such a way that it is indexable in all three axes and adjustable rotationally along the vertical axis. Finally, the headform mounting must be attached to a table that will slide away from the air cannon along the direction of ball travel after the impact. The standard contains drawings of a suggested testing set up (Figure 2) and an LBT with headform mount (Figure 3). [6]

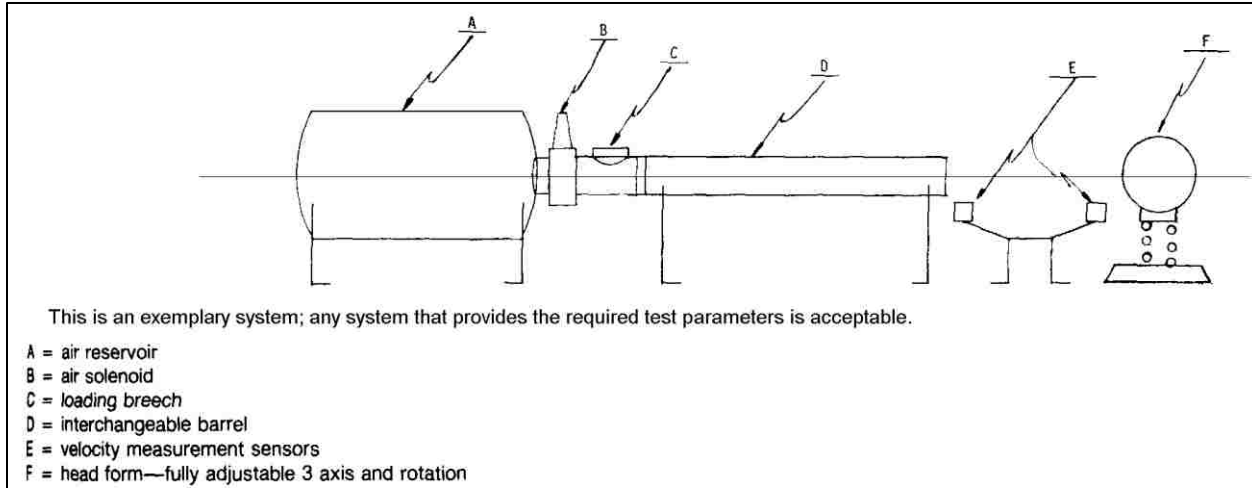


Figure 2: Drawing of NOCSAE Specified Air Cannon [6]

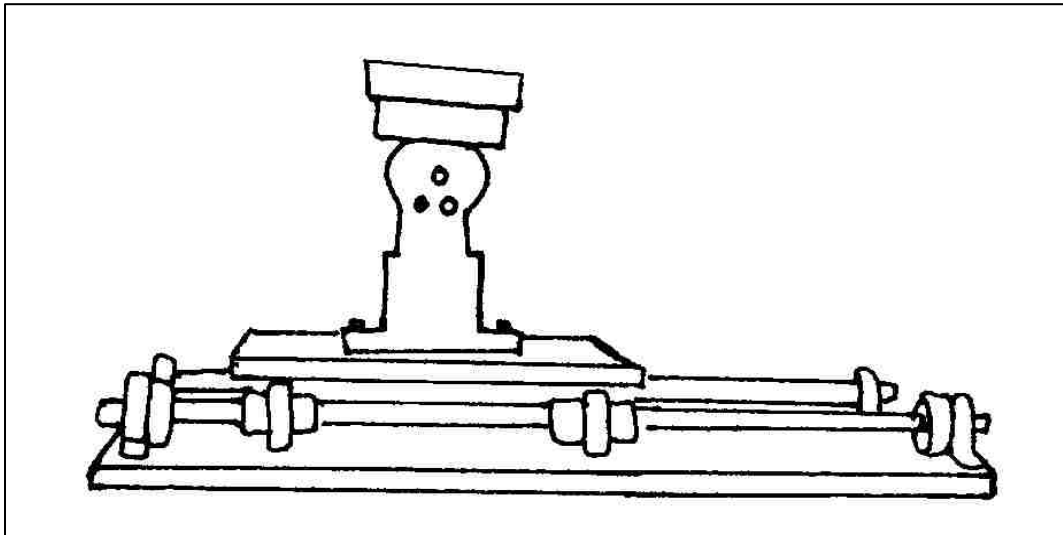


Figure 3: Drawing of NOCSAE Specified LBT [6]

The last two standards that deal with baseball helmet projectile impact testing are ND-022/023. ND-022 or “Standard Performance Specifications for Newly Manufactured Baseball/Softball Batter’s Helmets” specifies the conditions, projectile speeds and mounting

positions (Figure 4) of the helmets. The most important part of ND-022 is the pass/fail criteria specified in Section 6.2 that states, “The peak severity index of any impact shall not exceed 1200 SI.” [7] Lastly in ND-023 “Laboratory Procedural Guide for Certifying Newly Manufactured Baseball/Softball Batter’s Helmets” all of the information provided in the previous three standards is pulled together in single document outlining the entire procedure. [8] These documents are the up to date and reflect the current state of helmet projectile impact testing.

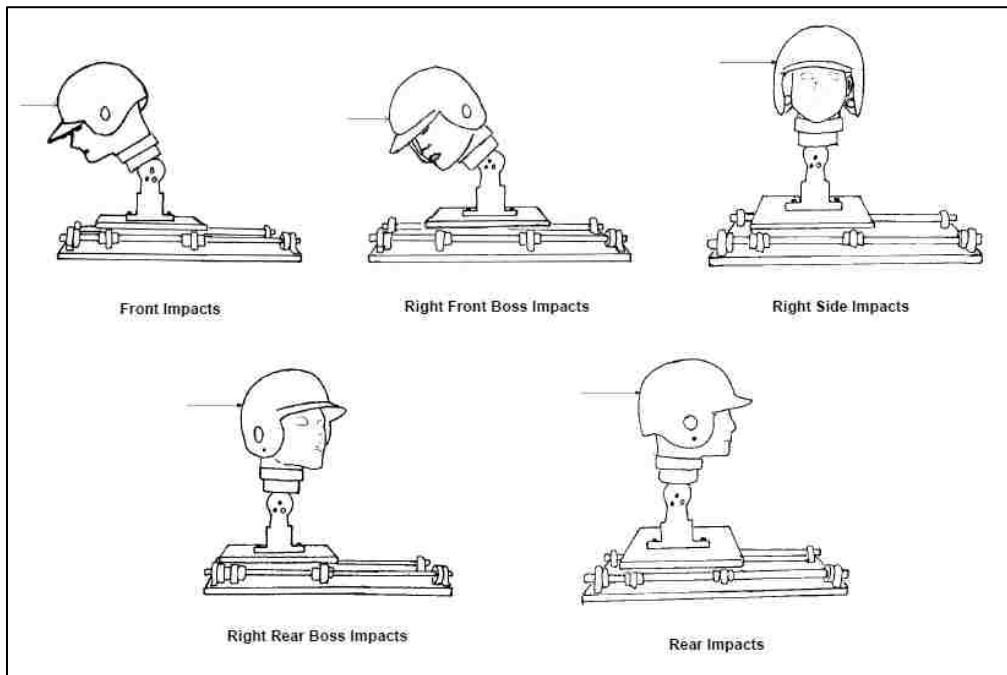


Figure 4: Helmet Positioning for Projectile Impact Testing [7]

2.2. SI

The Severity Index was a head impact injury metric developed for the National Highway Traffic Safety Administration (NHTSA) in 1966 and 1972 respectively. It is based on the Wayne State Tolerance Curve (WSTC) developed in 1960 which “included six points that represented the relationship between acceleration level and pulse duration (in the range of 1 to 6 ms) found to

produce linear skull fracture in embalmed cadaver heads [4].” The SI was the work of C.W. Gadd who plotted the WSTC on log-log plot and then used a straight-line approximation of the result to find a slope which is the exponent in the SI function seen in equation 1-1. [4] The standard that was created for NOCSAE in 1971 was a SI of 1200 as maximum. It must be stressed that SI is measure of the likelihood of skull fracture and is not directly related to TBI.

As previously stated, SI is not a direct measure of TBI but since SI has been adopted by NOCSAE in 2003 Pellman, Viano and Tucker et al. attempted to correlate the SI values to the probability of a concussion in the paper “*Concussion in professional football: reconstruction of game impacts and injuries.*” They analyzed professional football game films between 1996 and 2001 and stated that a majority of concussions occurred at or above a SI value of 300. [9] These SI values were considered the pass/fail limit during the development of the modified test procedure discussed in this report. However, this analysis is applicable to either the NOCSAE mandated SI or these lower values.

2.3. TBI’s in Soccer

American football has been the major focus of safety research and this lead to the current state of safety regulations in all of the major helmet sports. But due to recent media attention on TBI’s, there is now a conversation about player safety in non-helmet sports like soccer. There are several instances during normal game play in soccer that the head may be impacted including: head to head player collisions, head to ground impacts during a fall, head to goal post collisions and deliberately hitting the soccer ball with the head or “heading” the ball. In the report ‘National High School Sports-Related Injury Surveillance Study, 2014-2015 School Year’ the number of injuries during a single year in boys and girls high school soccer is recorded. [2] In Tables 1-4 and figures 5-6 the number of injuries in boys’ and girls’ soccer, the type of injuries

and the activity in which they were participating during the injury are shown for the year. It can be seen that for both boys' and girls' soccer a significant part of the injuries received are concussions and of those concussions 25-30% happen while the player is attempting to head the ball. This has led researchers to question if heading the ball is safe and whether or not adopting protective headgear could lower the instances of concussion in soccer.

Table 1: Boys' Soccer Injury Rates by Type of Exposure, High School Sports-Related Injury Surveillance Study, US, 2014-2015 School Year [2]

| | # Injuries | # Exposures | Injury rate (per 1,000 athlete-exposures) |
|--------------|------------|----------------|--|
| Total | 575 | 330,072 | 1.74 |
| Competition | 376 | 101,172 | 3.72 |
| Practice | 199 | 228,900 | 0.87 |

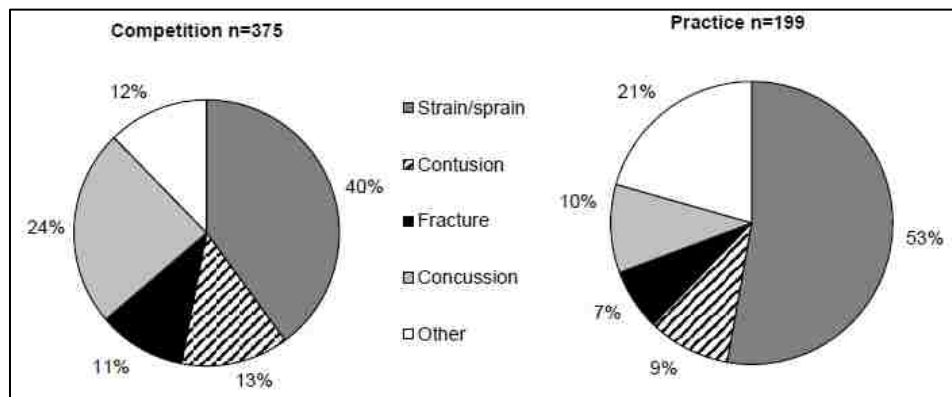


Figure 5: Diagnosis of Boys' Soccer Injuries by Type of Exposure, High School Sports-Related Injury Surveillance Study, US, 2014-15 School Year [2]

Table 2: Activity Resulting in Boys' Soccer Injuries by Injury Diagnosis, High School Sports-Related Injury Surveillance Study, US, 2014-15 School Year [2]

| Activity | Diagnosis | | | | | | | | | |
|-------------------------|---------------|-------------|-----------|-------------|-----------|-------------|------------|-------------|-----------|-------------|
| | Strain/Sprain | | Contusion | | Fracture | | Concussion | | Other | |
| | n | % | n | % | n | % | n | % | n | % |
| General play | 67 | 27.9% | 11 | 18.3% | 12 | 24.0% | 16 | 16.3% | 30 | 37.5% |
| Defending | 24 | 10.0% | 12 | 20.0% | 4 | 8.0% | 20 | 20.4% | 6 | 7.5% |
| Ball handling/dribbling | 24 | 10.0% | 8 | 13.3% | 5 | 10.0% | 3 | 3.1% | 3 | 3.8% |
| Chasing loose ball | 31 | 12.9% | 6 | 10.0% | 6 | 12.0% | 9 | 9.2% | 7 | 8.8% |
| Heading ball | 4 | 1.7% | 4 | 6.7% | 3 | 6.0% | 24 | 24.5% | 6 | 7.5% |
| Other | 90 | 37.5% | 19 | 31.7% | 20 | 40.0% | 26 | 26.5% | 28 | 34.9% |
| Total | 240 | 100% | 60 | 100% | 50 | 100% | 98 | 100% | 80 | 100% |

Table 3: Girls' Soccer Injury Rates by Type of Exposure, High School Sports-Related Injury Surveillance Study, US, 2014-15 School Year [2]

| | # Injuries | # Exposures | Injury rate (per 1,000 athlete-exposures) |
|--------------|------------|----------------|--|
| Total | 832 | 308,502 | 2.70 |
| Competition | 582 | 98,288 | 5.92 |
| Practice | 250 | 210,214 | 1.19 |

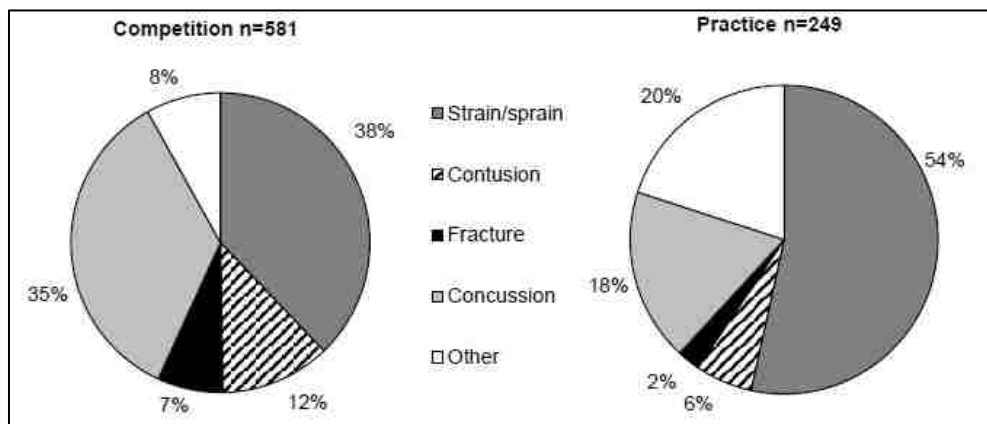


Figure 6: Diagnosis of Girls' Soccer Injuries by Type of Exposure, High School Sports-Related Injury Surveillance Study, US, 2014-15 School Year [2]

Table 4: Activity Resulting in Girls' Soccer Injuries by Injury Diagnosis, High School Sports-Related Injury Surveillance Study, US, 2014-15 School Year [2]

| Activity | Diagnosis | | | | | | | | | |
|--------------------------|---------------|-------------|-----------|-------------|-----------|-------------|------------|-------------|-----------|-------------|
| | Strain/Sprain | | Contusion | | Fracture | | Concussion | | Other | |
| | n | % | n | % | n | % | n | % | n | % |
| General play | 74 | 23.1% | 11 | 14.9% | 2 | 4.8% | 36 | 15.9% | 33 | 35.5% |
| Defending | 53 | 16.5% | 23 | 31.1% | 8 | 19.0% | 43 | 19.0% | 9 | 9.7% |
| Chasing loose ball | 37 | 11.5% | 7 | 9.5% | 9 | 21.4% | 15 | 6.6% | 4 | 4.3% |
| Heading ball | 3 | 0.9% | 2 | 2.7% | 4 | 9.5% | 69 | 30.5% | 4 | 4.3% |
| Ball handling /dribbling | 46 | 14.6% | 8 | 10.8% | 6 | 14.3% | 11 | 4.9% | 14 | 15.1% |
| Other | 108 | 33.6% | 23 | 31.1% | 13 | 31.0% | 52 | 23.0% | 29 | 31.2% |
| Total | 321 | 100% | 74 | 100% | 42 | 100% | 226 | 100% | 93 | 100% |

CHAPTER 3 – PENDULUM BASED IMPACT TESTING DEVELOPED BY DARREN BENN

In his master's thesis Darren Benn outlines the design and construction of impact testing apparatus. The pendulum tests that Benn designed are all based around the NOCSAE headform manufactured by Southern Impact Research Center, LLC. (Figure 7). [1]



Figure 7: Southern Impact Research NOCSAE Headform Size Medium

3.1. Hardware Used in the Development of Benn's Apparatus

All of the test's performed by Benn and as well as in this series of experiments were mounted to a test stand. The test stand was an aluminum frame with a square base and top plate both two by two feet wide and supported by posts 9 feet tall. It was design to perform both impact and drop tower testing and can be seen in drop tower configuration in Figures 8-9. The

base of the frame was machined with T-slots so that anvils, headforms and the LBT (Figure 10) could be mounted depending on the test to be performed. On the top plate was mounted a winch to raise and lower the headform during drop testing and later used to raise and lower the pendulum. The stand also incorporated features like additional mounting points in the base and top plate for flexibility in reconfiguring the stand for future test modifications. For safety the frame also includes a circuit breaker for the winch and a limit switch to prevent the operator from over winding the winch and colliding the overhaul weight.

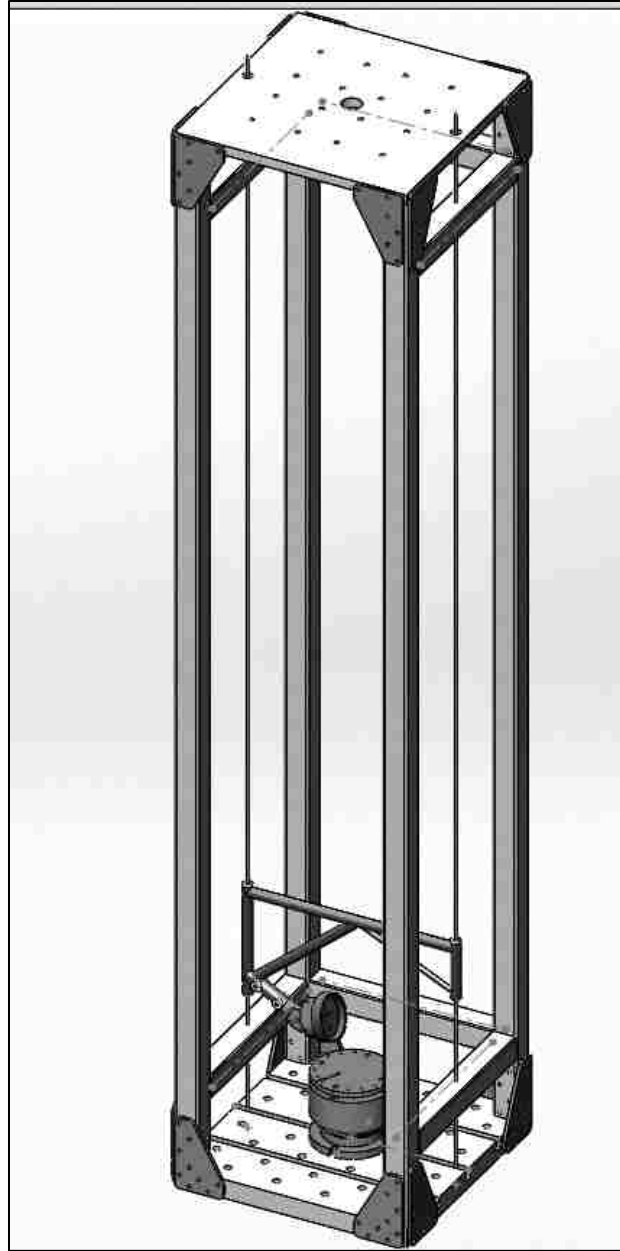


Figure 8: SolidWorks® Model of the Test Frame in Drop Tower Configuration [1]



Figure 9: Test Frame in Drop Tower Configuration [1]

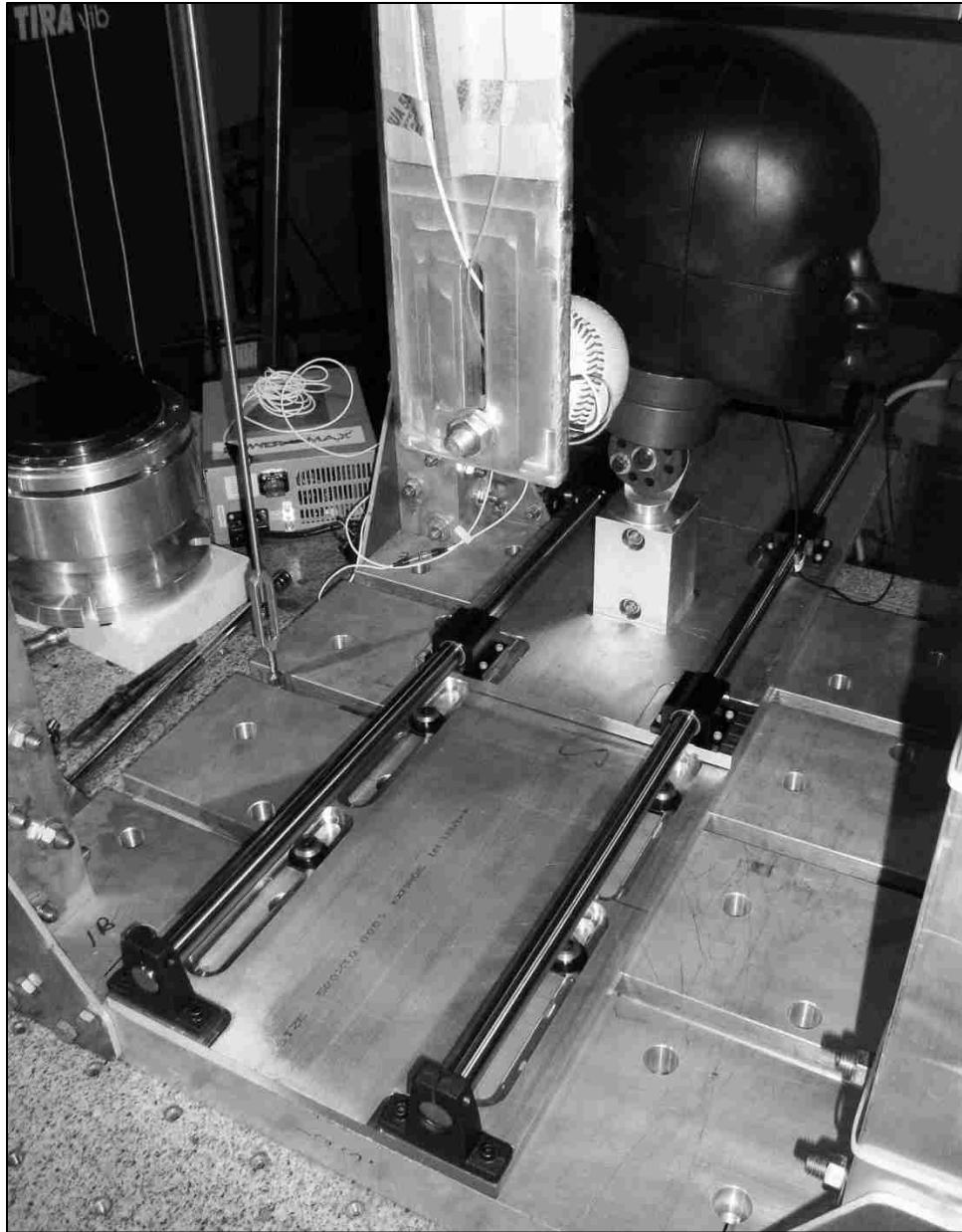


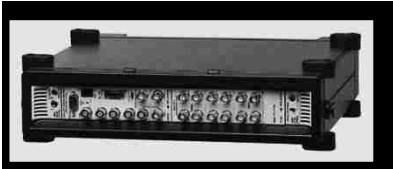



Figure 10: Test Frame with LBT Mounted to the Base [1]

In addition to the mechanical components in the test there is was also the data acquisition (DAQ) equipment to consider. All of the data recorded in previous experiments as well as these tests was logged using a Brüel & Kjær data acquisition module and the DAQ software PULSE®. Using this equipment all of the forces and accelerations were recorded from the transducers

mounted on the impactors and at the centroid of the Headform. Also for the LBT tests and additional accelerometer was mounted to the carriage. The manufacture and specifications of the DAQ hardware used in these tests is list in Table 5.

Table 5: Specifications of Data Acquisition Hardware Components

| Component | Manufacturer /Purpose | Specifications |
|---|---|--|
|  | <p>PCB Piezotronics/ Measurement Device: Accelerometer placed on baseball adapter and the carriage on the LBT.</p> | <p>Sens. ($\pm 15\%$) = $0.25 \text{ mV}/(\text{m/s}^2)$ Meas. Range = $\pm 19600 \text{ m/s}^2$ peak Freq. Range ($\pm 5\%$) = 1.0 to 10000 Hz Freq. Range ($\pm 10\%$) = 0.7 to 13 kHz Freq. Range ($\pm 3 \text{ dB}$) = 0.3 to 20000 Hz Res. Freq. = $\geq 80 \text{ kHz}$ Broadband. Res. (1) = 0.1 m/s^2 rms Temp. Range = -65 to $250 \text{ }^\circ\text{F}$ Excitation Voltage = 18 ~ 30 VDC Current Excitation = 2~20 mA Height/Weight = .14in/.02oz</p> |
|  | <p>Dytran/ Measurement Device: Dytran model 1051V4 is an IEPE force sensor. Placed between Pendulum and baseball.</p> | <p>10 mV/lbf sensitivity 500 lbf compression range 500 lbf tension range 10,000 lbf maximum compression 500 lbf maximum tension 10-32 radial connector 1/4-28 tapped holes top and bottom 28 grams, Stainless steel High natural frequency IEPE</p> |
|  | <p>Brüel & Kjær / Data Acquisition Module. Link between measurement devices and analysis software.</p> | <p>25 kHz analysis frequency range Six input channels Two generators with 25 kHz frequency range</p> |
|  | <p>Dytran/ Measurement Device: Dytran model 3023A Triaxial Accelerometer. Mounted in Headform.</p> | <p>10 mV/g sensitivity 500g range 1.5 to 10,000 Hz frequency range ($\pm 15\%$-5%) 4-pin 1/4-28 radial connector Adhesive mount 3 grams Titanium Hermetic Lightweight Triaxial IEPE</p> |

3.2. The Pendulum

Benn made two modifications to the NOCSAE baseball impact test procedure. The first modification was the use of a pendulum impactor instead of an air cannon for propelling a ball toward the NOCSAE headform. This facilitated the use of additional instrumentation to analyze the effects of head impacts. A drawing of the pendulum and a photograph of the pendulum impactor and the NOCSAE headform mounted to the LBT with the pendulum in the ready position is shown in Figures 11-12. The pendulum impactor allows for the instrumentation of the ball so the force and acceleration of the ball can be measured directly during head/helmet impact.

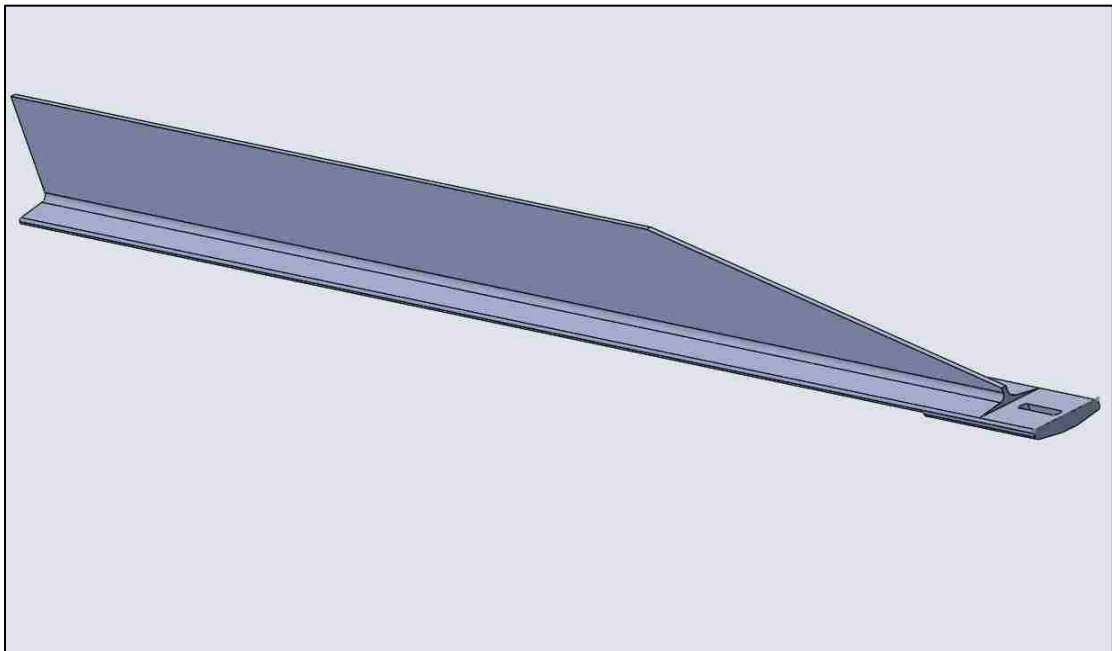


Figure 11: SolidWorks® of the Pendulum [1]

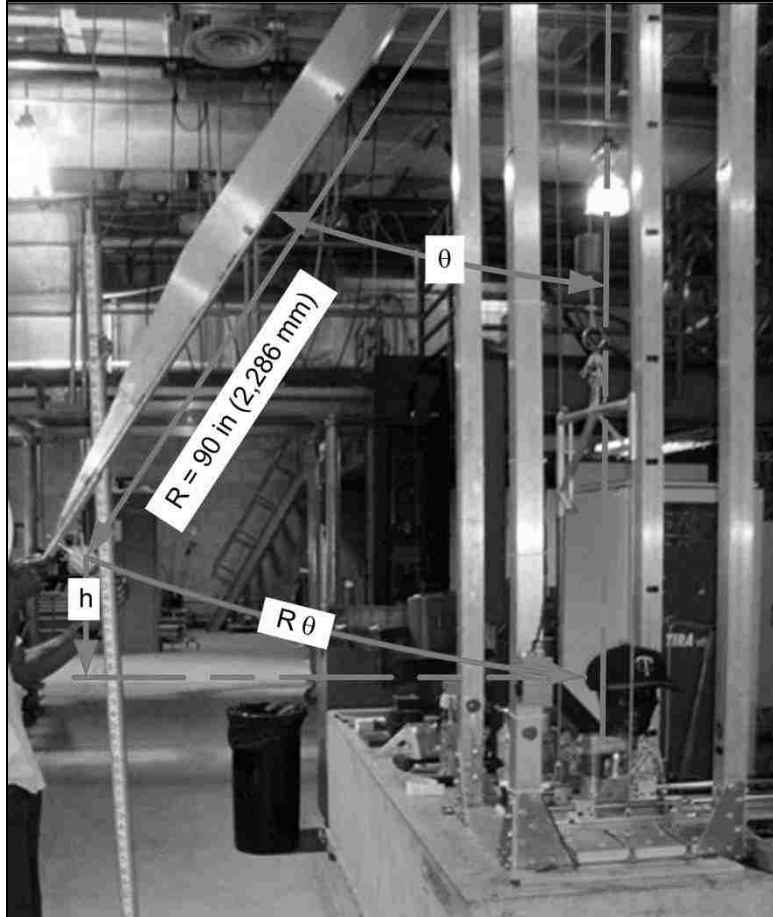


Figure 12: Headform on LBT Mounted to the Test Frame and Pendulum Impactor Held in Ready Position [1]

3.3. Rigid Pedestal Mount

The second modification to the NOCSAE test procedure to use a rigid pedestal mount for the headform to compare against the response of the LBT. A solid model of the pedestal mount is shown in Figure 10 and it can also be seen mounted to the base of the test frame in Figures 13-14. The pedestal provides a rigid support for the headform so the deceleration pulse can be measured and compared to LBT where the deceleration is neglected. However, the neck has some

compliance. Therefore, the actual acceleration experienced by the head will be less than that measured using the rigid pedestal mount.

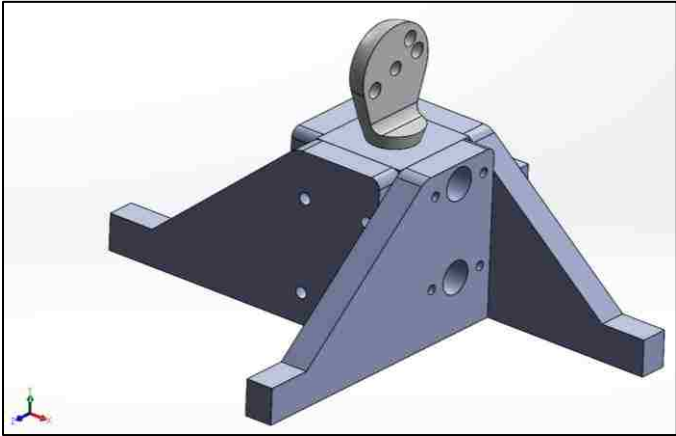


Figure 13: SolidWorks® Model of the Pedestal Mount [1]

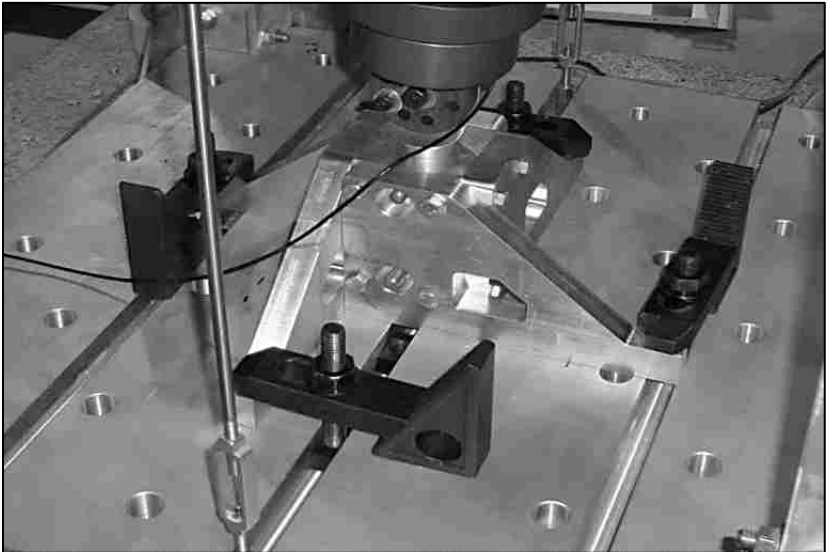


Figure 14: Pedestal Mount Attached to Test Frame Base [1]

CHAPTER 4 - MODIFICATIONS MADE TO THE PENDULUM IMPACT TEST

Moving forward from the work of Darren Benn modifications were made to the test stand and LBT to improve the repeatability of the tests and generate more consistent results. When the impact tests were performed prior to this work the measurement drop height, pendulum release and the measurement of the rebound height of the pendulum were all performed by hand. So in order to remove any operator error from the procedure these tasks were automated. Also there were problems with the old LBT that created unreliable results so more robust LBT was constructed. Finally, after the improvements to the test stand were completed, it was modified to perform impact testing with soccer as well as baseballs.

4.1. Addition of a Mechanical Release and Pendulum Angle Measurement

The pendulum impact test was operated manually was seen in Figure 12. The operator would grab the end of the pendulum and lift it to the desired test height measured with a yard stick. Then once the DAQ was activate the operator would let go of the pendulum and then after the impact attempt to catch it in order to measure the rebound height again with the yard stick. This method creates several opportunities for operator error including:

1. Misreading the yard stick when measuring the drop height.
2. Accidentally moving the pendulum before the drop.
3. Accidentally introducing an extra force when releasing the pendulum.
4. No guarantee that the pendulum was caught at exactly the maximum rebound height.

4.1.1. Mechanical Release

To address problems 2 and 3, the operator holding and dropping the pendulum was replaced with a mechanical release. A boom and pulley were constructed and attached to the top of the test frame using the existing mounting locations. Then the winch, cable and mechanical release used in the drop tower testing was rerouted so that it could be attached to the end of the pendulum (Figures 15-16). Now the pendulum can be held reliable at exactly the specified height. It can be raised and lowered with the winch (Figure 17) and when the DAQ is activated it can be mechanically released (Figure 18) with no incidental force being applied to the end pendulum.

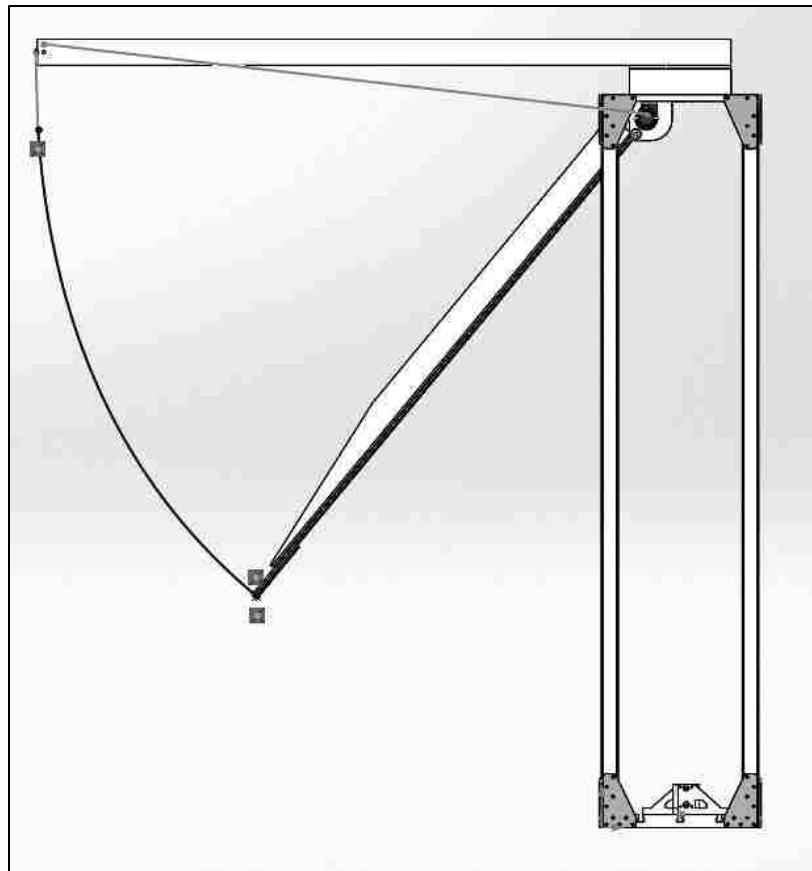


Figure 15: SolidWorks® Model of Test Frame with Pendulum Impactor

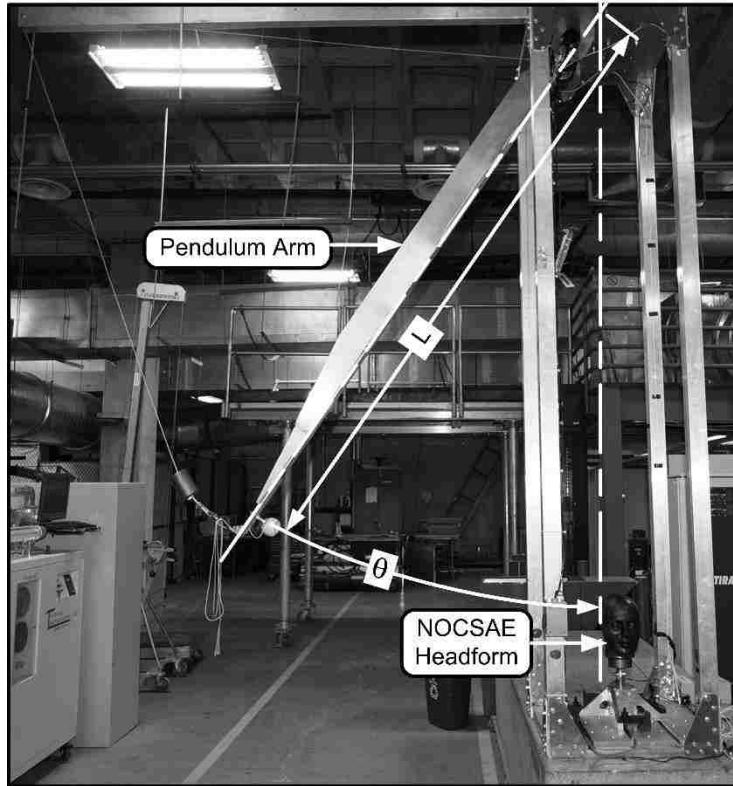


Figure 16: NOCSAE Headform Pedestal mounted to the Test Frame with Pendulum Impactor in the Ready Position

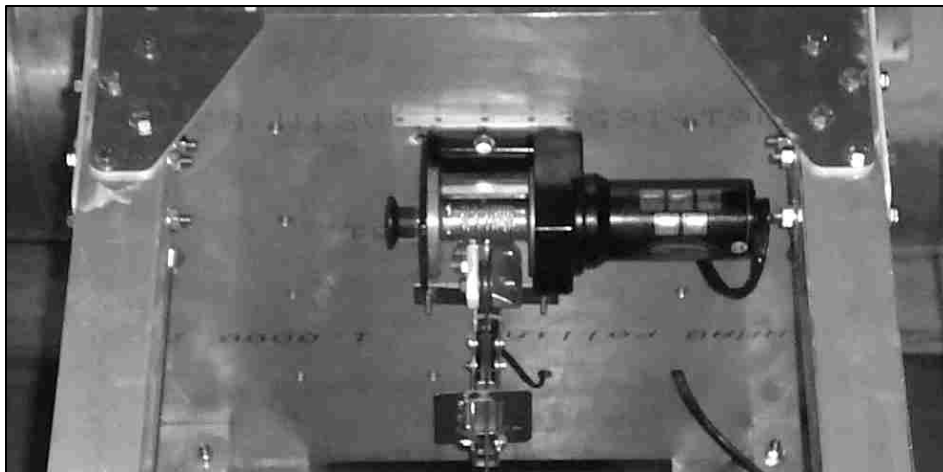


Figure 17: Winch Used to Raise and Lower the Pendulum

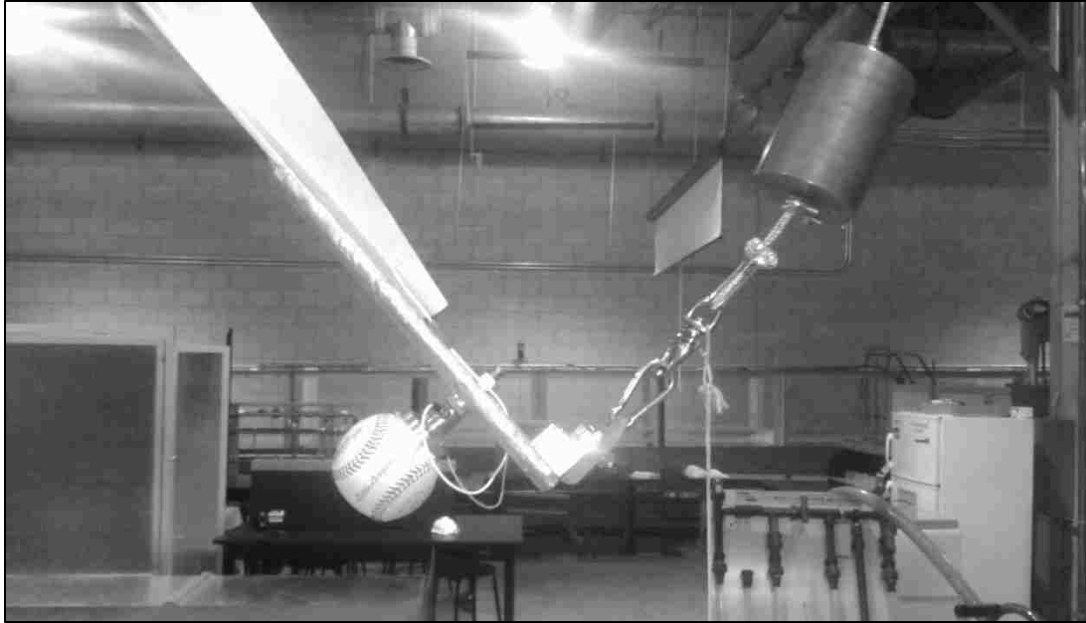


Figure 18: Pendulum Held in Ready Test Position by Mechanical Release

4.1.2. Potentiometer

The solution to the first and last problem identified was to replace the manual height measurements with an electronic measurement. A single turn potentiometer was used to find the angular position of the pendulum. The potentiometer was mounted to left side of the pendulum and the potentiometer shaft was connected to the pendulum axle shaft with a coupler (Figure 19). The potentiometer was indexed so that it measured zero degrees when the pendulum was in the horizontal position. Then as the pendulum swings down the potentiometer will measure an angle of 90 degrees at the moment of impact. The rationale for this index is that some compression can be expected in the ball as well as flex in the headform at the moment of impact. Any angle measured greater than 90 degrees can be used as a measure of this compression or compliance. Then, having an accurate measurement of the angle, and knowing the pendulum geometry

(Figure 12) a simple application of trigonometry gives the pendulum height as a function of the angle.

$$h_{\text{pendulum}} = L_{\text{pendulum}} \left[1 - \cos\left(\frac{\pi}{2} - \theta\right) \right] \tag{4-1}$$

Where h is the pendulum height at the point of impact, L is the length of the pendulum from the center of rotation to the point of impact (88 inches in these tests) and theta is the angle measured by the potentiometer in radians. Figure 20 shows an example of recorded values of pendulum angle and height for a 75 inch drop height. This data or level of precision was not possible with manual height measurements.

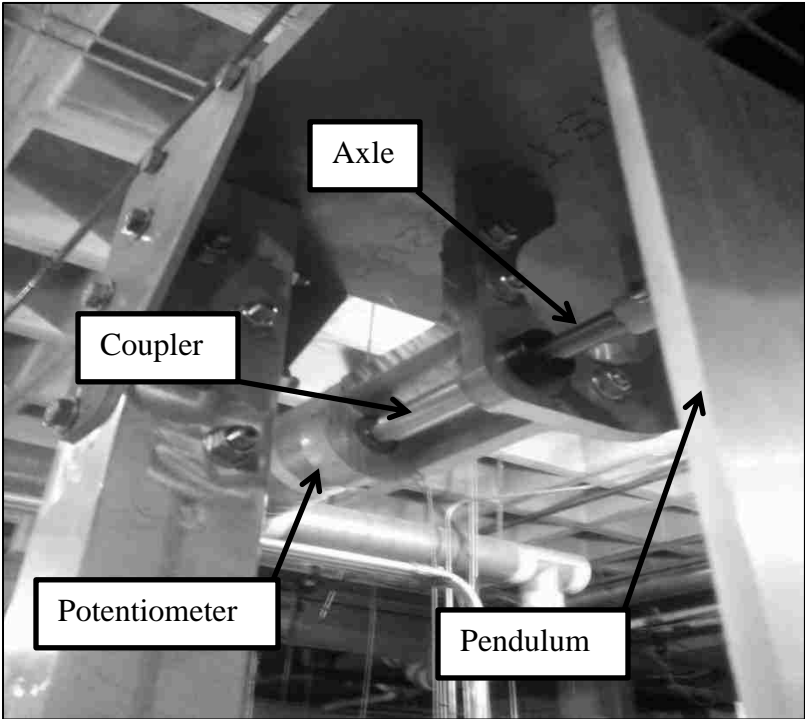


Figure 19: Potentiometer Mounted to the Pendulum Axle Shaft

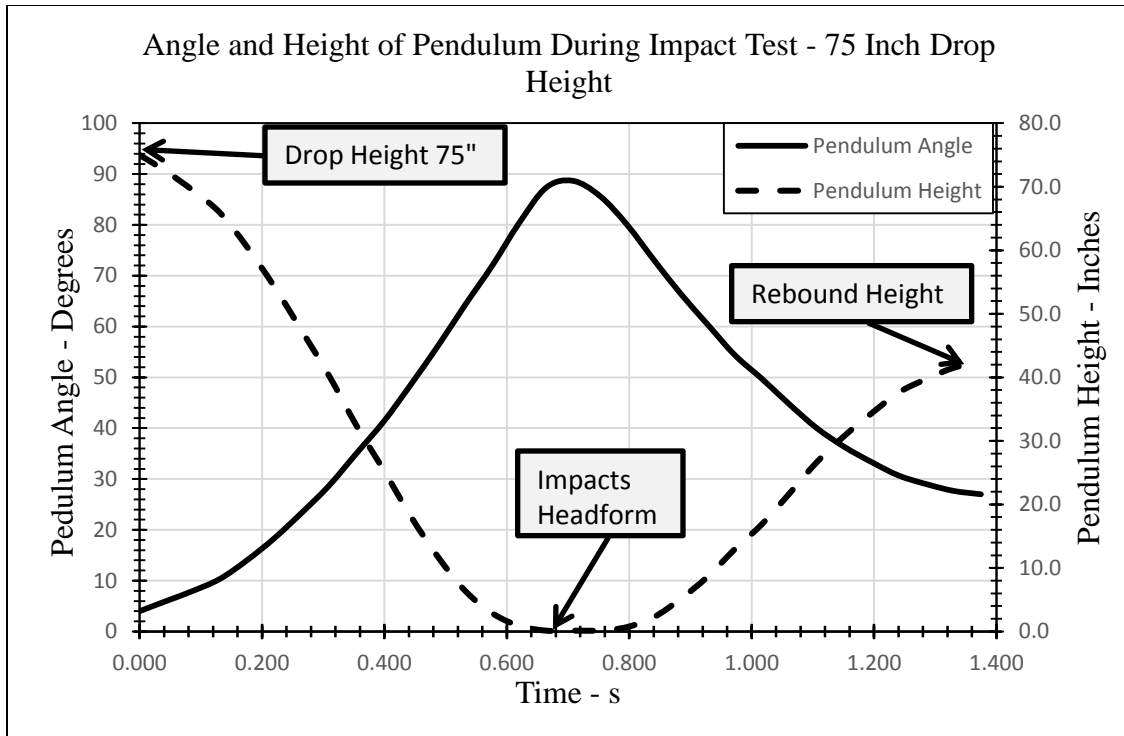


Figure 20: Pendulum Angle and Height Measured from the Potentiometer, Starting from a Drop Height of 75 Inches

4.2. Improved LBT

The LBT designed and constructed by Benn, when tested, was not sufficient rigid enough or long enough use for helmet impact testing. During a test the impactor would hit the headform or helmet and instead of simply travelling along the LBT it would move but also excite a substantial amount of vibration in the LBT guide rails. And during testing at the higher pendulum drop heights the carriage/headform would travel the full length of the LBT and impact the far end. Part of this analysis involves a summation of energy transfers in the system during the impact so the additional collision and vibrations in the rails would add irreconcilable energy losses when performing the calculations.

The new LBT was reinforced by increasing the diameter of the guide rails from 5/8" to 3/4". Also the old LBT guide rails were only supported from the ends, on the new LBT the guide rails are supported for their entire length. One last measure to avoid exciting vibration in the rails was to replace the bushings used on the old headform/carriage with precision bearings. And to avoid having the carriage/headform collide with the end of the LBT the upgrade was an additional three feet longer than the old one. Figure 21 shows the original design of the new LBT including additional reinforcements on each side of the base plate along its entire length. When the new LBT was constructed and attached to the test frame it proved to be sufficiently rigid and the additional side plates were not installed. During the initial testing the bearing resistance was found to be so low that the carriage still collided with the back of the LBT. To prevent the collision, the LBT was mounted with 3.6 degrees of upward slope (Figure 22). That way instead of a collision at the end of the track where an unknown amount of energy was dissipated, the kinetic energy was simply converted into the potential energy of the elevation change and was readily quantifiable.

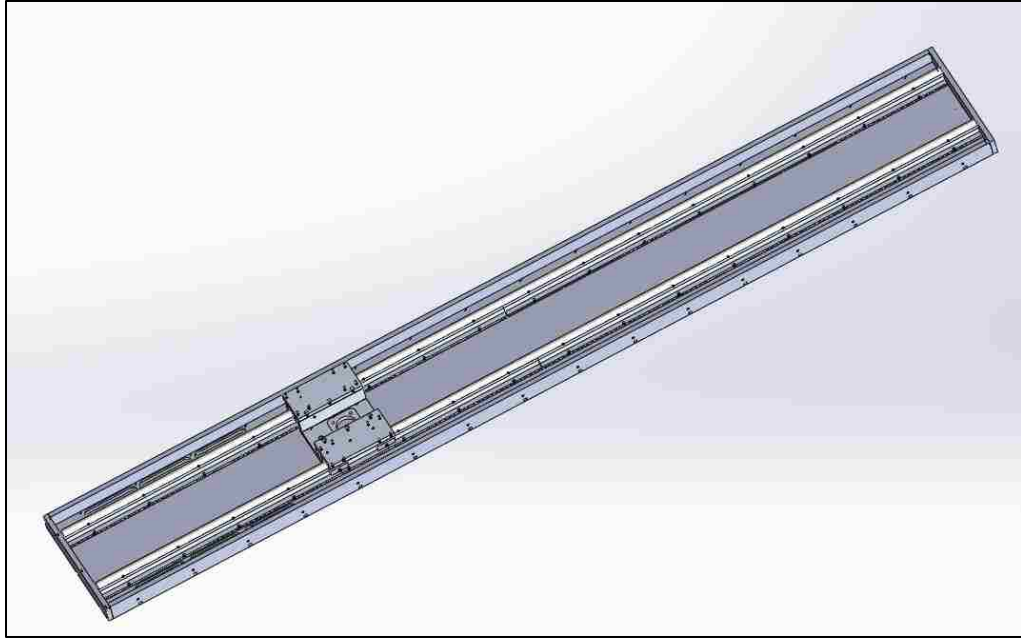


Figure 21: SolidWorks® Model of the Improved LBT

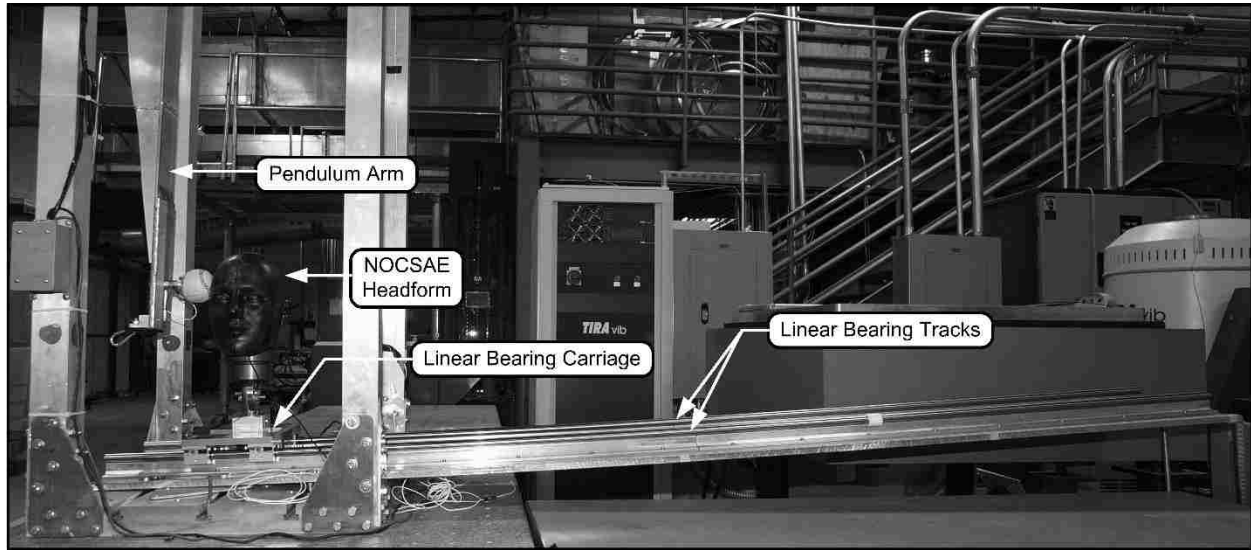


Figure 22: The LBT Mounted to the Test Frame with Headform in Ready Test Position

4.3. Equipment Setup for Baseball Helmet Testing

The equipment setup used in this testing is almost identical to the testing performed by Benn but bears repeating for the sake of clarity. In Figure 23 the Rawlings® S100 Pro Comp Helmet is mounted on the NOCSAE size medium headform. The headform is mounted to the frame with the pedestal mount but this setup is in every other way identical for LBT testing. To left of the headform the pendulum is shown indexed to impact the headform exactly 90 degrees from the horizontal. Mounted at the end of the pendulum with the concave adapter is the Rawlings® Corked/Rubber Pill Yarn Wound Core ball. The ball was within specification with a weight of 141.7 grams and a circumference of 9 inches. In between the ball adapter and the pendulum, the transducers are mounted that measure both ball force and acceleration. Once all of the components are setup and the instrumentation is verified functional and calibrated the helmet is ready to be tested. Then the pendulum is simply raised with the winch to the desired height and once the DAQ is activated it is released triggering on impact the measurements of ball force, ball acceleration, pendulum angle and headform acceleration. Once the impact is over and the test results are verified, the operator simple needs to reposition the helmet, check that the setup is unchanged and repeat as many times as necessary.

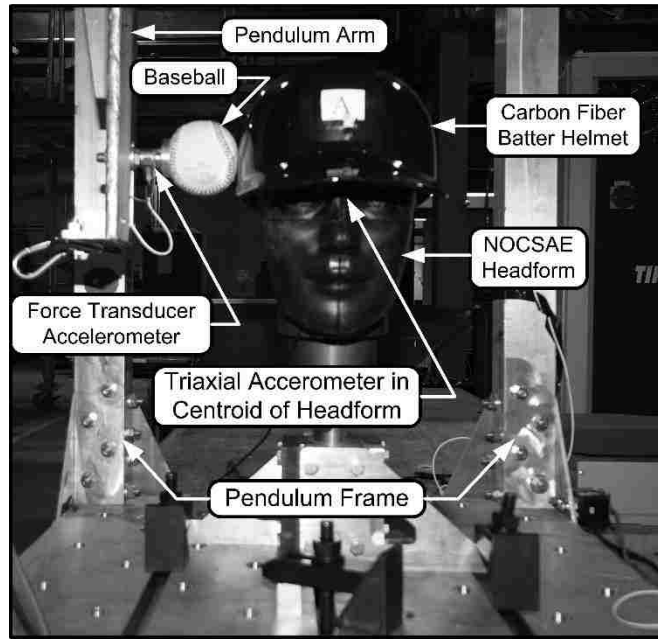


Figure 23: Baseball Helmet Set Up for Right Side Impact Testing

4.4. Adapting the Test to Soccer

The impact test adapted to soccer is actually in almost every way identical to the baseball test. The diameter of the soccer ball is larger so it requires a larger adapter (Figure 24). The Vizari® Club V90 size 5 soccer ball is a regulation for high school soccer and was used to design the adapter and in testing. Because it is an air inflated ball the pressure in the ball must be verified between 9-11 psi and it must be weighed at proper inflation, in this case the ball weighed 0.97 lbs. The soccer ball was mounted to the end of the pendulum with the concave ball mounting adaptor. A force transducer and accelerometer were placed between the ball mounting adaptor and the pendulum arm as before and the headform mounting was moved to the right to accommodate the larger ball diameter. This testing set up with the Gamebreaker® Helmets Soft Padded Soccer Headgear mounted to the headform is shown in Figures 25 for both right side

impact testing. During actual testing the procedure is exactly the same as baseball with one difference. Because the soccer ball is air inflated it responds as an air spring so the rebound height after the impact is significantly higher than in baseball.

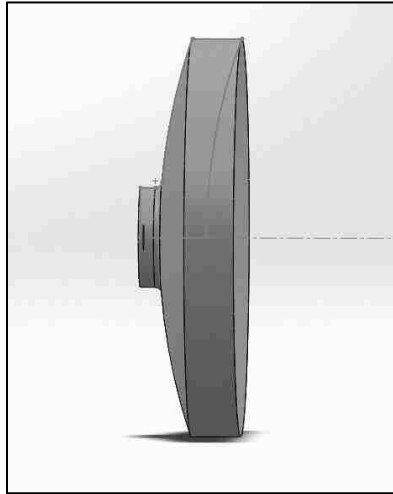


Figure 24: SolidWorks® Soccer Ball Adapter for Pendulum Mounting

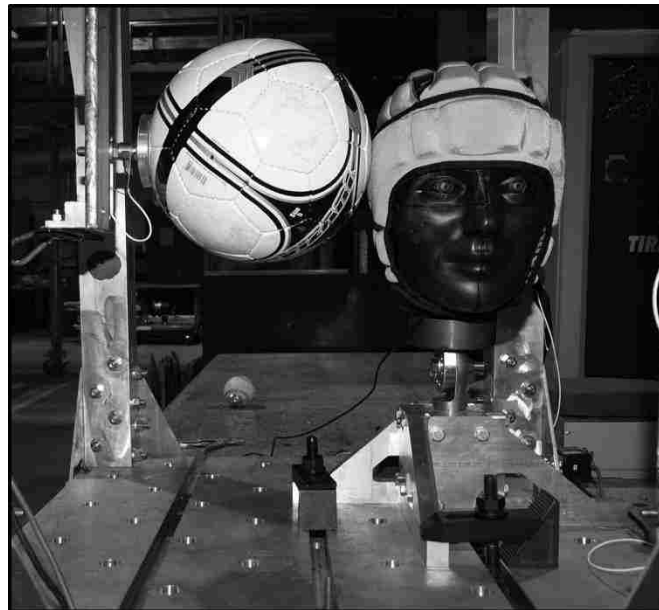


Figure 25: Soccer Soft Helmet Set Up for Adapted NOCSAE Right Side Impact Test

CHAPTER 5 - ANALYSIS OF THE BASEBALL AND SOCCER HELMET IMPACT TESTS

The methods for testing sports helmets has been outlined in the preceding sections and the following analysis was used to interpret the acceleration data. The accelerations will be used to calculate the values according to equations 1-1. The accelerations measured will also be used to find the velocities in these impacts so energy and momentum analysis can be performed. There are two different tests to consider: the LBT impact test and the rigid pedestal impact test. The analysis is going to vary between the tests because in the case of the LBT momentum is conserved in the collision but energy is not conserved, however, for the pedestal test energy is conserved in the collision. In both cases the analysis needs to be related back actual TBI's that result from a ball impacting the head/helmet at some velocity. In the NOCSAE standard they use the air cannon to propel balls at the mandated velocities into the headform. However, when using a pendulum to impact the NOCSAE headform the impacting mass is much larger but the velocities are lower, so instead the conservation of energy is used to calculate equivalent energy of a ball traveling at the mandated velocity. The potential energy PE_p of the pendulum when the pendulum mass is raised to its drop height equals the kinetic energy KE_{ball} of a ball traveling at some velocity. In equation form:

$$PE_p = KE_{ball} \quad (5-1)$$

where:

$$PE_p = m_p g h_{dh} \quad (5-2)$$

$$KE_{ball} = 0.5 m_b v_b^2 \quad (5-3)$$

h_{dh} is the pendulum drop height, m_p (lb/in./s²) is the effective mass of the pendulum at the end of the pendulum arm, $g = 386$ in./s², m_b is the mass of the ball (lb) and v_b (in./s) is the velocity of the ball at the point of impact with the NOCSAE headform. Substituting equations (5-2) and (5-3) into equation (5-1) yields:

$$m_p g h_{dh} = 0.5 m_b v_b^2 \quad (5-4)$$

Equation (5-4) can be rearranged to get:

$$v_b = \sqrt{2 \frac{m_p}{m_b} g h_{dh}} \quad (5-5)$$

v_b is the velocity a ball of mass m_b would have to be traveling to have the same energy as a pendulum of mass m_p at the point of impact with the NOCSAE headform that is associated with the pendulum drop height h_{dh} . In this way the headform can be affected with the same energy as a ball traveling at some prescribed velocity. This is the “effective” velocity that will be used to plot the SI values as well as the plots of energy transfer.

Also, as the energy and momentum analysis is developed, the theoretical velocities at every point in this analysis should be compared to measured velocities. Since the quantity measured in these tests is acceleration, integrating over the acceleration pulse will give measured velocities:

$$v = \int_{t_1}^{t_2} a(t) dt \quad (5-6)$$

where $a(t)$ (in./s²) is the instantaneous acceleration at the point of impact, t_1 (s) is the time the impact begins, and t_2 (s) is the time the measurement ends. And in order to determine the position of the ball during impact the velocity can be integrated again to give the position:

$$x = \int_{t_1}^{t_2} v(t) dt \quad (5-7)$$

where $v(t)$ (in./s) is the instantaneous velocity at the point of impact, t_1 (s) is the time the impact begins, and t_2 (s) is the next incremental time step. The position is measured at the centroid of the ball which is attached to the end of the pendulum so the position is going to trace an arc. However, the position of interest will be during the impact resulting in a small pendulum angle so the small angle approximation can be made and the path of x treated as a straight line.

5.1. LBT Analysis

As mentioned earlier the energy is not conserved during the impact in the LBT test but the momentum is conserved. Therefore, the momentum transfer between the pendulum and the carriage/headform on the LBT can be described as:

$$m_{p1} v_{p1} + m_{c1} v_{c1} = m_{p2} v_{p2} + m_{c2} v_{c2} \quad (5-8)$$

where m_{p1} , v_{p1} , m_{c1} and v_{c1} are the masses and velocities of the pendulum and carriage before the impact and m_{p2} , v_{p2} , m_{c2} and v_{c2} are the masses and velocities after the impact. Before the impact the carriage velocity is zero and after the impact the pendulum velocity is zero so Equation 5-8 can be reduced to:

$$m_p v_p = m_c v_c \quad (5-9)$$

where m_p and v_p are the mass (lb) and velocity (in/s) of the pendulum before the impact and m_c and v_c are the mass (lb) and velocity (in/s) of the carriage/headform after the impact. With

Equation 5-9 the velocity of the carriage after the impact can be found and used to solve for the kinetic energy:

$$KE_{\text{carriage}} = 0.5 m_c v_c^2 \quad (5-10)$$

then solving Equation 5-9 for v_c and substituting in Equation 5-10,

$$KE_{\text{carriage}} = 0.5 \frac{(m_p v_p)^2}{m_c} \quad (5-11).$$

Using the energy balance between the potential energy of the pendulum when it is raised to its drop height and kinetic energy of the pendulum at the time of impact:

$$m_p g h_p = 0.5 m_p v_p^2 \quad (5-12)$$

where h_p is the pendulum drop height (in) and then solving for v_p :

$$v_p = \sqrt{2gh_p} \quad (5-13).$$

Finally, substituting Equation 5-13 into 5-11, the formula for the kinetic energy of the carriage is:

$$KE_{\text{carriage}} = \frac{m_p^2 g h_p}{m_c} \quad (5-14).$$

The carriage velocity and the pendulum velocity can also be measured directly from integrating the pulse of the accelerometers using Equation 5-6. These measured velocities should be used to verify the theoretical velocities of Equations 5-9 and 5-13.

After the impact the carriage and headform travel up the LBT and most of the kinetic energy becomes the potential energy of the elevation change. Some energy will be lost in transfer from kinetic to potential energy as friction:

$$KE_{\text{carriage}} - PE_{\text{carriage}} = E_{\text{friction}} \quad (5-15).$$

Then substituting in Equation 5-14 and the equation for gravitational potential energy:

$$\frac{m_p^2 g h_p}{m_c} - m_c g h_c = E_{\text{friction}} \quad (5-16)$$

where h_c is the change in height (in) of the carriage as it travels along the LBT. If the friction is sufficiently low the kinetic energy should be approximately equal to the potential energy in which case the change in elevation could be used as measure of the energy input into the headform.

5.2. Rigid Pedestal Analysis

Now for the headform mounted to the rigid pedestal the headform is stationary during the impact and the energy is conserved. Since the energy is conserved the development of the equation for the energy transferred into the headform is just a direct application of the energy balance:

$$KE_{p1} + E_{\text{head1}} = KE_{p2} + E_{\text{head2}} \quad (5-17)$$

where KE_{p1} and E_{head1} are the energies in the pendulum head immediately before the impact and KE_{p2} and E_{head2} are the energies immediately after the impact. The kinetic energy of the pendulum before and after the impact is equal to the gravitational potential energy based on the initial drop height of the pendulum and the rebound height of the pendulum after the impact as

described in by Equation 5-12. Also before the impact the energy in the head is zero so canceling E_{head1} and substituting in Equation 5-12 into 5-17:

$$m_p g h_1 - m_p g h_2 = E_{\text{head}} \quad (5-18)$$

where h_1 is the initial drop height (in) of the pendulum and h_2 is the rebound height (in) and the difference in potential energies is the energy E_{head} (lb*in) input into the headform.

In the case of an inflated ball such as the soccer ball used in this testing the energy balance of Equation 5-18 still holds but there is an intermediate step in the impact that should be considered. During the impact the soccer ball essentially behaves as an air spring which using the energy balance is:

$$KE_{p1} + E_{\text{head1}} = PE_{\text{ball2}} + E_{\text{head2}} = KE_{p3} + E_{\text{head3}} \quad (5-19)$$

As before E_{head1} cancels because there is no energy in the headform pre-impact but now as the ball collides with the headform the ball is compressed storing a significant part of KE_{p1} as potential energy. The ball reaches its maximum compression then releases this potential energy PE_{ball2} a majority of which is converted back into the kinetic energy KE_{p3} of the pendulum. The result of this spring effect is that the rebound of the pendulum is much higher than with a solid ball (baseball) and the energy transferred in to the head form E_{head} is much less. The energy balance of Equation 5-18 is still true but the intermediate step in Equation 5-19 should help illustrate why the accelerations measured in the soccer ball tests are of longer duration and lower magnitude than the baseball tests.

Using the analysis outlined in this section the SI values will be calculated using MATLAB plotted for a series of tests using the LBT and the rigid pedestal mount. A sample of the

MATLAB code used to perform these calculations can be seen in Appendix A-4. The SI will then be compared against corresponding plots of the energy transferred into the headform in each test configuration. If the hypothesis that the LBT is an underestimate of the potential for TBI's in helmet impact testing is correct then the SI and energy transfer using the LBT should be significantly lower than when using the rigid pedestal.

5.3. Test's Performed in this Experiment

Fifteen data sets were generated for analysis using the aforementioned testing procedures. First the baseball tests were performed at drop heights of 12, 26, 32 and 45 inches for both the LBT and the rigid pedestal. The LBT was tested with the unprotected headform in the right side impact position to generate a baseline data set for comparison with the rigid pedestal. Then the rigid pedestal was also tested with the unprotected headform in the right side impact position. Next the LBT and rigid pedestal were used to test two different baseball helmets shown in Figure 26 in the right side impact positions. Finally, soccer ball tests were also conducted at drop heights of 15, 25, 35, 45, 55, 65 and 75 inches using the rigid pedestal. The headform was again tested unprotected in the right side impact positions to set a baseline for SI with the soccer ball. Then the Gamebreaker® Helmets Soft Padded Soccer Headgear (Figure 27) and a pad constructed from a material for helmet padding called Lite by D3O® were both tested for soccer ball impact attenuation in the right side impact positions.



Figure 26: (A) Rawlings® S100 Pro Comp Helmet and New Era® isoBLOX® protective pitcher's cap



Figure 27: Gamebreaker® Helmets Soft Padded Soccer Headgear

CHAPTER 6 – RESULTS AND DISCUSSION

The results of these experiments are all from testing performed on the pendulum apparatus and all measurements were made using the same DAQ hardware and software (Brüel & Kjær Pulse). All measurements are reported using the English units of inch-pound-second and the necessary parts were weighed prior to testing (Table 6). These are the weights used in all calculations of energy and momentum.

Table 6: Weights of the Pendulum, Balls and Carriage/Headform Used in These Tests

| Weights Used in Calculation (As Measured on a Digital Scale) | |
|--|------------|
| Baseball | 0.312 (lb) |
| Soccerball | 0.997 (lb) |
| Pendulum (Baseball) | 11.6 (lb) |
| Pendulum (Soccer) | 12.6 (lb) |
| Carriage/Headform | 24.63 (lb) |

6.1. LBT Headform Test Results

The velocities for the LBT tests conducted with the unprotected headform are listed in Table 7. The theoretical values for the pendulum velocities was calculated using the energy balance in equation 5-12. The actual velocities of the pendulum were measured from integrating the acceleration pulses in Figure 28. The theoretical carriage velocities were calculated using the momentum balance equation 5-9. The actual carriage velocities are measured from integrating under the first acceleration pulse in Figure 30. Figure 29 shows the headform acceleration in response to the impact. Then in Figure 31 the SI values are plotted against effective ball velocity

using the first headform acceleration peak (per NOCSAE) to calculate the SI of initial acceleration and the second (negative) peak to calculate any secondary contribution to SI from the deceleration of the headform. The first peak is assumed to be contributing to the coup and the second peak the contrecoup of a biphasic TBI event.

Table 7: Theoretical and Measured Velocities in LBT Tests

| LBT Test Velocities | | | | |
|--|------|-------|-------|-------|
| Drop Height (in) | 12 | 26 | 32 | 45 |
| Theoretical Pendulum Velocity (in/s) | 96.2 | 141.7 | 157.2 | 186.4 |
| Measured Pendulum Velocity (in/s) | 96.0 | 140.6 | 155.4 | 184.9 |
| % Error | 0.21 | 0.78 | 1.14 | 0.80 |
| Equivalent Ball Velocity (mph) | 33.3 | 48.7 | 53.8 | 64.1 |
| Theoretical Carriage Velocity Post-Impact (in/s) | 45.2 | 66.2 | 73.2 | 87.1 |
| Measured Carriage Velocity Post-Impact (in/s) | 43.6 | 62.4 | 68.9 | 80.1 |
| % Error | 3.53 | 5.68 | 5.89 | 8.00 |

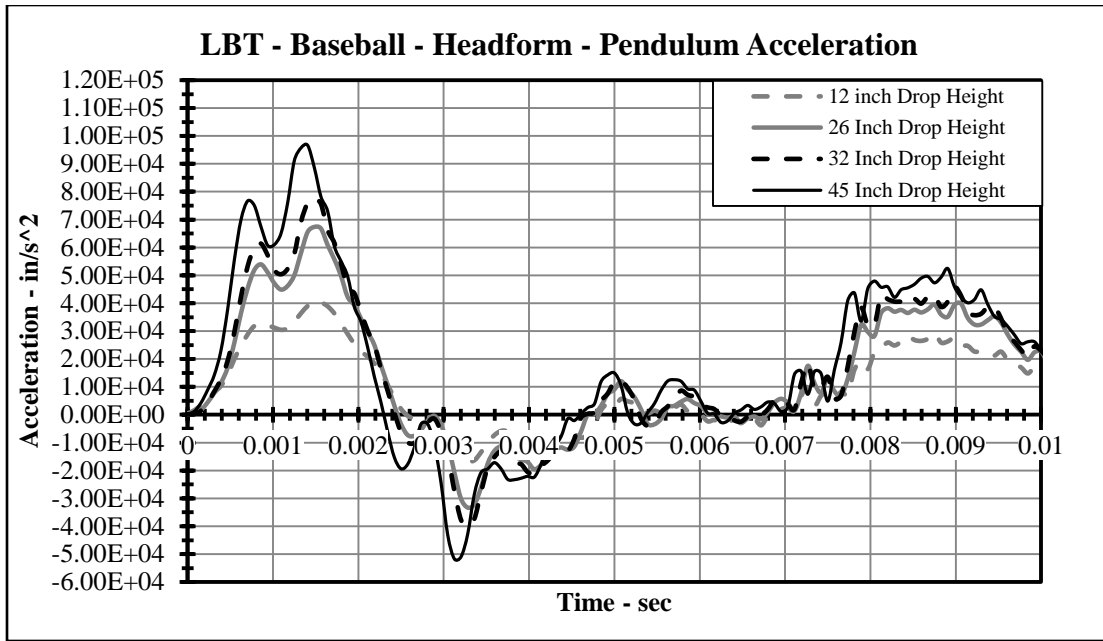


Figure 28: LBT Tests Pendulum Acceleration

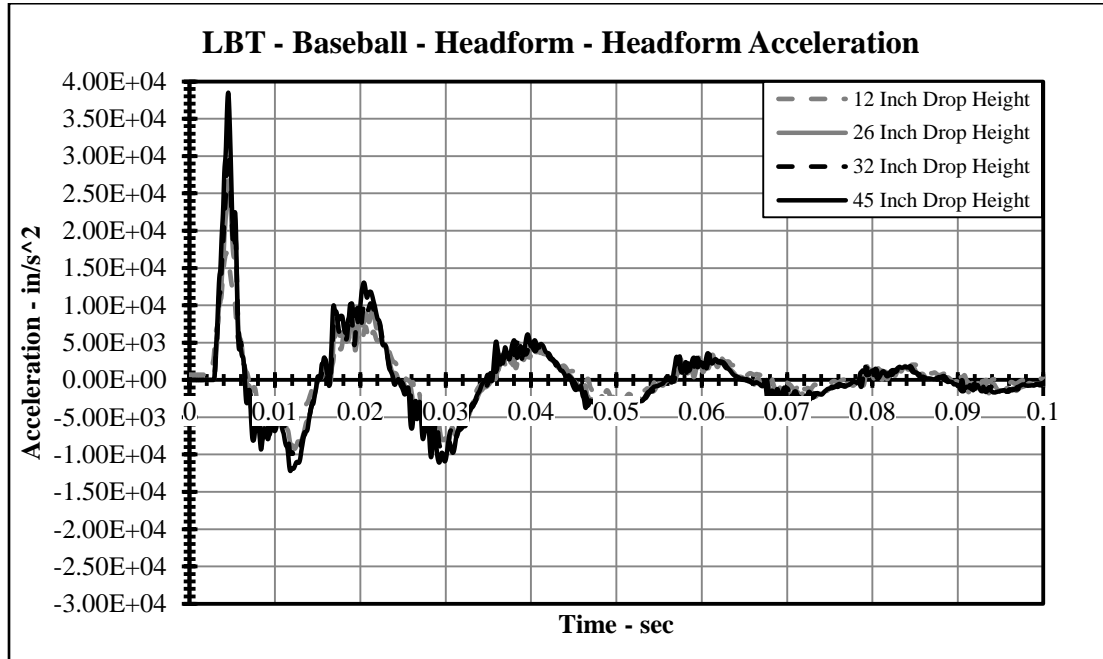


Figure 29: LBT Tests Headform Acceleration after Impact

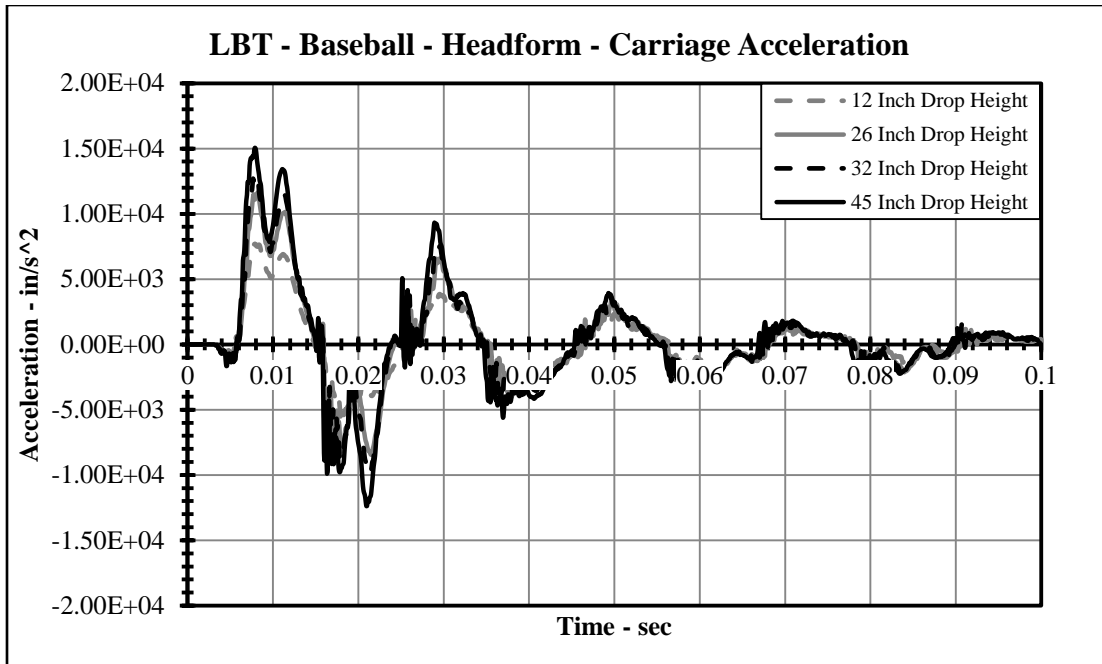


Figure 30: LBT Tests Carriage Acceleration After Impact

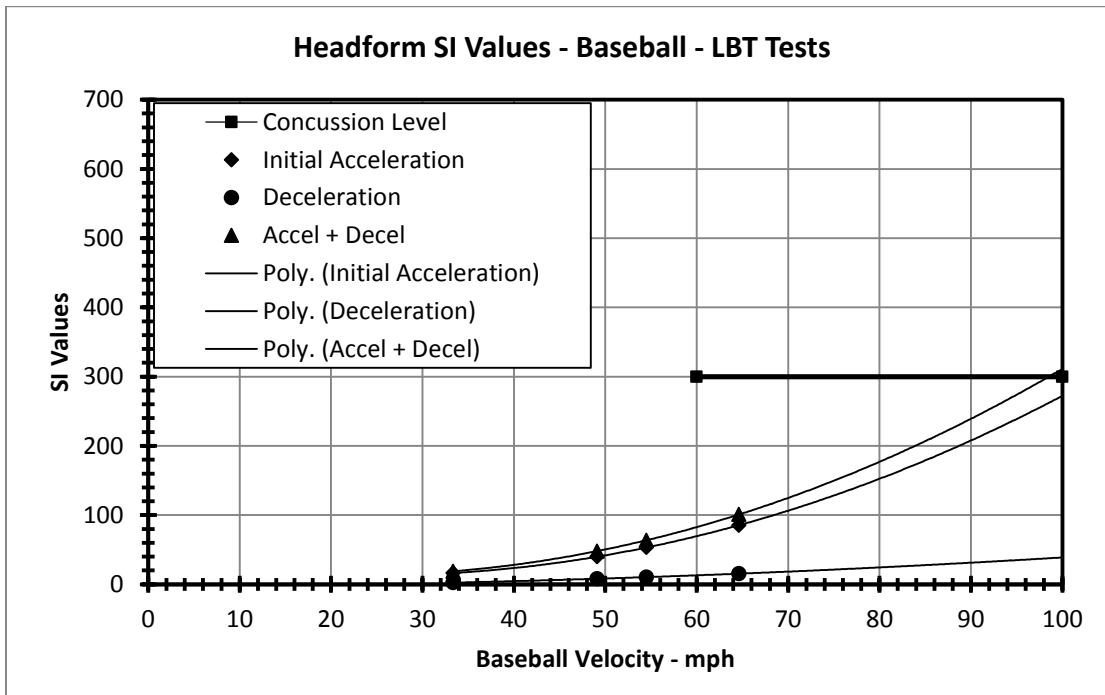


Figure 31: LBT Tests SI Values

6.2. Pedestal Headform Test Results

The velocities for the rigid pedestal tests conducted with the unprotected headform are listed in Table 8. The theoretical value for the pendulum velocity was calculated using the energy balance in equation 5-12. The actual velocities of the pendulum were measured from integrating the acceleration pulses in Figure 33. Figure 33 shows the acceleration headform in response to the impact. Then in Figure 34, the SI values are again plotted against effective ball velocity using the first headform acceleration peak (per NOCSAE) to calculate the SI of initial acceleration and the second (negative) peak to calculate any secondary contribution to SI from the deceleration of the headform.

Table 8: Theoretical and Measured Velocities in Pedestal Tests

| Rigid Pedestal Test Velocities | | | | |
|--------------------------------------|------|-------|-------|-------|
| Drop Height (in) | 12 | 26 | 32 | 45 |
| Theoretical Pendulum Velocity (in/s) | 96.2 | 141.7 | 157.2 | 186.4 |
| Measured Pendulum Velocity (in/s) | 93.1 | 138.7 | 155.2 | 184.0 |
| % Error | 3.28 | 2.10 | 1.27 | 1.28 |
| Equivalent Ball Velocity (mph) | 32.3 | 48.1 | 53.8 | 63.7 |

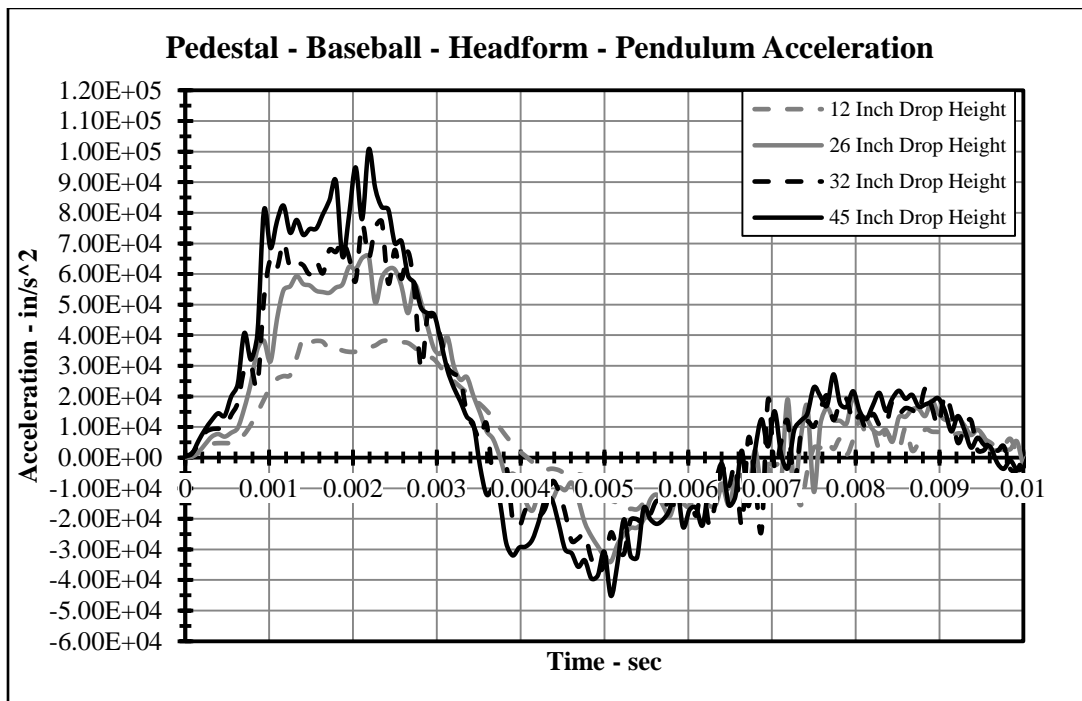


Figure 32: Pedestal Tests Pendulum Acceleration

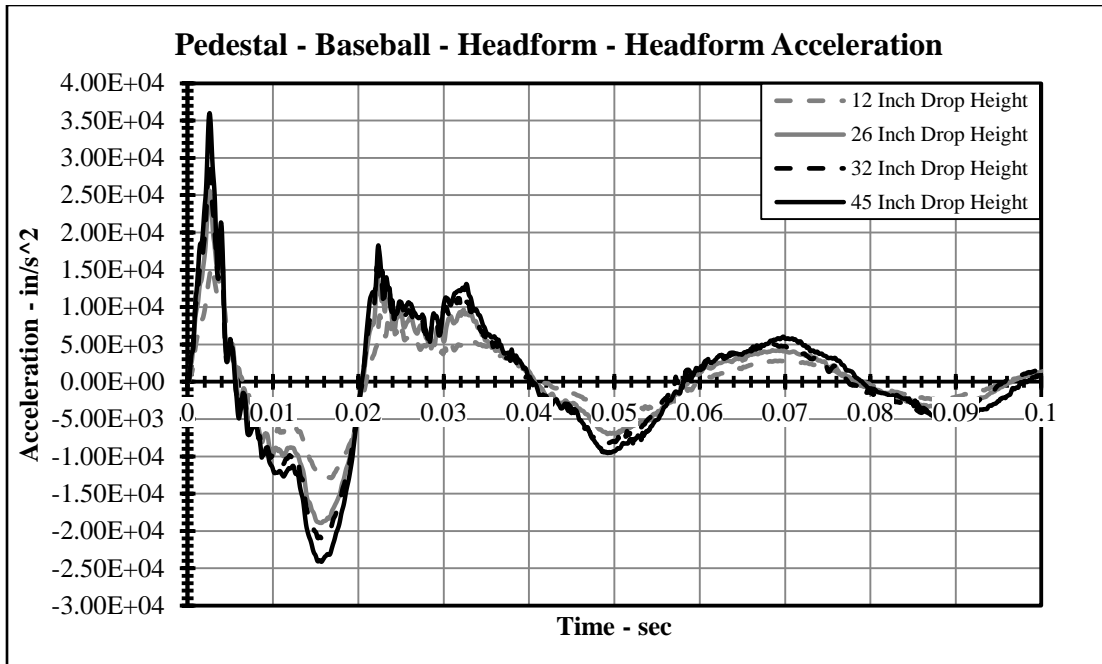


Figure 33: Pedestal Test Headform Accelerations After Impact

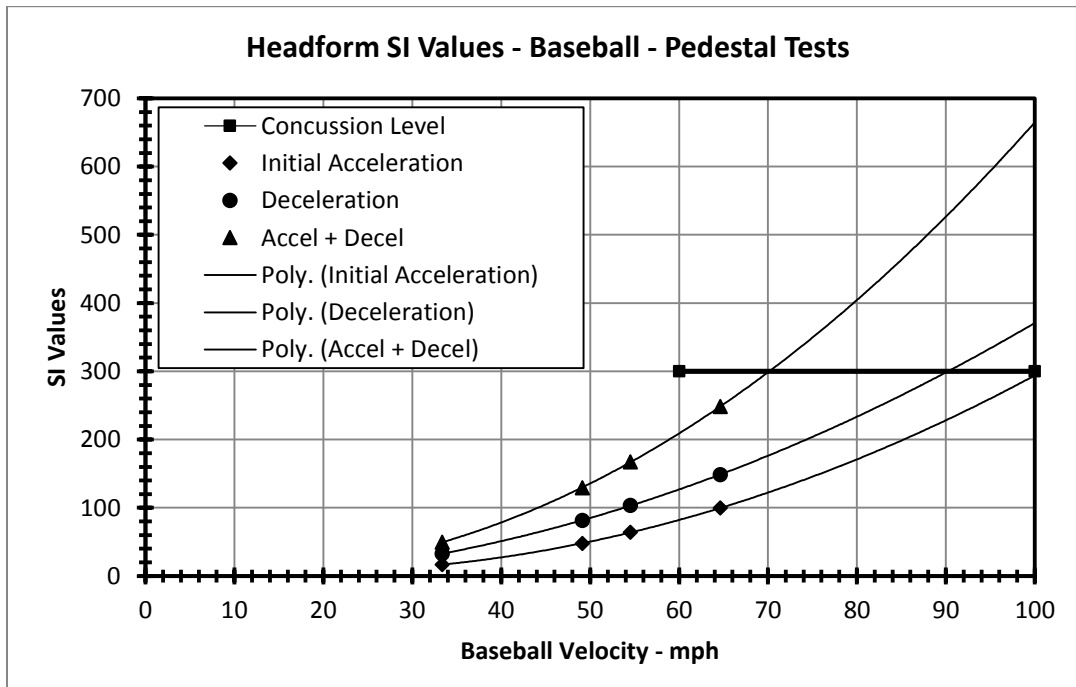


Figure 34: Pedestal Tests SI Values

6.3. LBT and Pedestal Comparison

In Table 9 and Figure 35 the SI values for the LBT and the rigid pedestal test are laid out next to each other and it appears that the pedestal mounting has a significant effect. Consider the SI values measured at the 45 inch drop height:

1. The SI resulting from the initial acceleration is 16% higher with the rigid pedestal.
2. The SI resulting from the deceleration is 8.5 times higher with the rigid pedestal.
3. If the impact is considered biphasic as the literature suggests then the total SI is 2.5 higher with the rigid pedestal.

These results agree with the original measurements made by Darren Benn in 2015 [1]. The accompanying plots of the energy transferred into the headform based on the equations developed in chapter 5 can be seen in Figure 36. The energy transferred into the headform is greater for the pedestal test and in the case of the 45 inch drop height 2 times larger than with the LBT. It seems reasonable that twice the energy input in to the head form could result in an SI 2.5 time greater.

Table 9: SI Values for LBT and Pedestal Tests

| SI Values for LBT and Pedestal Headform Tests | | | | |
|--|-------|-------|-------|---------------|
| Height (in) | 12 | 26 | 32 | 45 |
| Effective Velocity (mph) | 33.4 | 49.1 | 54.5 | 64.6 |
| LBT Pendulum | 178.0 | 515.9 | 692.0 | 1111.5 |
| LBT Headform Initial Acceleration | 16.4 | 39.9 | 53.3 | 85.4 |
| LBT Headform Deceleration | 2.5 | 8.2 | 10.3 | 15.5 |
| LBT Headform Accel + Decel | 18.9 | 48.1 | 63.6 | 100.9 |
| Pedestal Pendulum | 177.4 | 539.2 | 751.6 | 1190.8 |
| Pedestal Headform Initial Acceleration | 16.7 | 47.8 | 64.0 | 99.6 |
| Pedestal Headform Deceleration | 32.9 | 81.3 | 103.4 | 148.6 |
| Pedestal Headform Accel + Decel | 49.6 | 129.2 | 167.4 | 248.2 |

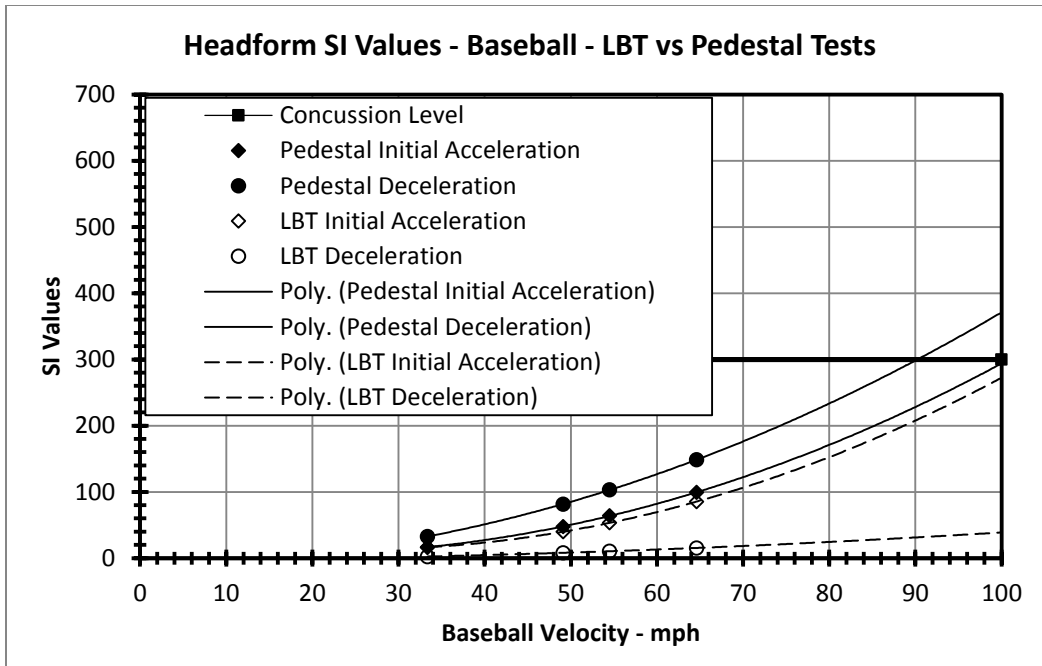


Figure 35: Comparison of SI from the Initial Acceleration and the Deceleration in LBT and Pedestal Tests

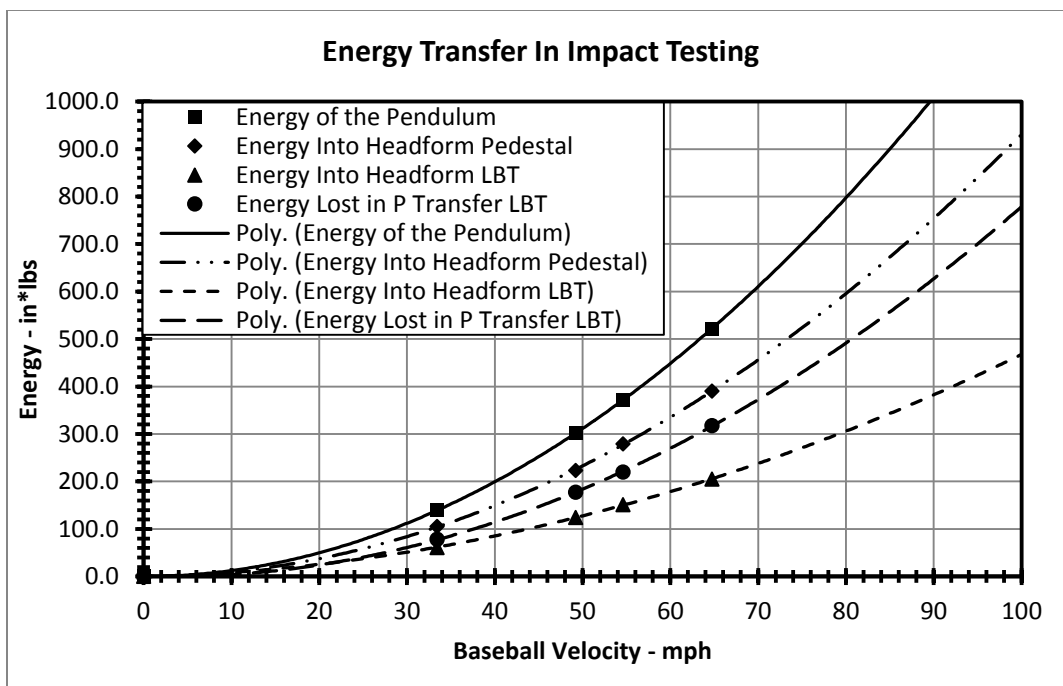


Figure 36: Impact Energy Transferred into the Headform During LBT and Pedestal Testing.

The results of the SI and the energy analysis would seem to validate the original hypothesis that the LBT is an under estimate of the injury potential when the deceleration is included in the measurement. When the headform acceleration response to a 45 inch drop for LBT and rigid pedestal are compared directly (Figure 37) the large contribution of the deceleration is apparent.

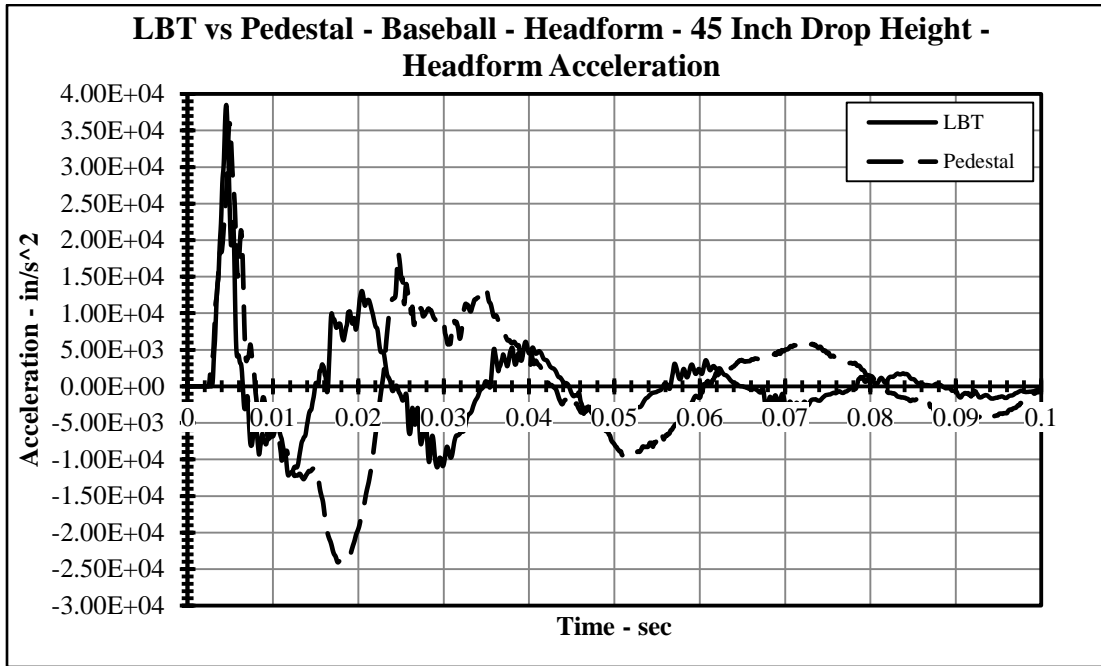


Figure 37: Response of the Headform to LBT and Pedestal Tests

The initial acceleration pulse (the first/highest positive impulse as defined by NOCSAE) of the LBT and the pedestal test are close in peak magnitude. However, the pedestal deceleration pulse peaks much higher and has twice the duration of the LBT. The SI values for both the acceleration and the deceleration in all experiments to date were calculated considering the entire first and second impulses. This seemed a reasonable assumption but on closer consideration of the biphasic TBI event as described in the literature additional velocity and displacement analysis was performed (Figure 38-39).

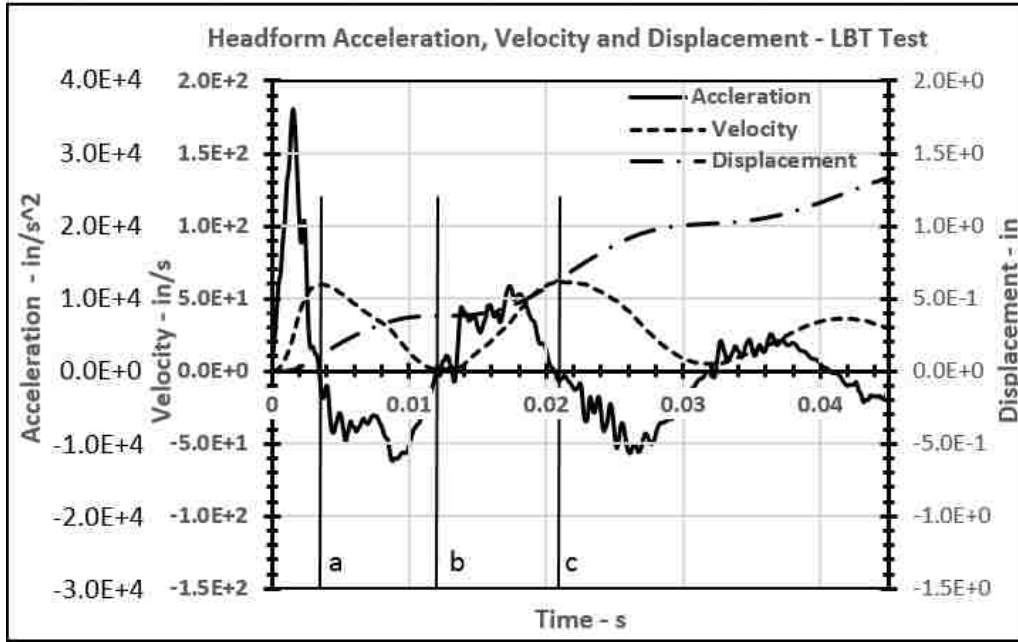


Figure 38: LBT Headform Response from Times: 0 to a) Initial Acceleration (TBI Phase 1), Velocity Peaks. a to b) Deceleration (TBI Phase 2), Velocity Approaches Zero. b to c) Velocity and Displacement Increase. Carriage/Headform Travels Up the LBT.

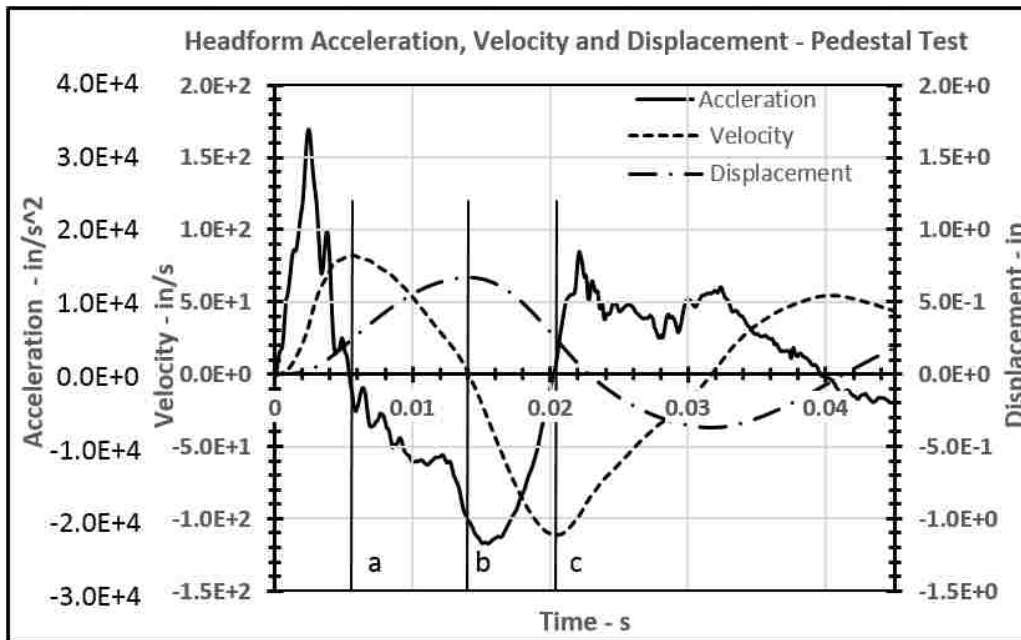


Figure 39: Pedestal Headform Response from Times: 0 to a) Initial Acceleration (TBI Phase 1), Velocity Peaks, a to b) Deceleration (TBI Phase 2), Velocity Goes to Zero, Max Displacement Before Rebound. b to c) Velocity Changes Direction and Increases, Displacement Goes to Zero (TBI Phase 2 if Rebound is Considered in SI/HIC Calculation).

In the responses for both the LBT and the pedestal test from time zero to the end of the initial acceleration (a) the velocity of the headform reaches its maximum as the positive acceleration goes to zero, as one would expect. This response should correspond to the first half of the TBI event, the coup. The second half of the TBI event (contrecoup) should result from the deceleration of the head resulting in a cranial velocity that approaches zero and a collision of the brain still in motion with the back of the skull. In the case of the LBT this happens as the deceleration pulse and the resulting velocity from time b to c approach 0 and the displacement reaches a local maximum. This was assumed to be the case when SI was calculated for contrecoup and in the case of the LBT is a valid assumption. However, by calculating the contrecoup SI for the pedestal test over the entire deceleration pulse (from time a to c) without considering the velocity or displacement, the SI was inadvertently calculated much higher than it should have been by considering acceleration after the velocity had returned to zero and the headform had reach maximum displacement. The reason the deceleration pulse was so much larger and longer in the case of the pedestal test was a result of the rigid mounting behaving as a spring. The negative acceleration persisted after the headform had reached its maximum displacement because this “spring” unloaded as is returned to its initial position. Mechanically it is reasonable for the system to behave this way but it is not representative of an actual human response to this kind of impact. So in the case of the pedestal tests the SI was recalculated (Table 10, Figure 40) over the acceleration from time a to b because even though the deceleration was not zero, the velocity was zero and the displacement there was maximum which should more closely represent the contrecoup.

Table 10: Corrected SI Values for LBT and Pedestal Tests

| Corrected Values of SI for LBT and Pedestal Headform Tests | | | | |
|--|-------|-------|-------|---------------|
| Height (in) | 12 | 26 | 32 | 45 |
| Effective Velocity (mph) | 33.4 | 49.1 | 54.5 | 64.6 |
| LBT Pendulum | 178.0 | 515.9 | 692.0 | 1111.5 |
| LBT Headform Initial Acceleration | 16.4 | 39.9 | 53.3 | 85.4 |
| LBT Headform Deceleration | 2.5 | 8.2 | 10.3 | 15.5 |
| LBT Headform Accel + Decel | 18.9 | 48.1 | 63.6 | 100.9 |
| Pedestal Pendulum | 177.4 | 539.2 | 751.6 | 1190.8 |
| Pedestal Headform Initial Acceleration | 16.7 | 47.8 | 64.0 | 99.6 |
| Pedestal Headform Deceleration | 8.7 | 18.8 | 24.2 | 35.2 |
| Pedestal Headform Accel + Decel | 24.8 | 61.9 | 81.8 | 126.9 |

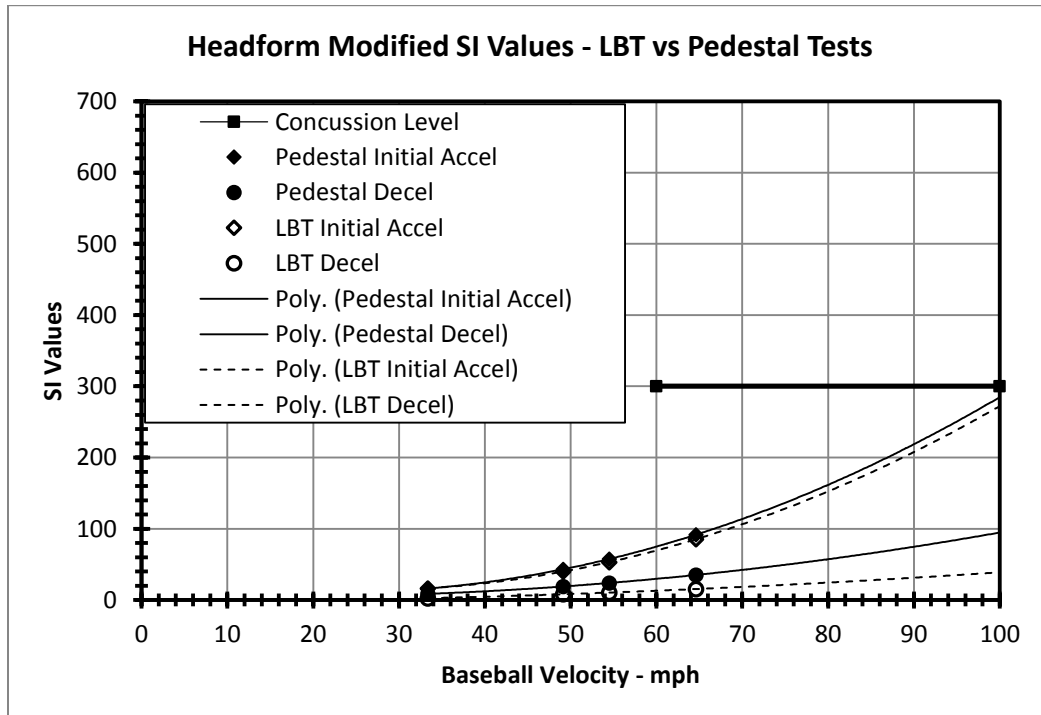


Figure 40: Comparison of Corrected SI from the Initial Acceleration and the Deceleration in LBT and Pedestal Tests

If the corrected SI is assumed to a more reasonable measure of injury potential in the case of the rigid pedestal test, then the SI no longer appears to correlate with the energy input into the head presented in figure 36. If the SI is taking to be correct then the problem must lie in a fundamental assumption made while developing the energy analysis. The assumption in pedestal testing was that energy was conserved in the collision and there was approximately perfect energy transfer from the pendulum to the headform. In reality the energy transfer is likely not close enough too ideal to reasonably make that assumption and a significant portion of that energy is being lost to deformation of the baseball, energy transfer to the test frame and frictional losses. One possible solution considered was to calculate the work done on the headform by multiplying the average force exerted on the headform measured by the load cell over the time from 0 to the time when the headform displacement was maximum as integrated from the accelerometer. The equation then would take the form:

$$W = F_{average}d \quad (6-1)$$

where W is the work done on the headform, F is the average force exerted on the headform over the displacement d . Using equation (6-1) the energy (work) was recalculated using the force measurements (Figure 41). The work input in to the headform was less than when using the energy balance between the drop and rebound heights, in particular the 45 inch drop height was shifted down by 140 in*lbs. The new value for work/energy input to the headform at 45 inches was 25% higher than the energy input during the LBT test which would correlate with the corrected SI for the pedestal test which was also approximately 25% higher than the LBT. However, no substantial claim about the correlation between energy and SI can be made at this time because these force

measurements are extremely short, highly transient and need further investigation to justify this type of analysis.

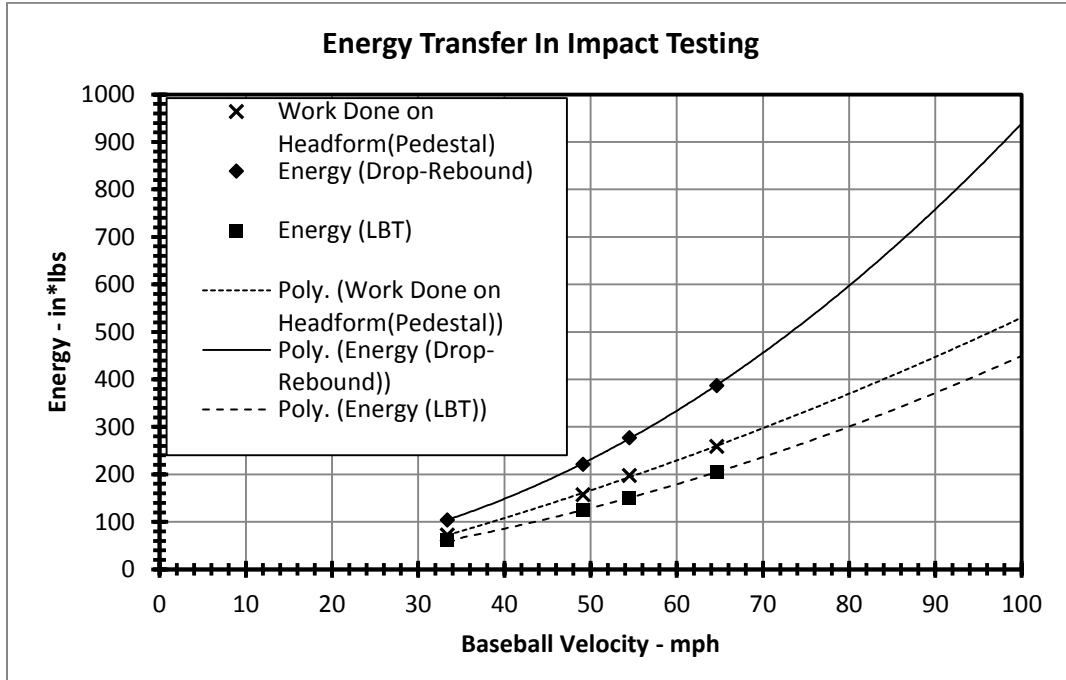


Figure 41: Work done on the headform using force measurement versus Drop-Rebound energy balance and LBT Energy.

6.4. Baseball Helmet Results

Helmet A and the pitcher hat were tested using both the LBT and the rigid pedestal to compare the SI values. In all tests the coup and the contrecoup SI were considered separately and then as combined value to evaluate the contribution of the contrecoup which is neglected in the current standards.

6.4.1. Pedestal Tests

The headform was tested at 4 different drop heights to establish the baseline for unprotected impacts. Then Helmet A and the pitcher hat were tested at the 4 drop height (12 inches to 45 inches). Velocities for each drop height were calculated and compared against the measured values in Table 11. The plots of the pendulum acceleration and the headform acceleration for the 45 inch drop height (Figures 42-43) showed attenuation of the peak values and an increase in the duration of the impacts when the protective headgear was used. This trend is also reflected in the SI values, (Table 12 and Figures 44-46), where the addition of Helmet A provided some protection and the pitcher hat showed even greater attenuation of these kinds of impacts. The plots of the pendulum accelerations and the headform responses for drop heights 12-32 inches are shown in Appendix A-1.

Table 11: Baseball Pedestal Test Velocities

| Rigid Pedestal Baseball Test Velocities | | | | |
|--|------|-------|-------|-------|
| Drop Height (in) | 12 | 26 | 32 | 45 |
| Theoretical Pendulum Velocity (in/s) | 96.2 | 141.7 | 157.2 | 186.4 |
| Headform Measured Pendulum Velocity (in/s) | 93.1 | 138.7 | 155.2 | 184.0 |
| % Error | 3.28 | 2.10 | 1.27 | 1.28 |
| Equivalent Ball Velocity (mph) | 32.3 | 48.1 | 53.8 | 63.7 |
| Helmet A Measured Pendulum Velocity (in/s) | 92.2 | 136.3 | 154.1 | 180.9 |
| % Error | 4.21 | 3.80 | 1.95 | 2.93 |
| Equivalent Ball Velocity (mph) | 31.9 | 47.2 | 53.4 | 62.7 |
| Pitcher Hat Measured Pendulum Velocity (in/s) | 92.7 | 138.4 | 154.0 | 183.8 |
| % Error | 3.72 | 2.32 | 2.01 | 1.41 |
| Equivalent Ball Velocity (mph) | 32.1 | 47.9 | 53.4 | 63.7 |

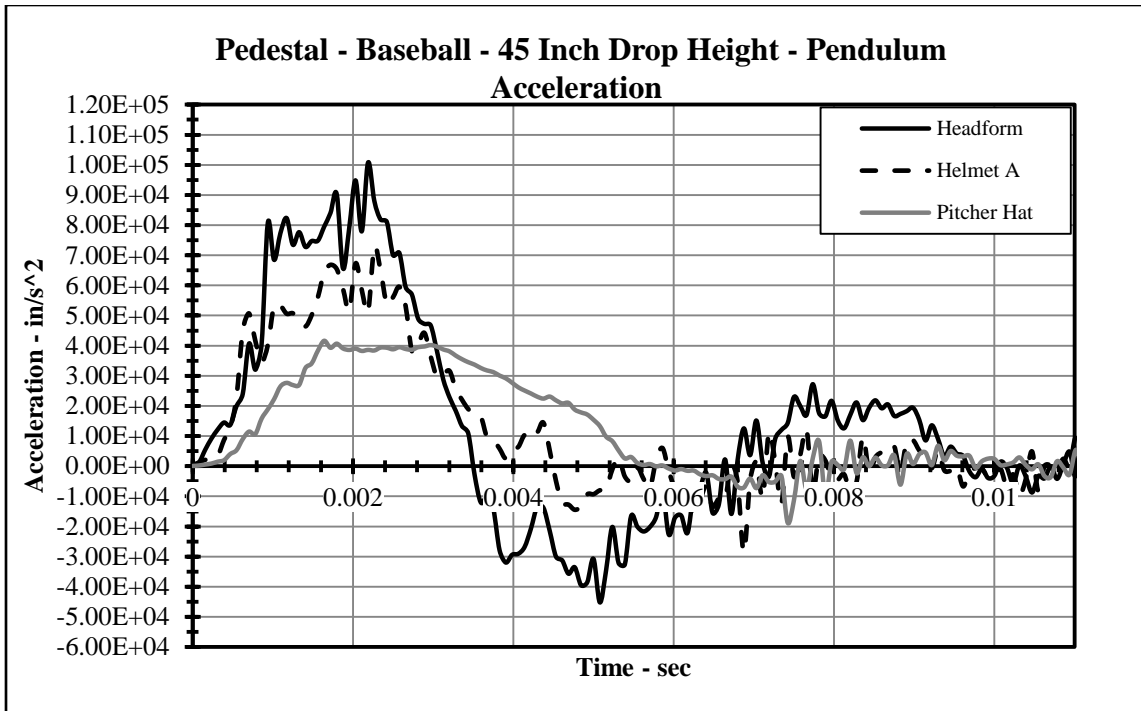


Figure 42: Rigid pedestal baseball helmet testing, 45 inch drop height, pendulum acceleration.

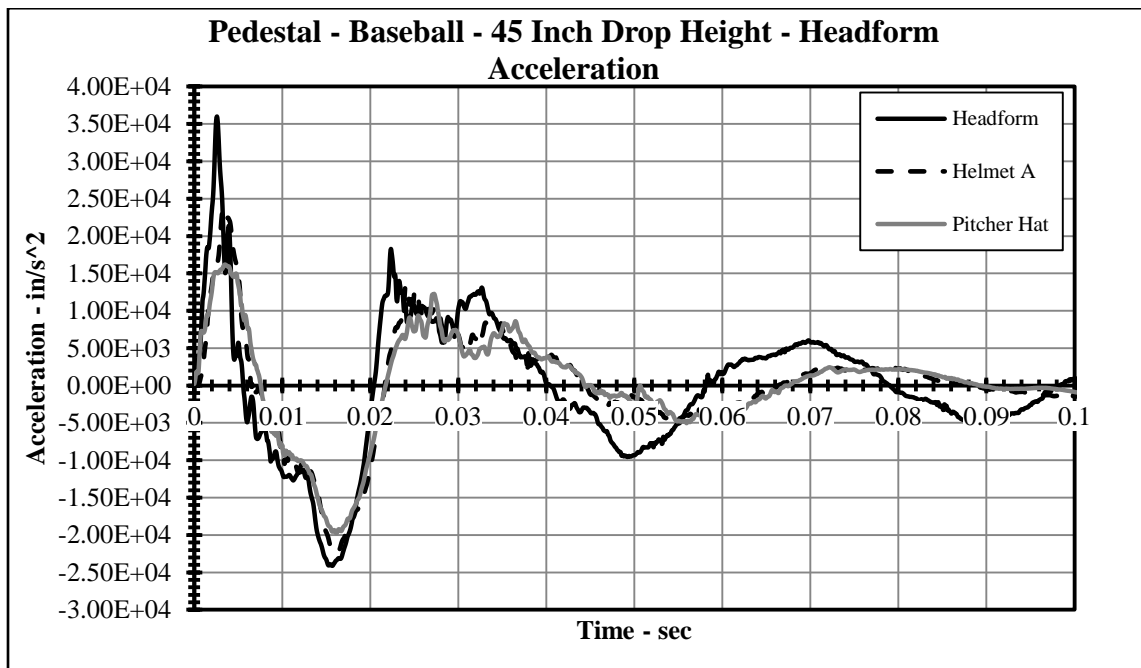


Figure 43: Rigid pedestal baseball helmet testing, 45 inch drop height, headform acceleration.

Table 12: Rigid pedestal baseball helmet tests SI values.

| Values of SI for Pedestal Baseball Helmet Tests | | | | |
|---|-------|-------|-------|---------------|
| Height (in) | 12 | 26 | 32 | 45 |
| Effective Velocity (mph) | 33.4 | 49.1 | 54.5 | 64.6 |
| Pedestal Pendulum | 177.4 | 539.2 | 751.6 | 1190.8 |
| Pedestal Headform Initial Acceleration | 16.7 | 47.8 | 64.0 | 99.6 |
| Pedestal Headform Deceleration | 8.7 | 18.8 | 24.2 | 35.2 |
| Pedestal Headform Accel + Decel | 24.8 | 61.9 | 81.8 | 126.9 |
| Pedestal Pendulum | 84.1 | 267.4 | 346.8 | 573.3 |
| Pedestal Helmet A Initial Acceleration | 9.5 | 24.6 | 32.2 | 51.9 |
| Pedestal Helmet A Deceleration | 7.7 | 17.2 | 21.8 | 31.8 |
| Pedestal Helmet A Accel + Decel | 17.2 | 41.8 | 54.0 | 83.7 |
| Pedestal Pendulum | 46.2 | 129.9 | 170.9 | 264.2 |
| Pedestal Pitcher Hat Initial Acceleration | 5.6 | 15.1 | 20.0 | 29.4 |
| Pedestal Pitcher Hat Deceleration | 6.3 | 15.2 | 19.5 | 27.7 |
| Pedestal Pitcher Hat Accel + Decel | 11.9 | 30.3 | 39.5 | 57.1 |

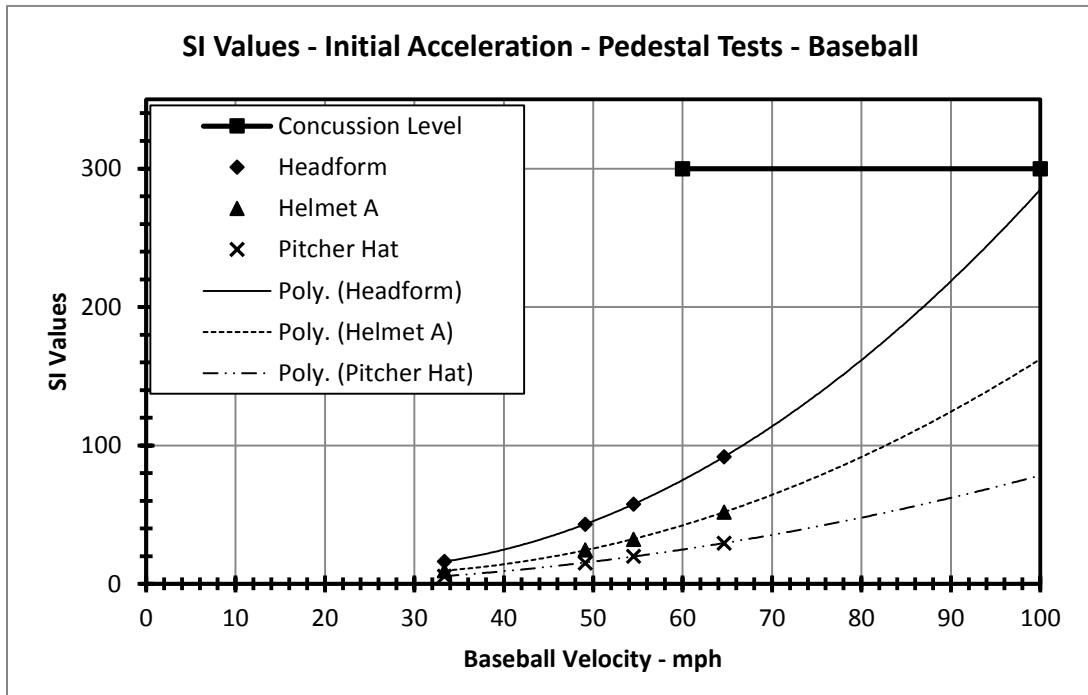


Figure 44: SI values for baseball pedestal helmet testing, initial acceleration.

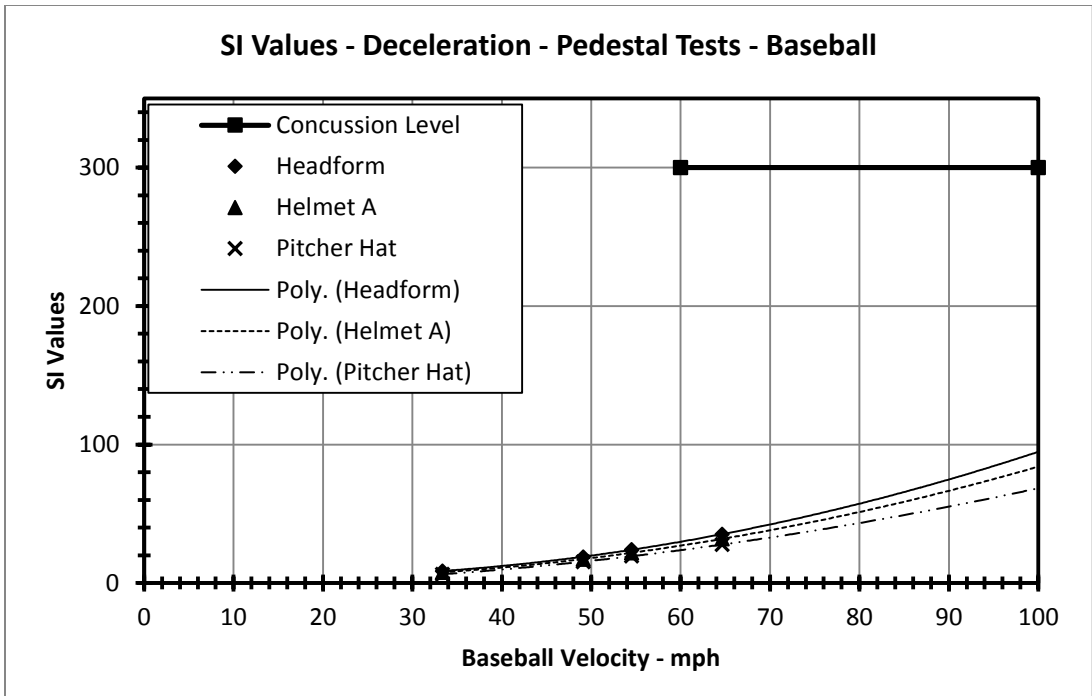


Figure 45: SI values for baseball pedestal helmet testing, deceleration.

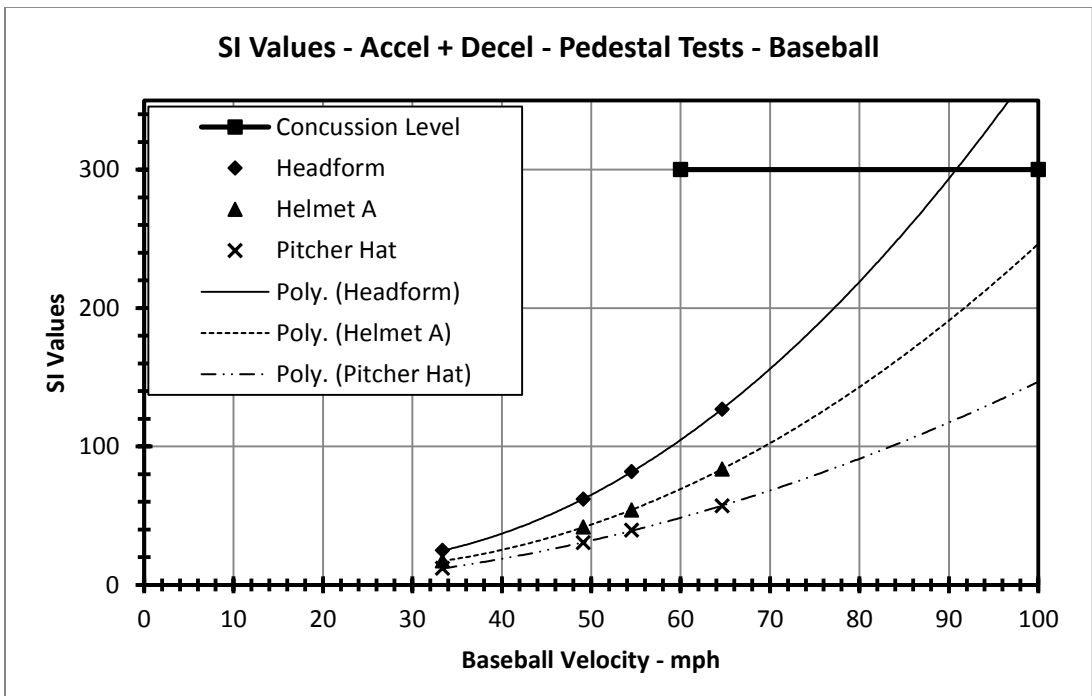


Figure 46: SI values for baseball pedestal helmet testing, acceleration and deceleration combined.

6.4.2. LBT Tests

The headform was again tested at 4 different drop heights to establish the baseline for unprotected impacts. Then Helmet A and the pitcher hat were tested at the 4 drop height (12 inches to 45 inches). Velocities for each drop height were calculated and compared against the measured values in Table 13. The plots of the pendulum acceleration and the headform acceleration for the 45 inch drop height (Figures 47-48) showed attenuation of the peak values and an increase in the duration of the impacts when the protective headgear was used. This trend is also reflected in the SI values, (Table 13 and Figures 49-51), where the addition of Helmet A provided some protection and the pitcher hat showed even greater attenuation of these kinds of impacts. The plots of the pendulum accelerations and the headform responses for drop heights 12-32 inches are shown in Appendix A-2.

Table 13: Baseball LBT test velocities.

| LBT Baseball Test Velocities | | | | |
|---|-----------|-----------|-----------|-----------|
| Drop Height (in) | 12 | 26 | 32 | 45 |
| Theoretical Pendulum Velocity (in/s) | 96.2 | 141.7 | 157.2 | 186.4 |
| Headform Measured Pendulum Velocity (in/s) | 94.8 | 140.6 | 155.4 | 184.9 |
| % Error | 1.46 | 0.76 | 1.13 | 0.78 |
| Equivalent Ball Velocity (mph) | 32.9 | 48.7 | 53.8 | 64.1 |
| Helmet A Measured Pendulum Velocity (in/s) | 95.9 | 141.1 | 156.2 | 185.9 |
| % Error | 0.40 | 0.41 | 0.60 | 0.25 |
| Equivalent Ball Velocity (mph) | 33.2 | 48.9 | 54.1 | 64.4 |
| Pitcher Hat Measured Pendulum Velocity (in/s) | 95.7 | 140.6 | 155.3 | 180.1 |
| % Error | 0.61 | 0.79 | 1.18 | 3.37 |
| Equivalent Ball Velocity (mph) | 33.1 | 48.7 | 53.8 | 62.4 |

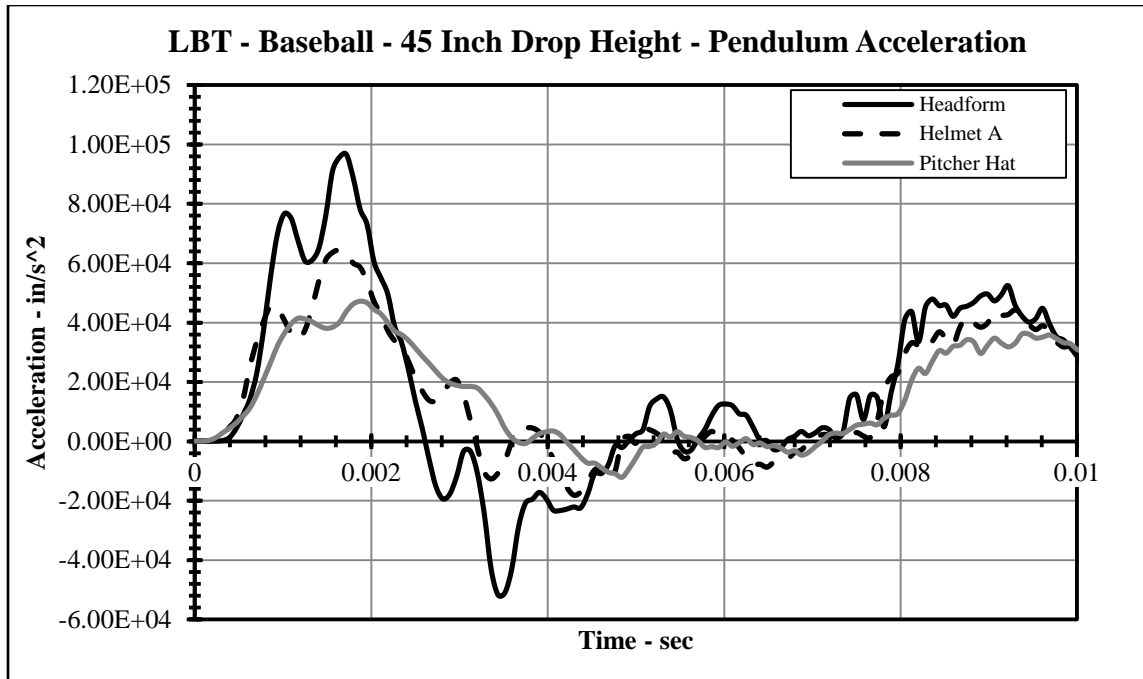


Figure 47: LBT baseball helmet testing, 45 inch drop height, pendulum acceleration.

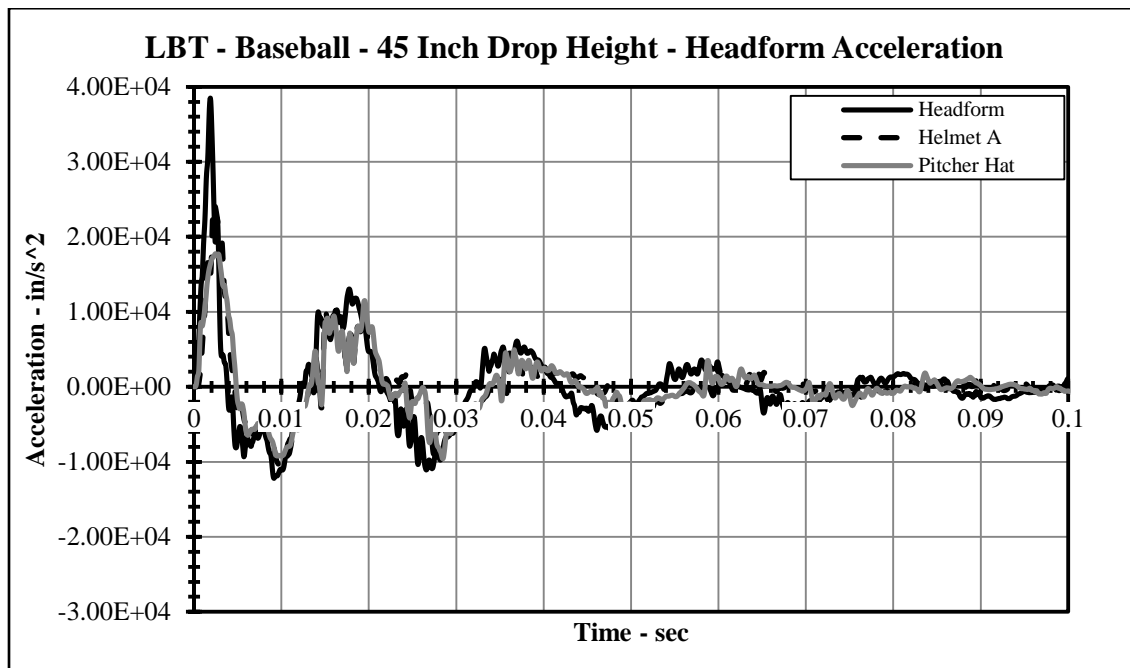


Figure 48: LBT baseball helmet testing, 45 inch drop height, headform acceleration.

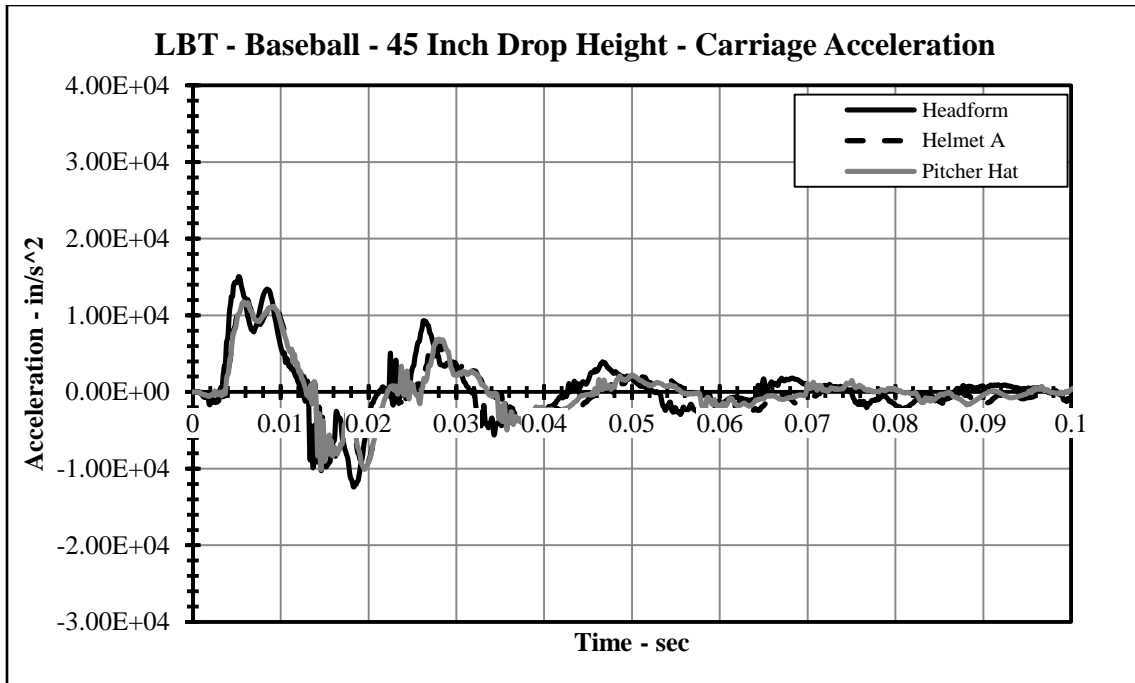


Figure 49: LBT baseball helmet testing, 45 inch drop height, carriage acceleration.

Table 14: LBT baseball helmet tests SI values.

| Values of SI for Pedestal Baseball Helmet Tests | | | | |
|---|-------|-------|-------|---------------|
| Height (in) | 12 | 26 | 32 | 45 |
| Effective Velocity (mph) | 33.4 | 49.1 | 54.5 | 64.6 |
| Pedestal Pendulum | 177.1 | 515.9 | 692.0 | 1111.5 |
| Pedestal Headform Initial Acceleration | 16.4 | 39.9 | 53.3 | 85.4 |
| Pedestal Headform Deceleration | 2.5 | 8.2 | 10.3 | 15.5 |
| Pedestal Headform Accel + Decel | 18.9 | 48.1 | 63.6 | 100.9 |
| Pedestal Pendulum | 94.2 | 273.4 | 359.3 | 548.2 |
| Pedestal Helmet A Initial Acceleration | 8.4 | 22.4 | 28.7 | 43.6 |
| Pedestal Helmet A Deceleration | 2.1 | 5.1 | 6.7 | 10.2 |
| Pedestal Helmet A Accel + Decel | 10.5 | 27.5 | 35.4 | 53.8 |
| Pedestal Pendulum | 76.3 | 195.7 | 251.1 | 366.5 |
| Pedestal Pitcher Hat Initial Acceleration | 5.9 | 15.1 | 19.8 | 29.3 |
| Pedestal Pitcher Hat Deceleration | 2.0 | 4.6 | 6.0 | 8.8 |
| Pedestal Pitcher Hat Accel + Decel | 8.0 | 19.7 | 25.7 | 38.2 |

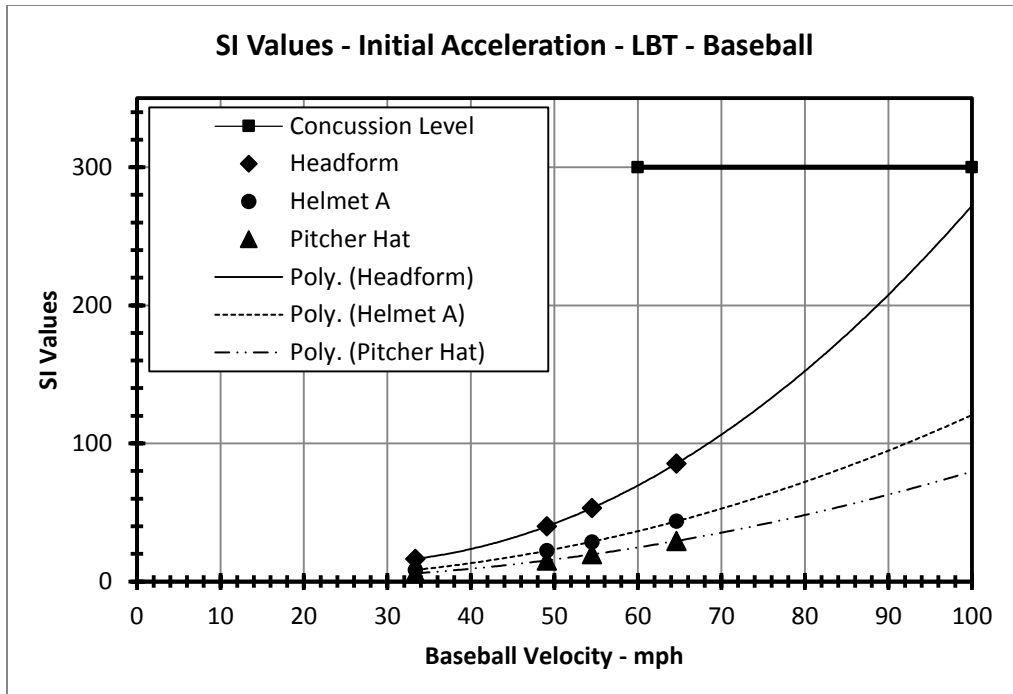


Figure 50: SI values for baseball LBT helmet testing, initial acceleration.

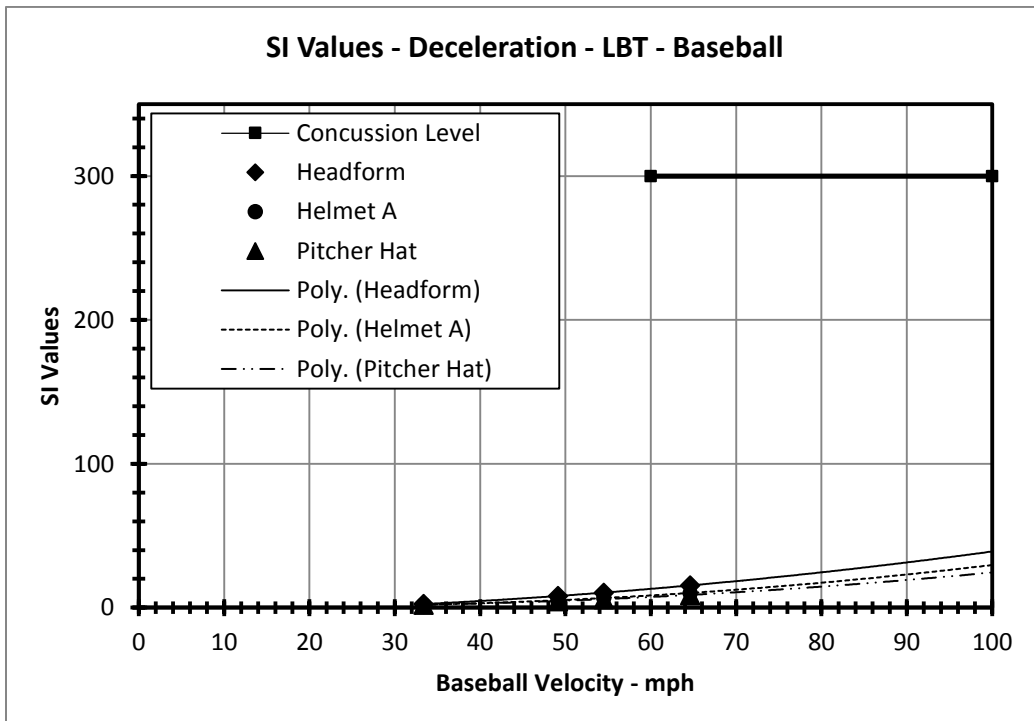


Figure 51: SI values for baseball LBT helmet testing, initial deceleration.

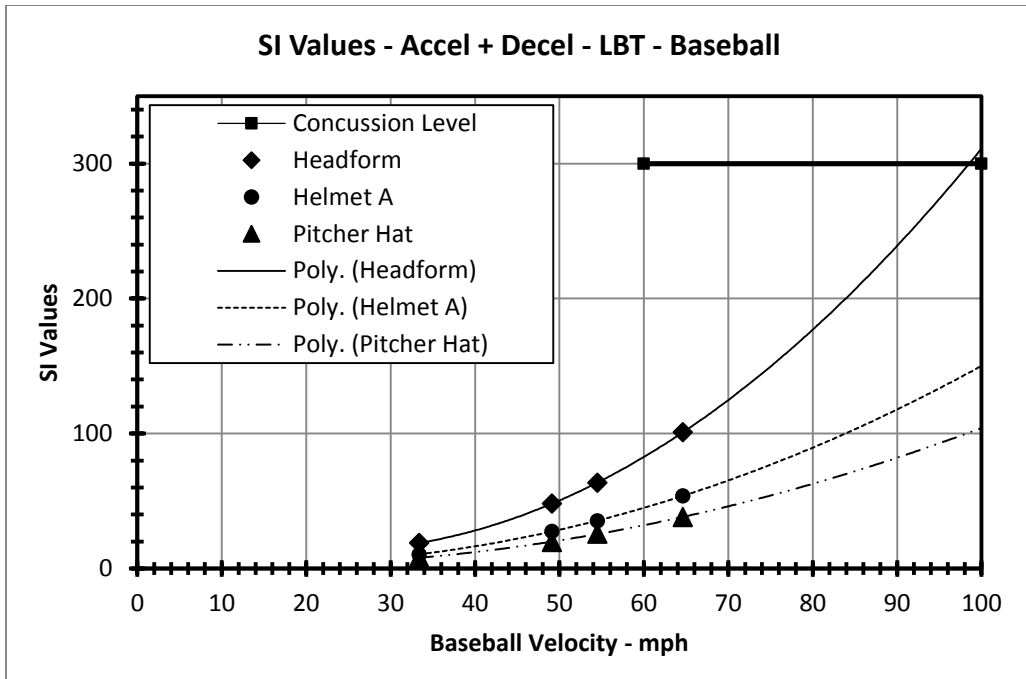


Figure 52: SI values for baseball LBT helmet testing, acceleration and deceleration combined.

6.4.3. SI Comparisons between LBT and Pedestal Helmet Tests

When the SI values from the rigid pedestal helmet testing is compared against the LBT (Table 15), in all cases there is an increase in measured SI with the pedestal. The SI from the initial acceleration pulse shows only a modest increase in SI peaking at 16% increase in the case of Helmet A. This could be meaningful if the helmet being tested is at the threshold of a pass/fail like that mandated by NOCSAE. The more interesting result is the SI values measured from the deceleration part of the response that is believed to be representative of the contrecoup that is neglected in the current standard. This SI is twice as high when the pedestal test is used and peaks at 68% higher than the LBT in the case of the pitcher hat. If the impact is indeed treated as a biphasic TBI event than the helmets tested as much as 20-35% higher for total SI value using the rigid pedestal. Even if only the LBT is considered which is the current standard method for

testing helmets, neglecting the deceleration (contrecoup) part of the event could still result in an underestimate of the SI by 25%.

Table 15: SI Comparison of Baseball Helmet Tests

| SI Comparison of Pedestal and LBT Baseball Helmet Tests at 45 inches | | | |
|---|-------|----------|-------------|
| | LBT | Pedestal | %diff |
| Headform Initial Acceleration | 85.4 | 99.6 | 14.3 |
| Headform Deceleration | 15.5 | 35.2 | 56.0 |
| Headform Accel + Decel | 100.9 | 126.9 | 20.5 |
| | | | |
| Helmet A Initial Acceleration | 43.6 | 51.9 | 16.0 |
| Helmet A Deceleration | 10.2 | 31.8 | 67.9 |
| Helmet A Accel + Decel | 53.8 | 83.7 | 35.7 |
| | | | |
| Pitcher Hat Initial Acceleration | 29.3 | 29.4 | 0.3 |
| Pitcher Hat Deceleration | 8.8 | 27.7 | 68.2 |
| Pitcher Hat Accel + Decel | 38.2 | 57.1 | 33.1 |

6.5. Soccer Helmet Results

The simulated soccer ball to head impact (heading) testing was conducted and the theoretical and recorded velocities calculated using the conservation of energy methodology can be seen in Table 15). The headform was tested at 7 different drop heights to establish the baseline for unprotected impacts. Then the soft helmet and D3O was tested at the 7 drop height (15 inches to 75 inches). The plots of the pendulum acceleration and the headform acceleration (Figures 53-54) showed little to no attenuation of the peak values or change in the duration of the impacts when the protective headgear was used. This trend is also reflected in the SI values, (Table 16 and Figures 55-57), where the addition of the soft helmet provided virtually no

protection against these kinds of impacts and the D3O actually increased the severity at higher velocities. The plots of the pendulum accelerations and the headform responses for drop heights 15-65 inches are shown in Appendix A-3.

Table 16: Soccer Pedestal Test Velocities

| Rigid Pedestal Soccer Ball Impact Test Velocities | | | | | | | |
|--|-------|-------|-------|-------|-------|-------|-------|
| Drop Height (in) | 15 | 25 | 35 | 45 | 55 | 65 | 75 |
| Theoretical Pendulum Velocity (in/s) | 107.6 | 138.9 | 164.4 | 186.4 | 206.1 | 224.0 | 240.6 |
| Headform Measured Pendulum Velocities (in/s) | 106.3 | 137.8 | 163.8 | 185.6 | 204.5 | 222.2 | 238.6 |
| % error | 1.2 | 0.8 | 0.3 | 0.4 | 0.8 | 0.8 | 0.8 |
| Equivalent Ball Velocity (mph) | 21.4 | 27.8 | 33.0 | 37.4 | 41.2 | 44.8 | 48.1 |
| Soft Helmet Measured Pendulum Velocities (in/s) | 107.1 | 138.1 | 163.5 | 185.3 | 205.3 | 222.9 | 239.8 |
| % error | 0.44 | 0.62 | 0.56 | 0.60 | 0.35 | 0.48 | 0.34 |
| Equivalent Ball Velocity (mph) | 21.6 | 27.8 | 33.0 | 37.4 | 41.4 | 45.0 | 48.4 |
| D30 Measured Pendulum Velocities (in/s) | 106.7 | 138.1 | 164.9 | 185.0 | 204.8 | 223.0 | 238.8 |
| % error | 0.82 | 0.60 | 0.35 | 0.73 | 0.59 | 0.45 | 0.74 |
| Equivalent Ball Velocity (mph) | 21.5 | 27.9 | 33.3 | 37.3 | 41.3 | 45.0 | 48.2 |

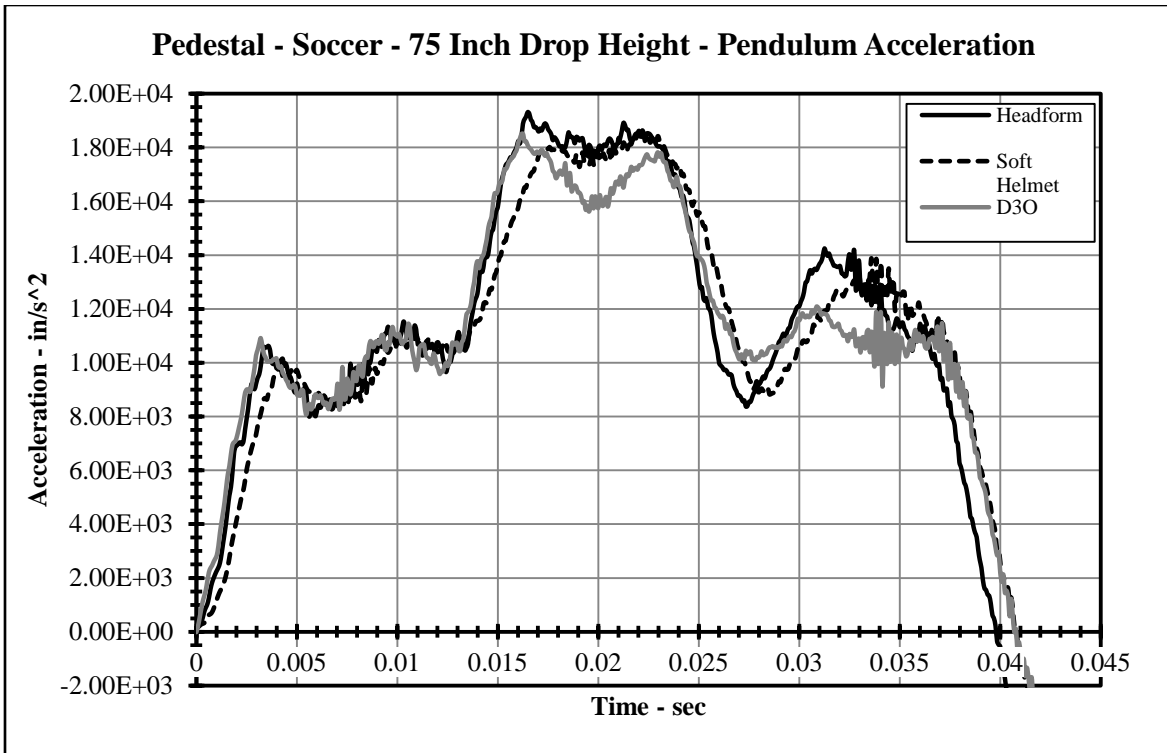


Figure 53: Rigid pedestal soccer helmet testing, 75 inch drop height, pendulum acceleration.

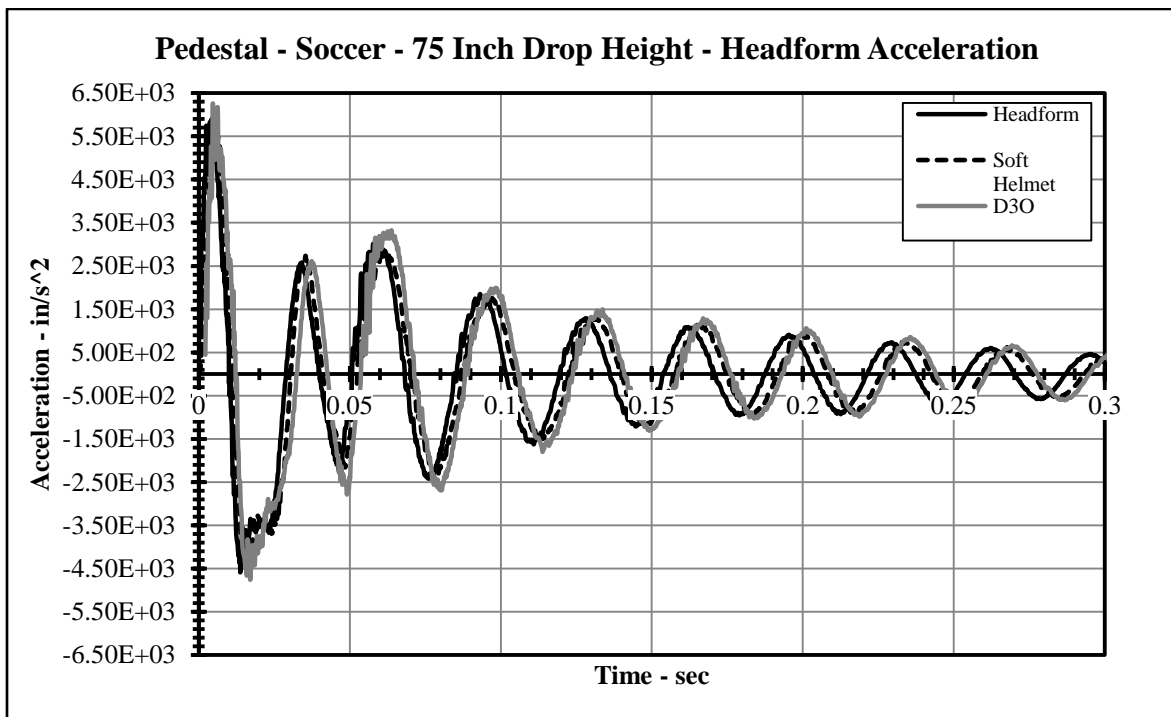


Figure 54: Rigid pedestal soccer helmet testing, 75 inch drop height, headform acceleration.

Table 17: Rigid pedestal soccer helmet tests SI values.

| SI Values for Pedestal Soccer Tests | | | | | | | |
|-------------------------------------|------|------|-------|-------|-------|-------|-------|
| Height (in) | 15 | 25 | 35 | 45 | 55 | 65 | 75 |
| Effective Velocity (mph) | 21.7 | 28.0 | 33.2 | 37.6 | 41.6 | 45.2 | 48.6 |
| Headform Pendulum | 51.0 | 80.3 | 109.7 | 139.9 | 179.6 | 219.5 | 258.0 |
| Headform Intitial Acceleration | 0.7 | 1.2 | 1.7 | 2.1 | 2.6 | 3.2 | 3.8 |
| Headform Deceleration | 1.5 | 2.1 | 2.4 | 2.6 | 2.9 | 3.3 | 3.9 |
| Headform Accel + Decel | 2.3 | 3.3 | 4.1 | 4.7 | 5.5 | 6.6 | 7.7 |
| Soft Helmet Pendulum | 47.1 | 75.7 | 104.1 | 137.3 | 172.9 | 209.0 | 246.8 |
| Soft Helmet Intitial Acceleration | 0.7 | 1.2 | 1.7 | 2.2 | 2.8 | 3.4 | 3.9 |
| Soft Helmet Deceleration | 1.8 | 2.3 | 2.6 | 2.9 | 3.3 | 3.6 | 4.0 |
| Soft Helmet Accel + Decel | 2.5 | 3.4 | 4.3 | 5.1 | 6.1 | 7.0 | 7.9 |
| D30 Pendulum | 50.2 | 78.2 | 107.8 | 135.3 | 169.3 | 200.3 | 237.0 |
| D30 Intitial Acceleration | 0.8 | 1.2 | 1.8 | 2.4 | 2.9 | 3.4 | 3.9 |
| D30 Deceleration | 2.0 | 2.5 | 2.8 | 3.1 | 3.4 | 3.7 | 4.1 |
| D30 Accel + Decel | 2.8 | 3.7 | 4.7 | 5.5 | 6.4 | 7.1 | 8.0 |

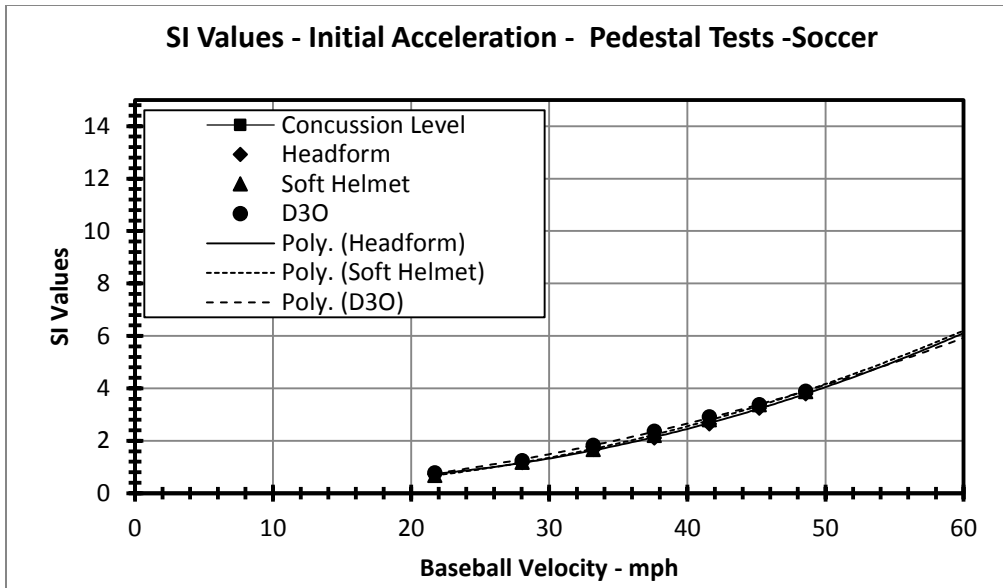


Figure 55: SI values for soccer pedestal helmet testing, initial acceleration.

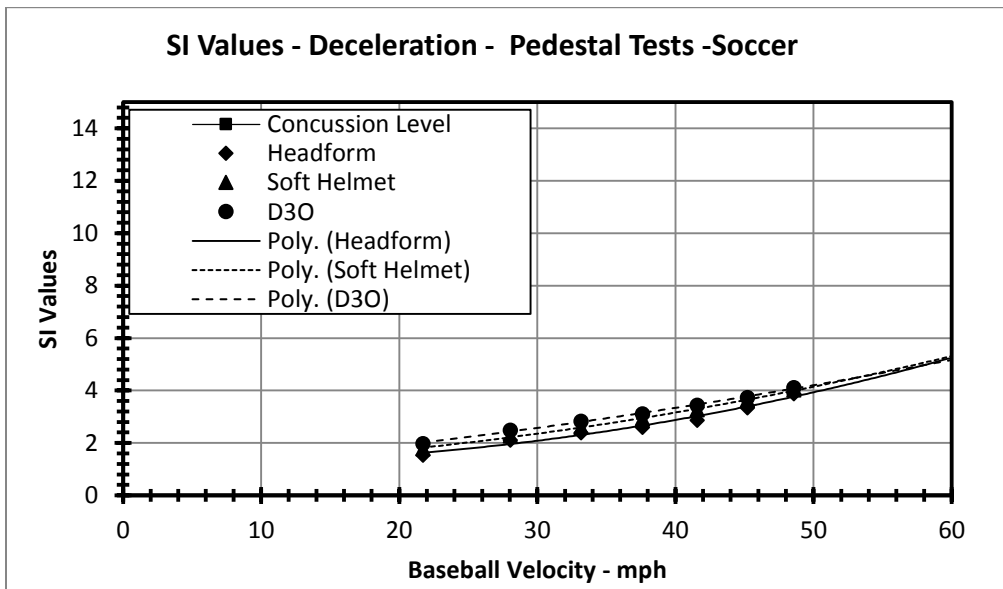


Figure 56: SI values for soccer pedestal helmet testing, deceleration.

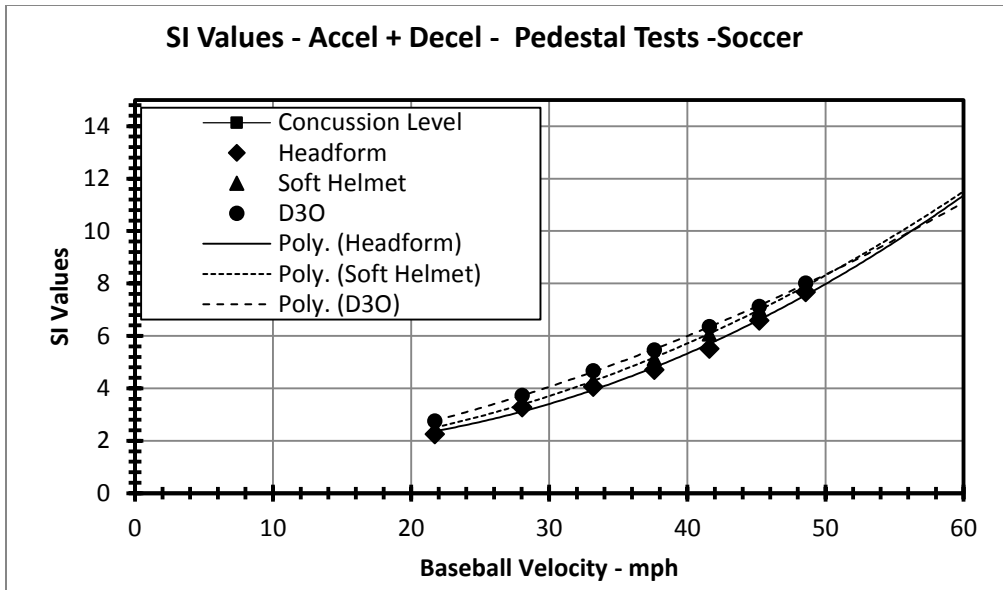


Figure 57: SI values for soccer pedestal helmet testing, acceleration and deceleration combined.

CHAPTER 7 – CONCLUSIONS

1. Headform baseball impact tests were conducted without a helmet utilizing the current LBT standard and the proposed rigid pedestal. Tests for several calculated baseball headform impacts with velocities up to 64 mph were conducted. The maximum SI value for the combined initial plus rebound headform responses was around 127. These was below the SI value of 300 for the possible onset of symptoms associated with a concussion, however the trend predicts that the threshold for concussion would be crossed at 90 mph.
2. The calculated pendulum velocities using the energy methods agreed with the measured velocities with a maximum variation of only 3%.
3. The assumption that the contrecoup SI should be calculated by integrating the entire second pulse (deceleration) proved to be reasonable for the LBT. When using the rigid pedestal however, velocity and displacement analysis was necessary to find the point at which the velocity approached zero and the displacement was maximum to define the end of the contrecoup. The additional magnitude and length of the deceleration pulse was a result of the rigid pedestal mounting behaving as a spring.
4. There is a correlation between the increased energy input into the head and the accompanying increase in SI, however the assumptions made in the energy analysis appear to be over simplified and a new model needs to be created in order to develop a more rigorous mathematical relationship.
5. The pedestal test showed a maximum increase of contrecoup SI by as much as 68% when compared to the LBT. And an overall increase in the SI of the total biphasic TBI event of between 20 and 35%. The pedestal test is likely an overestimate of the injury potential

because of the almost completely rigid nature of the “neck” mounting. The actual injury potential should lie somewhere between the LBT and the rigid pedestal values.

6. Regardless of the test methodology the coup-contrecoup model shows a significant increase in the SI value. Even in the case of the current LBT standard, SI could be underestimated by as much as 25% using the current testing methodology. Given the current state of medical understanding and the data recorded in these experiments, the current NOCSAE testing standards should be revisited to consider including the coup-contrecoup impact model.
7. Headform impact tests were conducted without a helmet using a soccer ball. Tests for several calculated soccer ball headform impacts with velocities up to 48 mph were conducted. The maximum SI value for the combined initial plus rebound headform responses was around 8. These are well below the SI value of 300 for the possible onset of symptoms associated with a concussion.
8. Headform impact tests were conducted with a soft foam-filled helmet. Tests were conducted at equivalent velocities between 22-48 mph. The soft helmet showed no attenuation of head impact energy when compared to similar test results without a helmet.
9. Headform impact tests were conducted with a helmet material labeled Lite by D3O. Tests were conducted at equivalent velocities between 22-48 mph. The Lite by D3O showed no attenuation of head impact energy when compared to similar test results without a helmet. At the 48 mph headform impact velocity, the material slightly increased the energy transmitted into the headform.
10. The results of all tests to date indicate the test apparatus and related test protocols being developed and investigated warrant continued development.

Further Work

The next step in the development of this testing methodology is twofold:

1) The energy analysis needs to be developed in order to find a rigorous mathematical relationship between input energy and SI. This may include some form of computational analysis such as FEA.

2) Some attempt should be made to develop either a mass-spring-damper for the LBT or some other form of “neck” system so that the test protocol has a higher bio-fidelity, more closely modeling an actual TBI event.

When these tests are complete, pictures of these types of impacts can be developed and compared to the NOCSAE standards currently in place. Rigid impactor tests will help to calculate the coefficient of restitution in the soccer ball impacts. Also the rigid impactor or some modification thereof may also be used to simulate other types of impacts such as head to head, head to goal post and head to ground.

APPENDIX

A-1. Baseball Pedestal Test Plots (12-32 Inch)

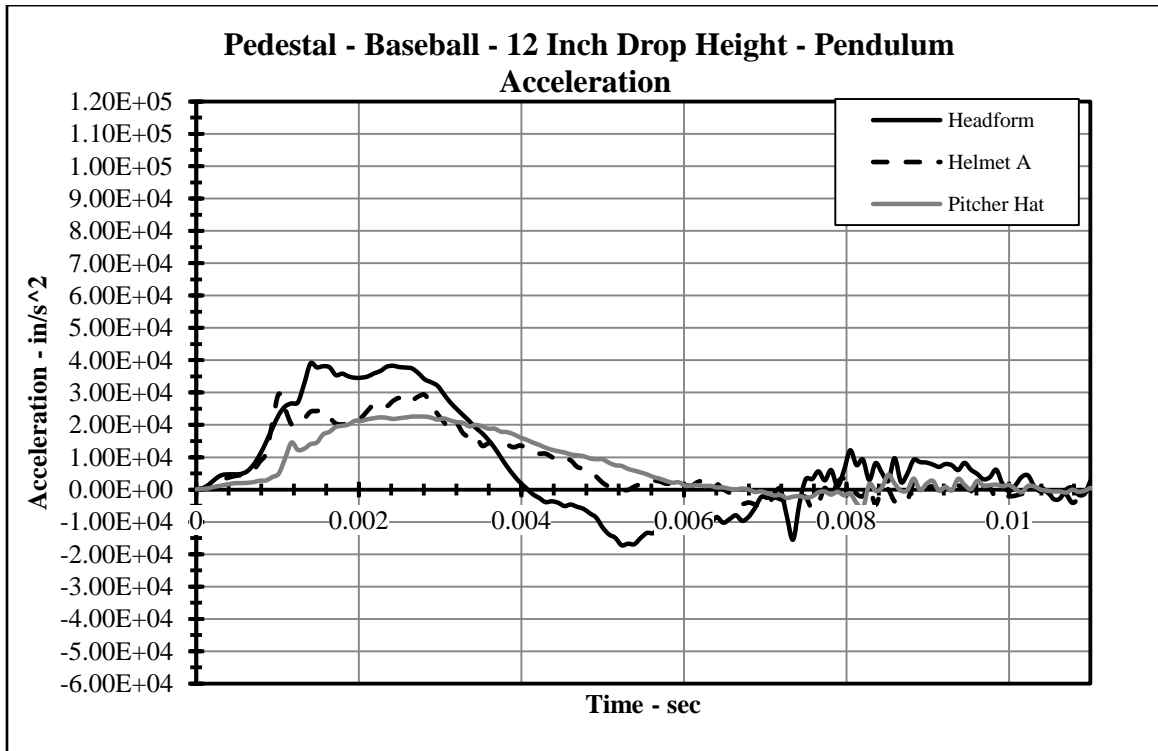


Figure 58: Rigid pedestal baseball helmet testing, 12 inch drop height, pendulum acceleration.

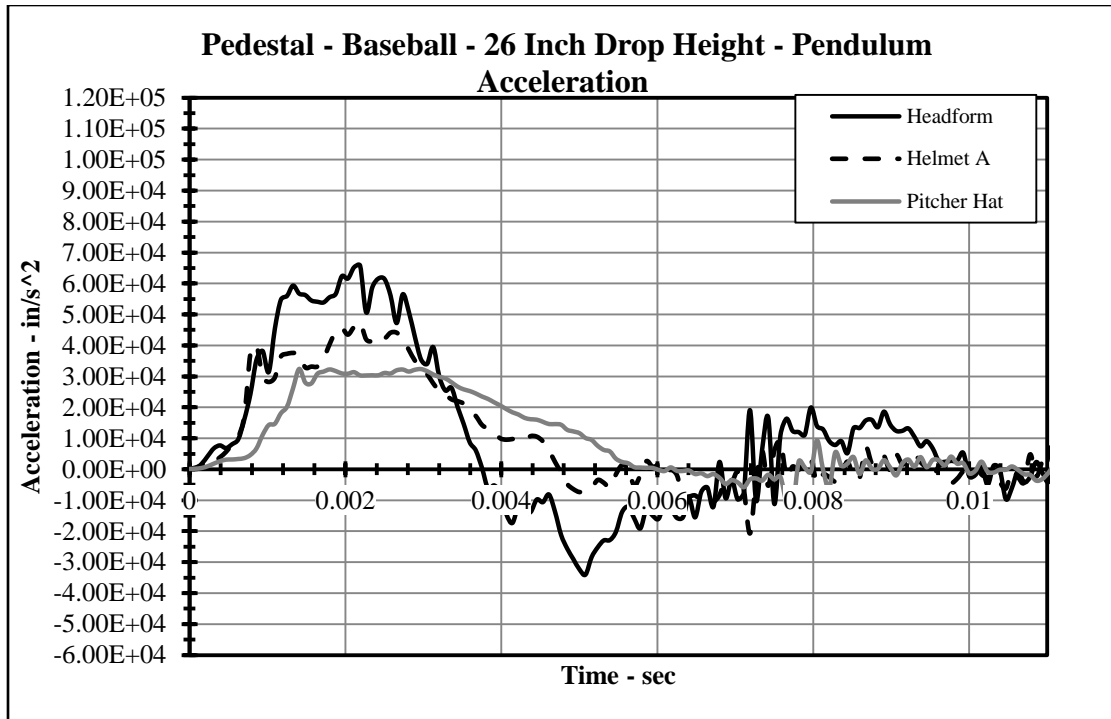


Figure 59: Rigid pedestal baseball helmet testing, 26 inch drop height, pendulum acceleration.

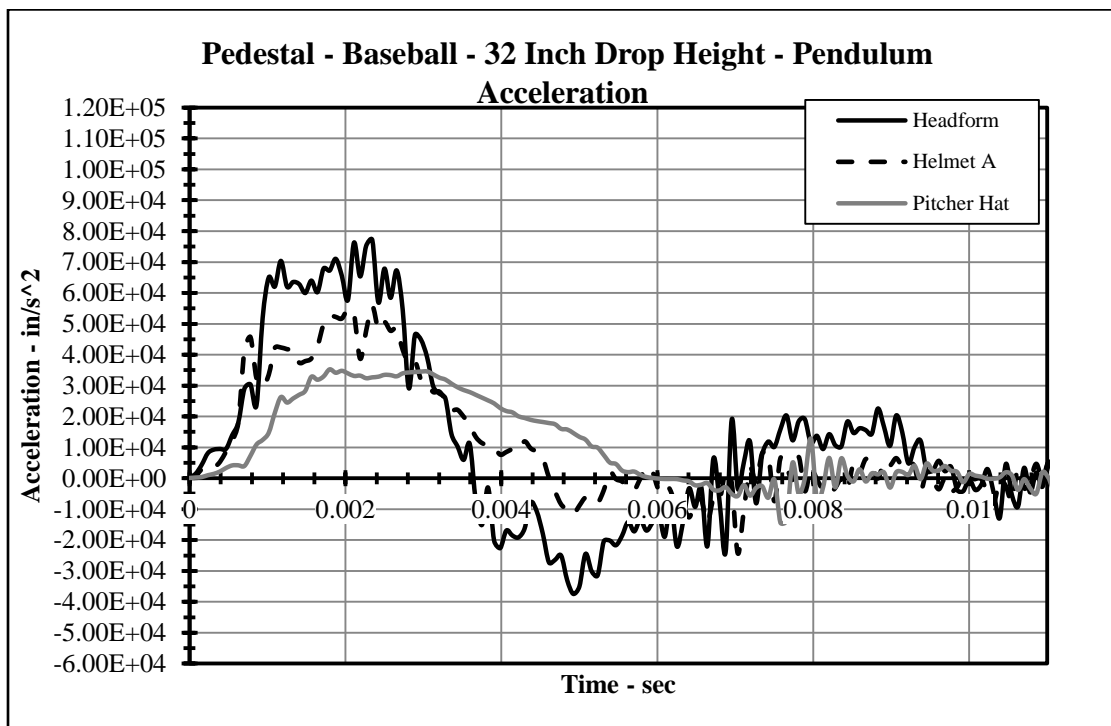


Figure 60: Rigid pedestal baseball helmet testing, 32 inch drop height, pendulum acceleration.

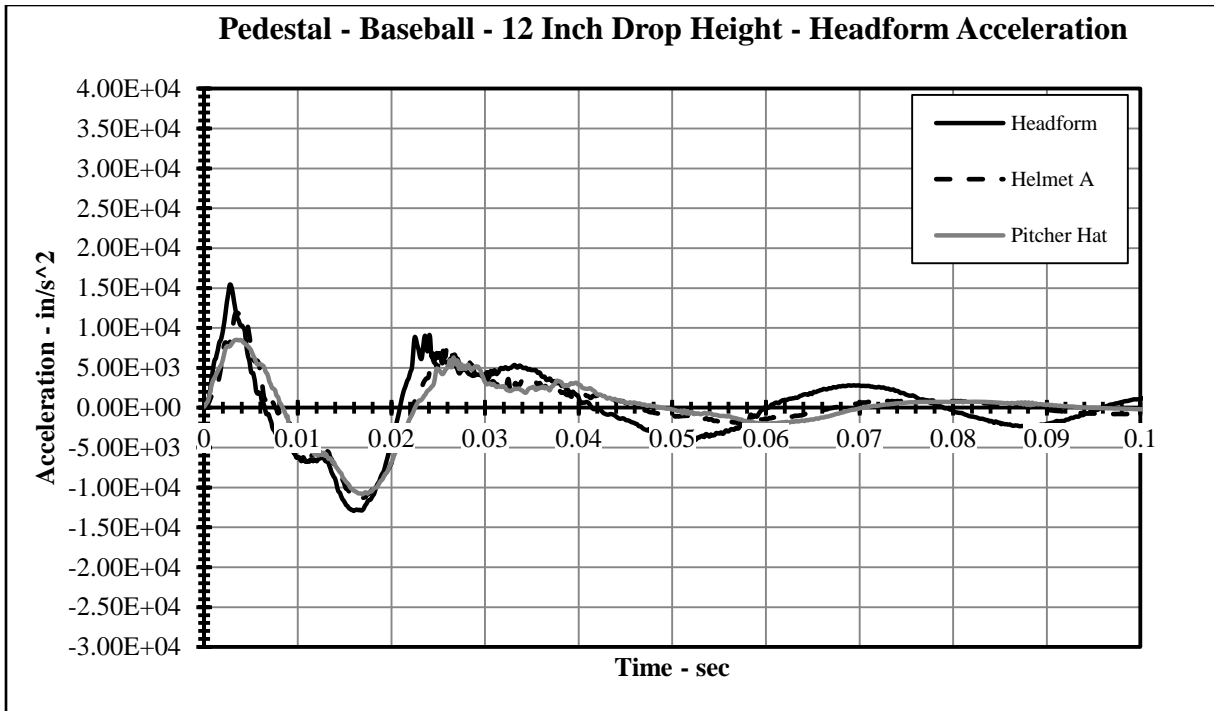


Figure 61: Rigid pedestal baseball helmet testing, 12 inch drop height, headform acceleration.

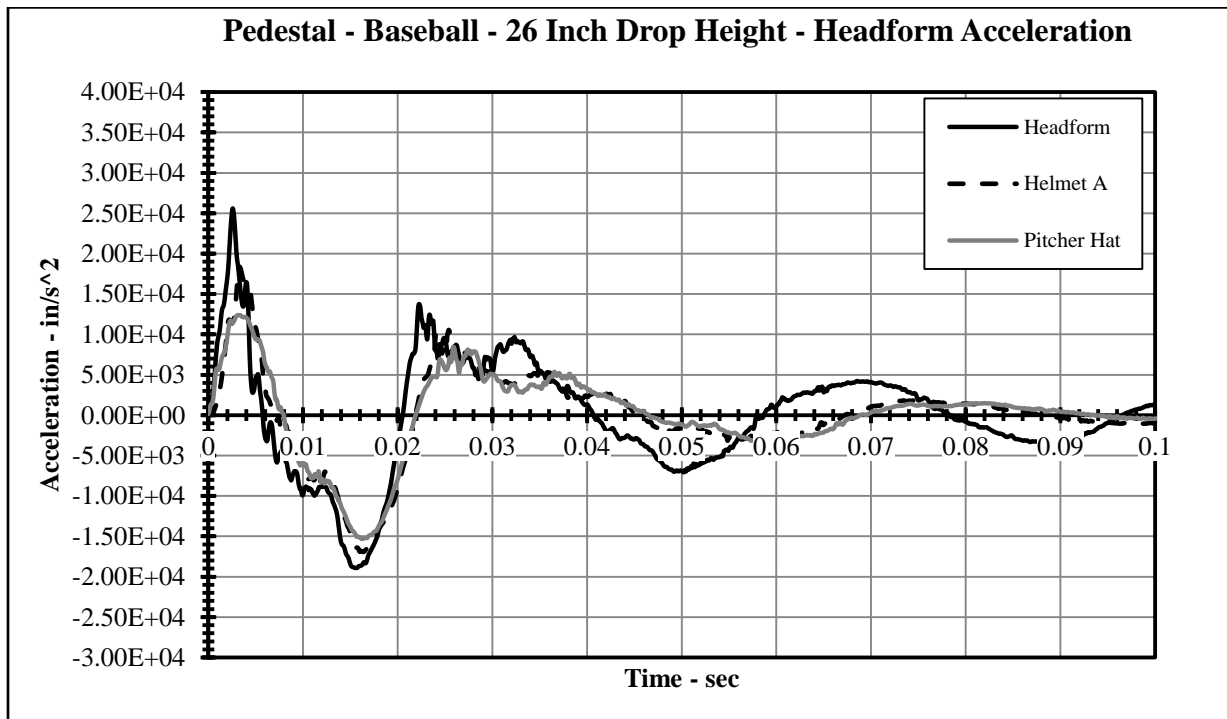


Figure 62: Rigid pedestal baseball helmet testing, 26 inch drop height, headform acceleration.

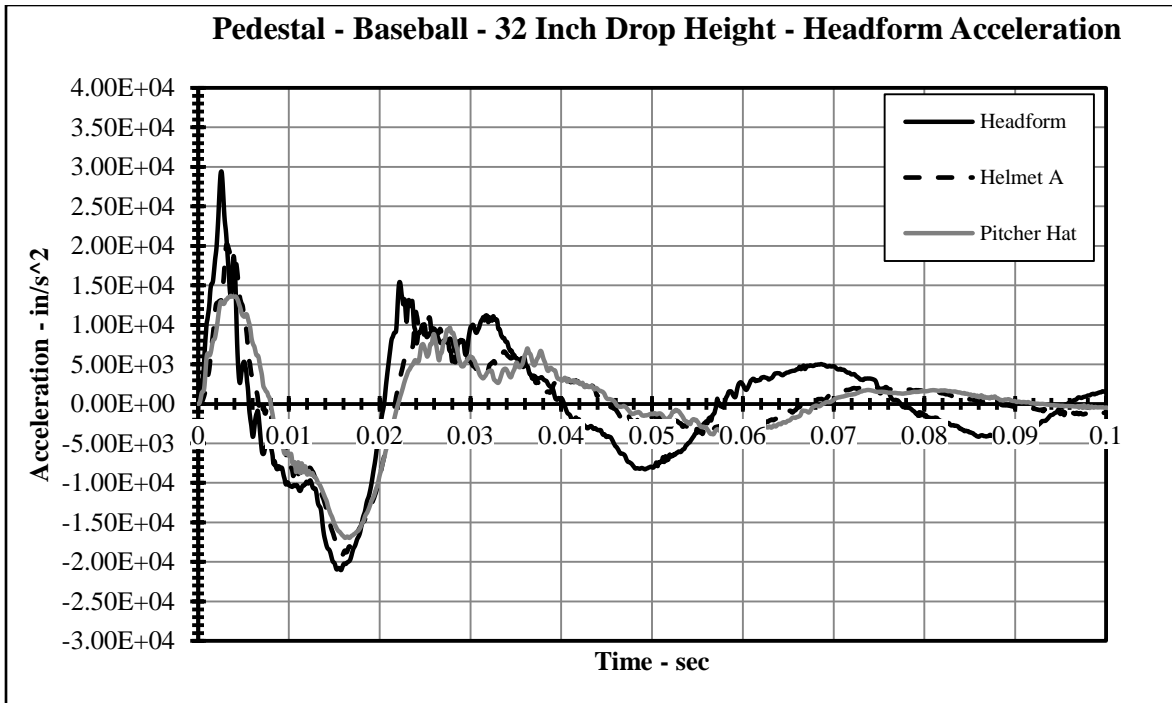


Figure 63: Rigid pedestal baseball helmet testing, 32 inch drop height, headform acceleration.

A-2. Baseball LBT Test Plots (12-32 Inch)

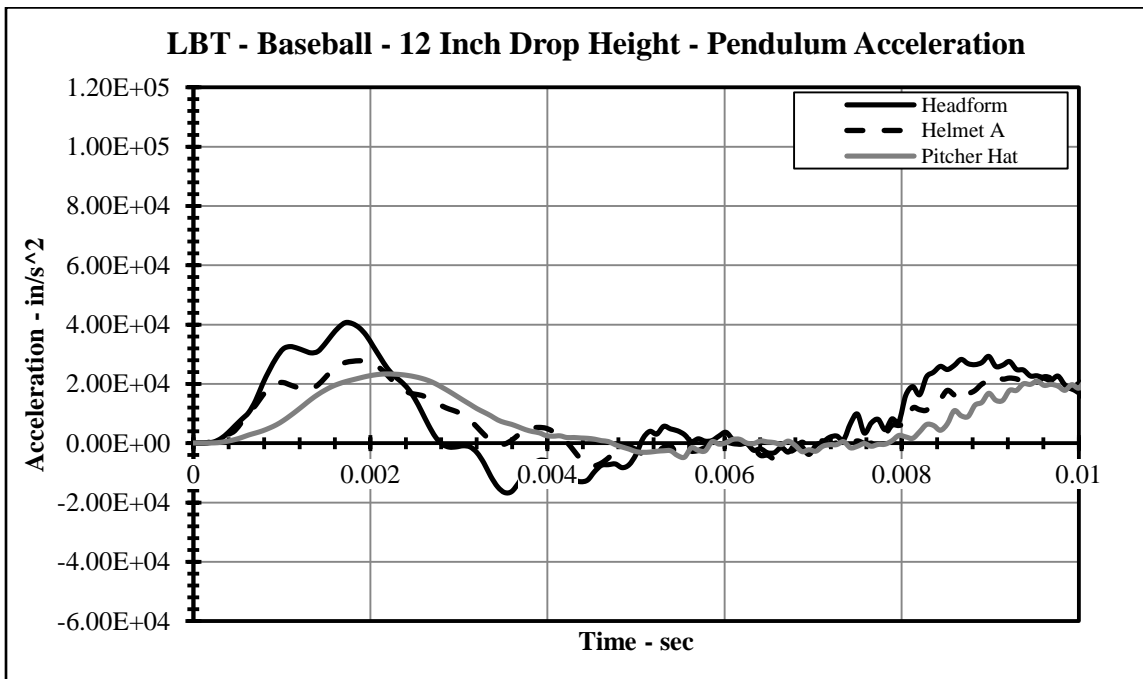


Figure 64: LBT baseball helmet testing, 12 inch drop height, pendulum acceleration.

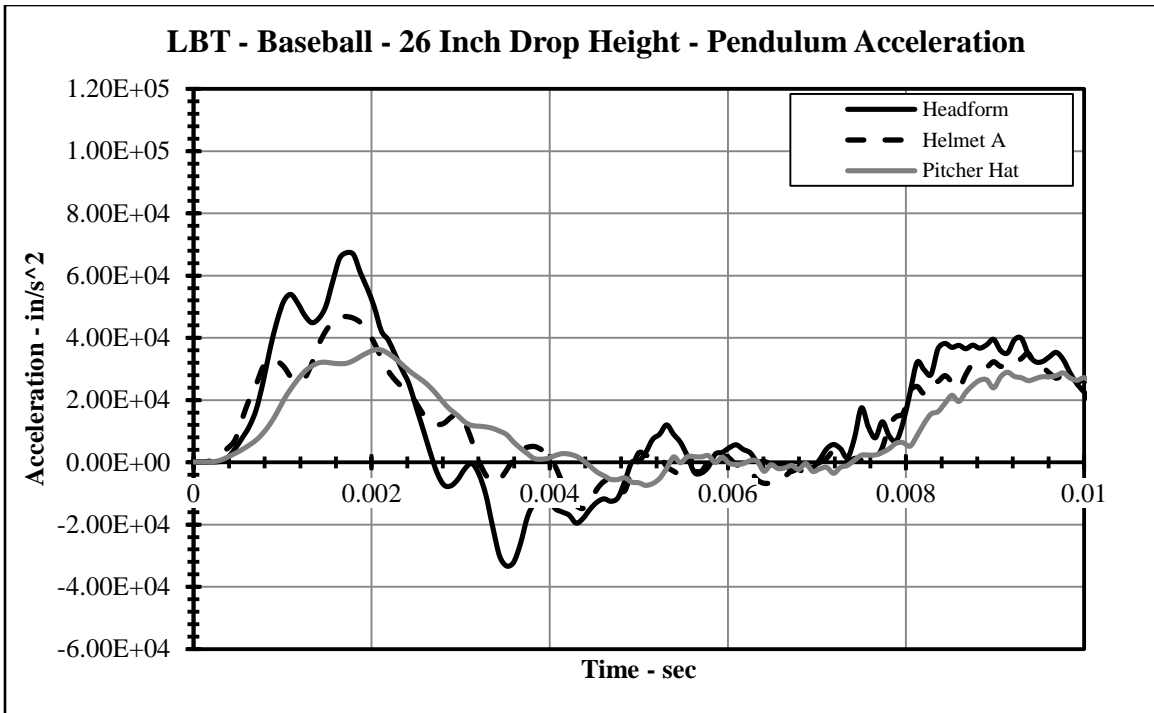


Figure 65: LBT baseball helmet testing, 26 inch drop height, pendulum acceleration.

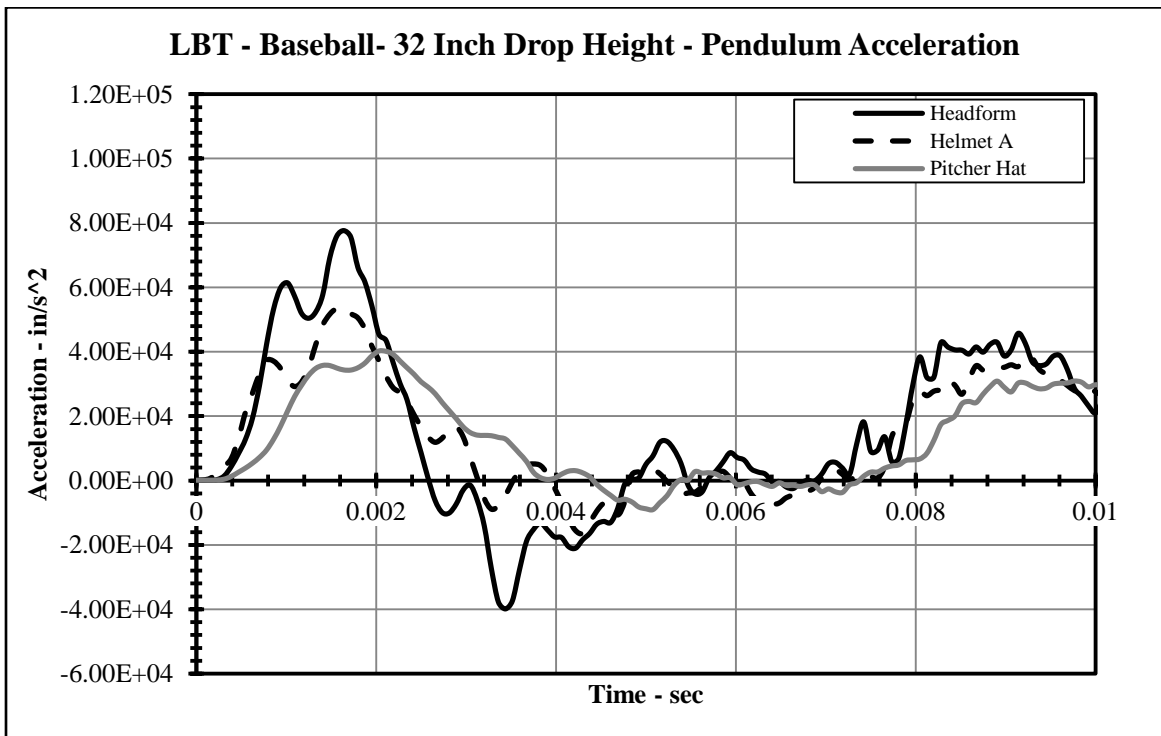


Figure 66: LBT baseball helmet testing, 32 inch drop height, pendulum acceleration.

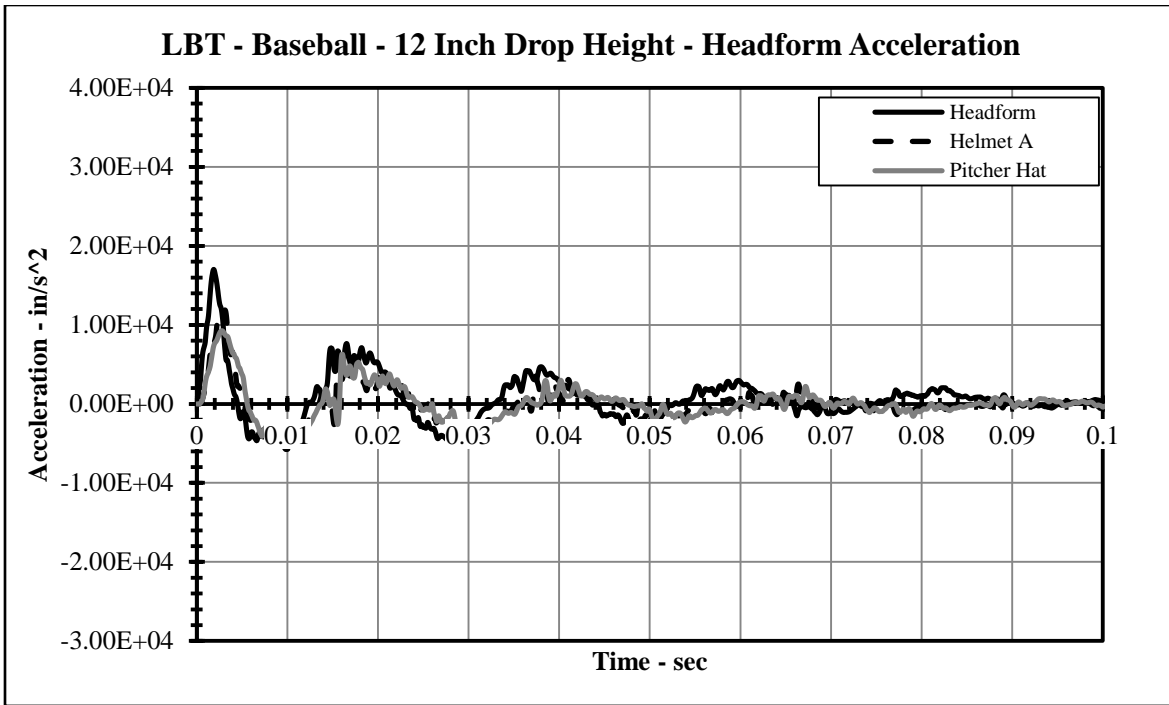


Figure 67: LBT baseball helmet testing, 12 inch drop height, headform acceleration.

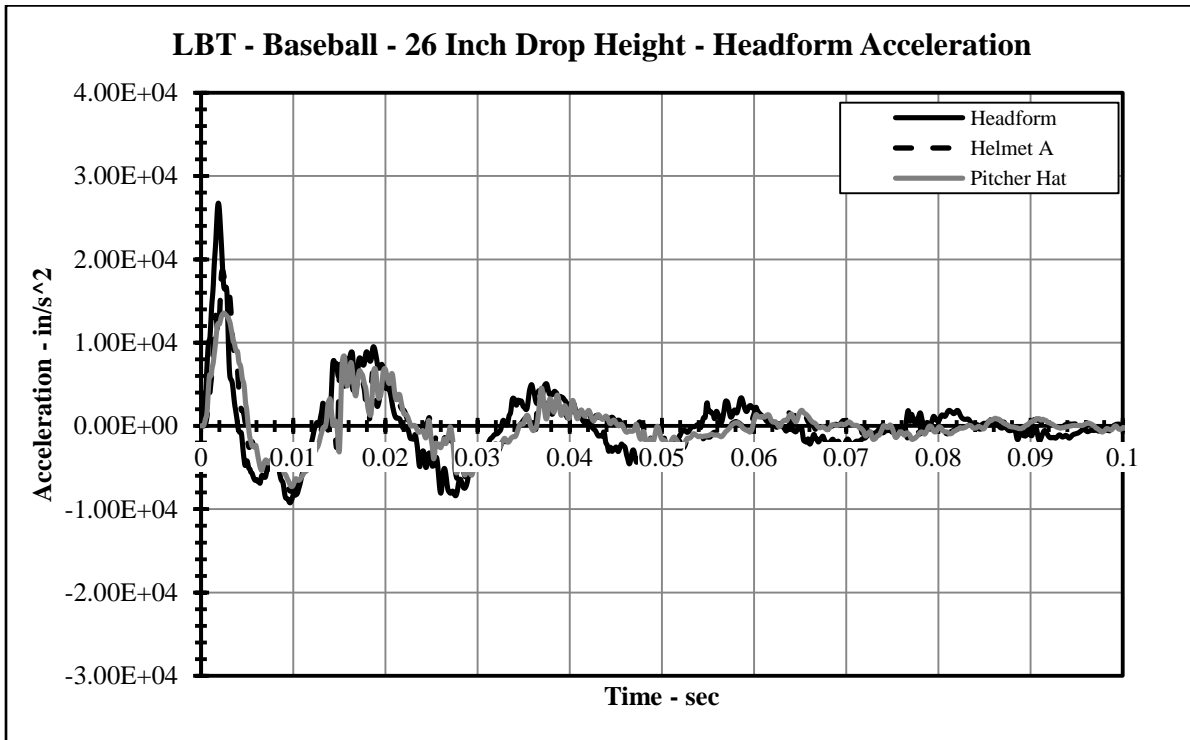


Figure 68: LBT baseball helmet testing, 26 inch drop height, headform acceleration.

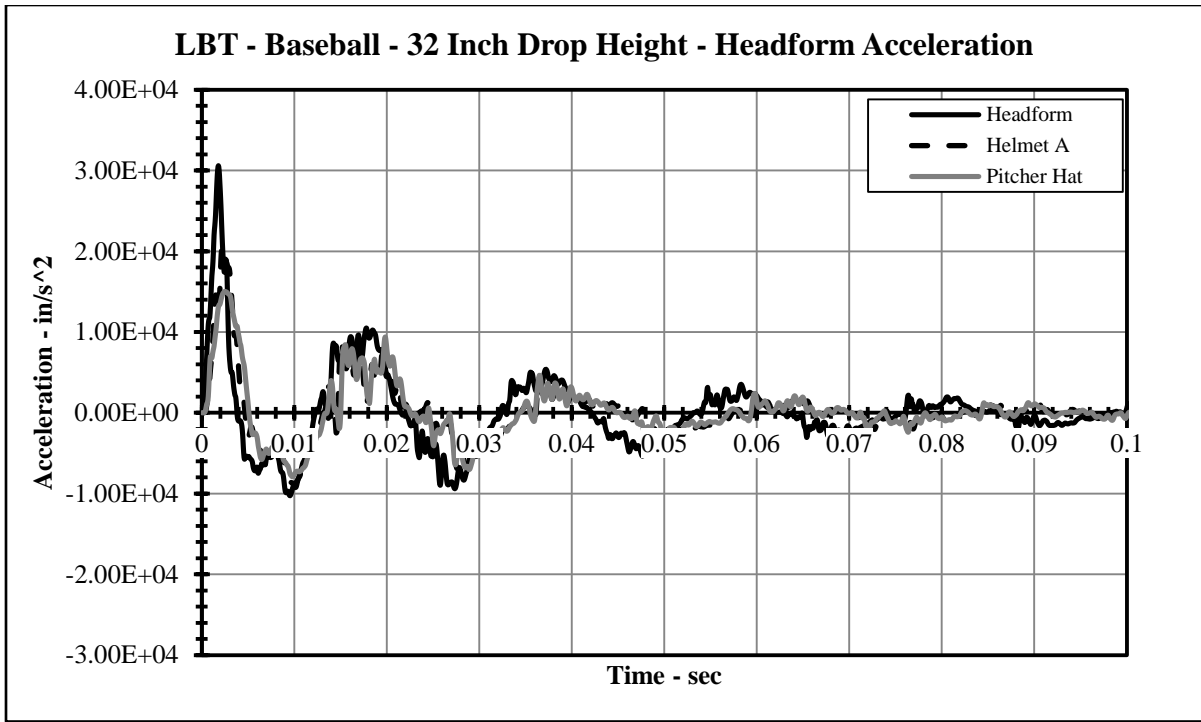


Figure 69: LBT baseball helmet testing, 32 inch drop height, headform acceleration.

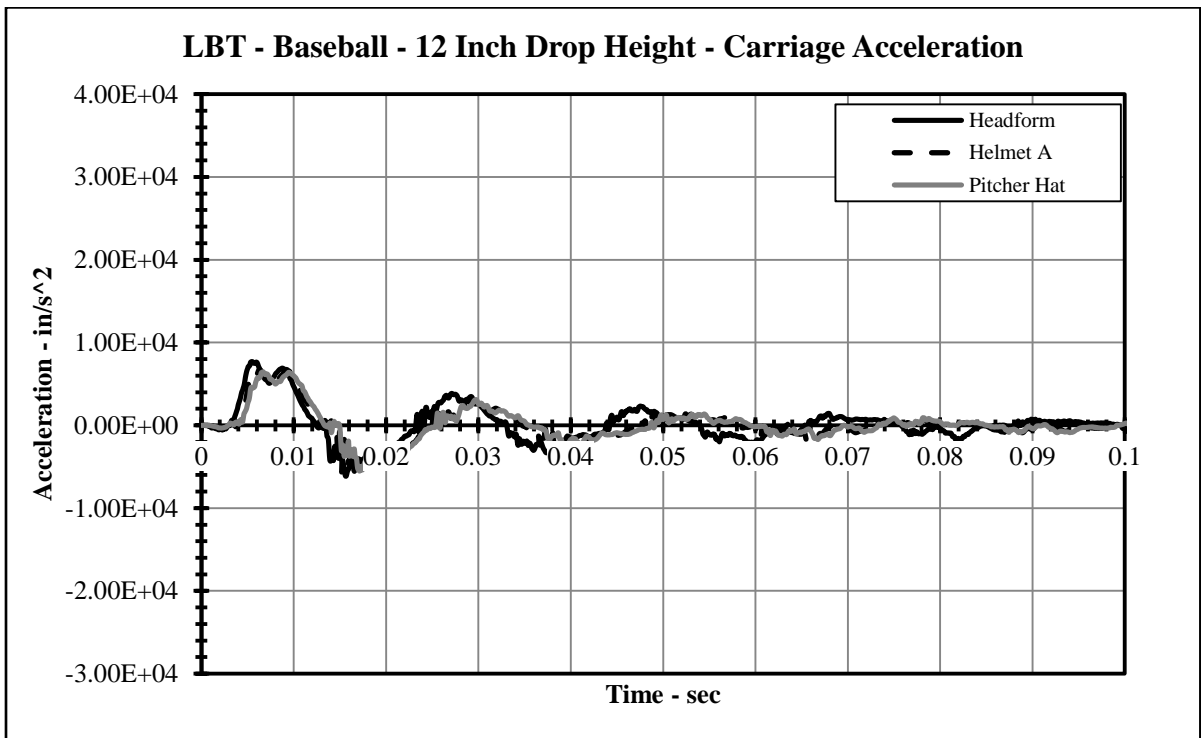


Figure 70: LBT baseball helmet testing, 12 inch drop height, carriage acceleration.

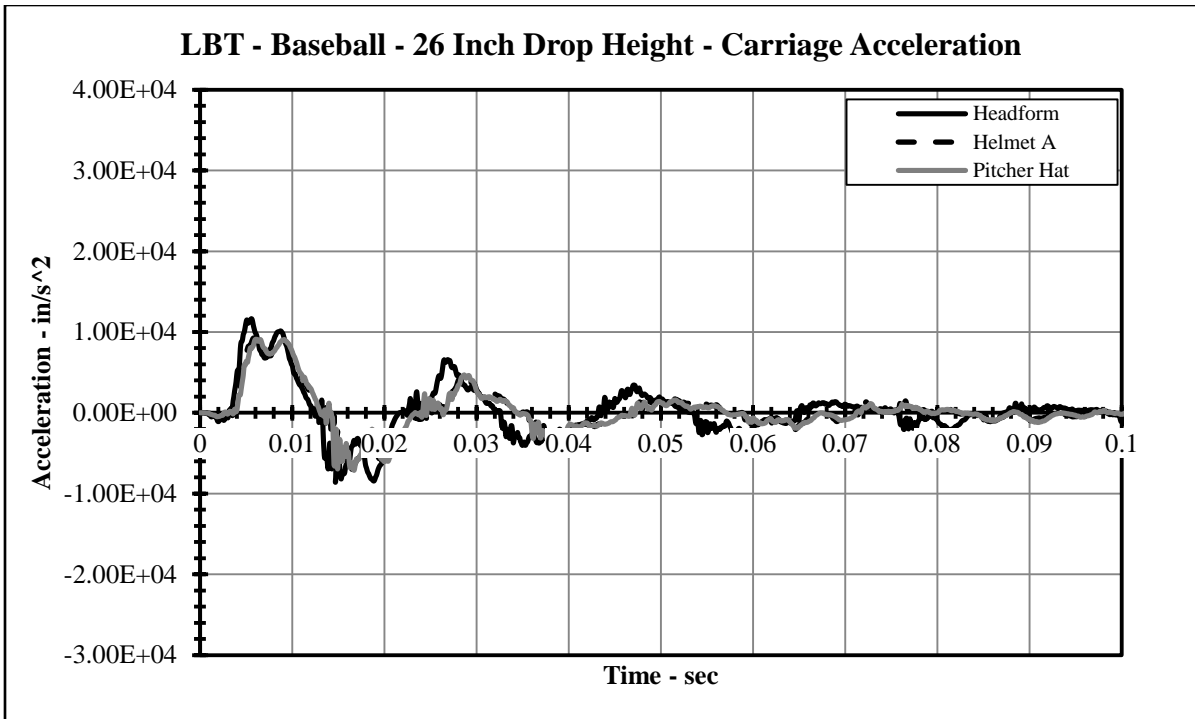


Figure 71: LBT baseball helmet testing, 26 inch drop height, carriage acceleration.

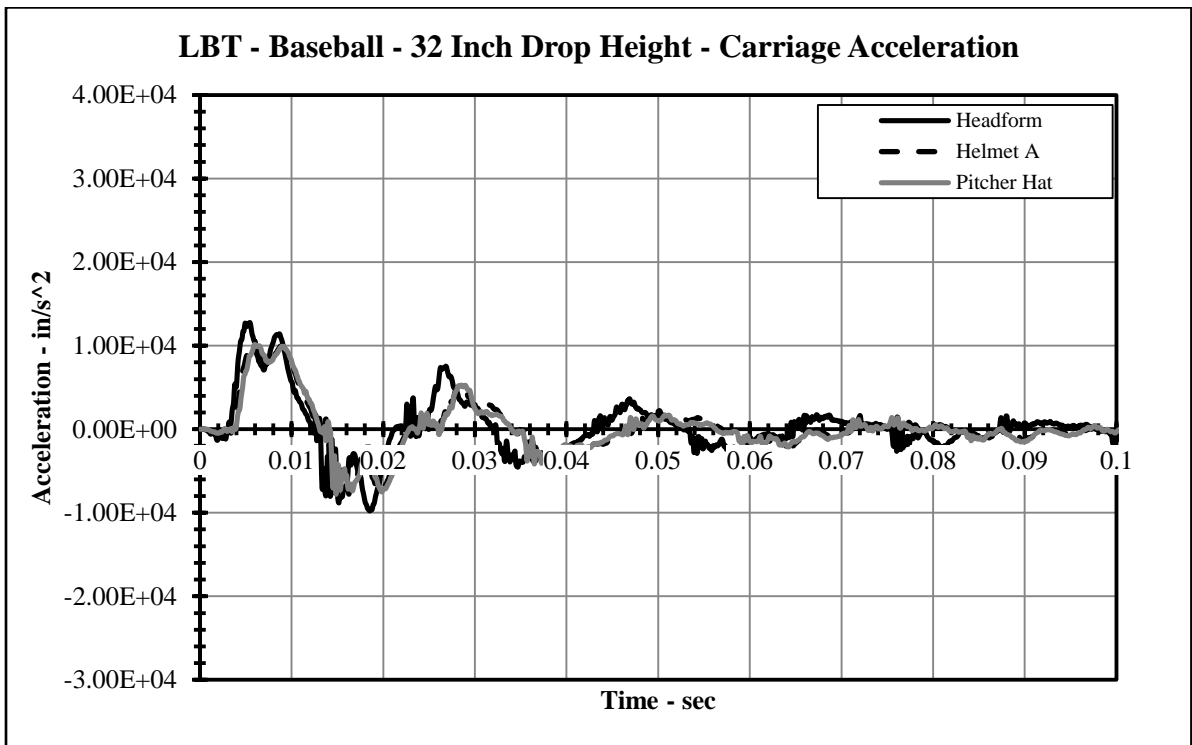


Figure 72: LBT baseball helmet testing, 32 inch drop height, carriage acceleration.

A-3. Soccer Pedestal Test Plots (15-65 Inch)

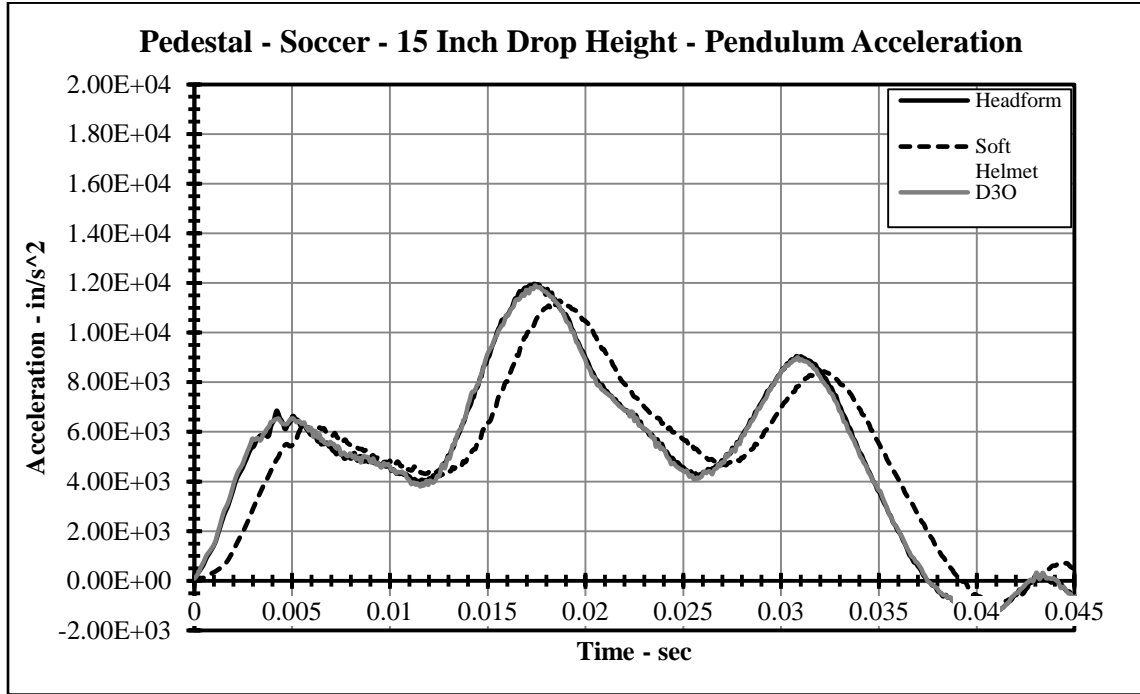


Figure 73: Rigid pedestal soccer helmet testing, 15 inch drop height, pendulum acceleration.

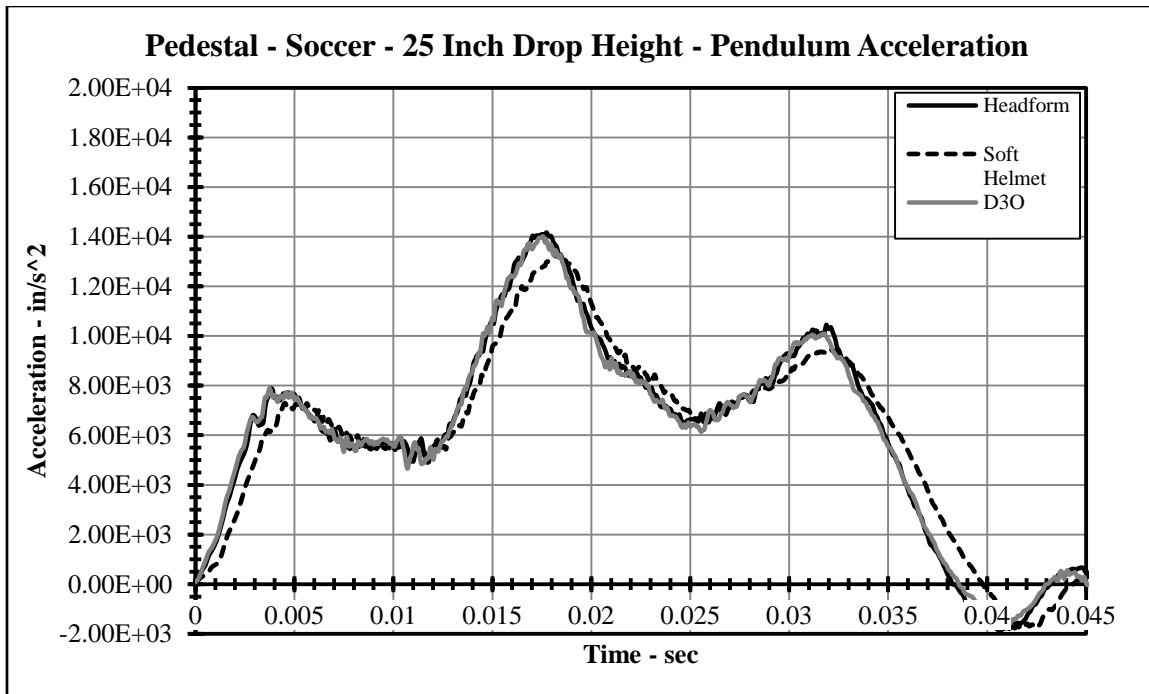


Figure 74: Rigid pedestal soccer helmet testing, 25 inch drop height, pendulum acceleration.

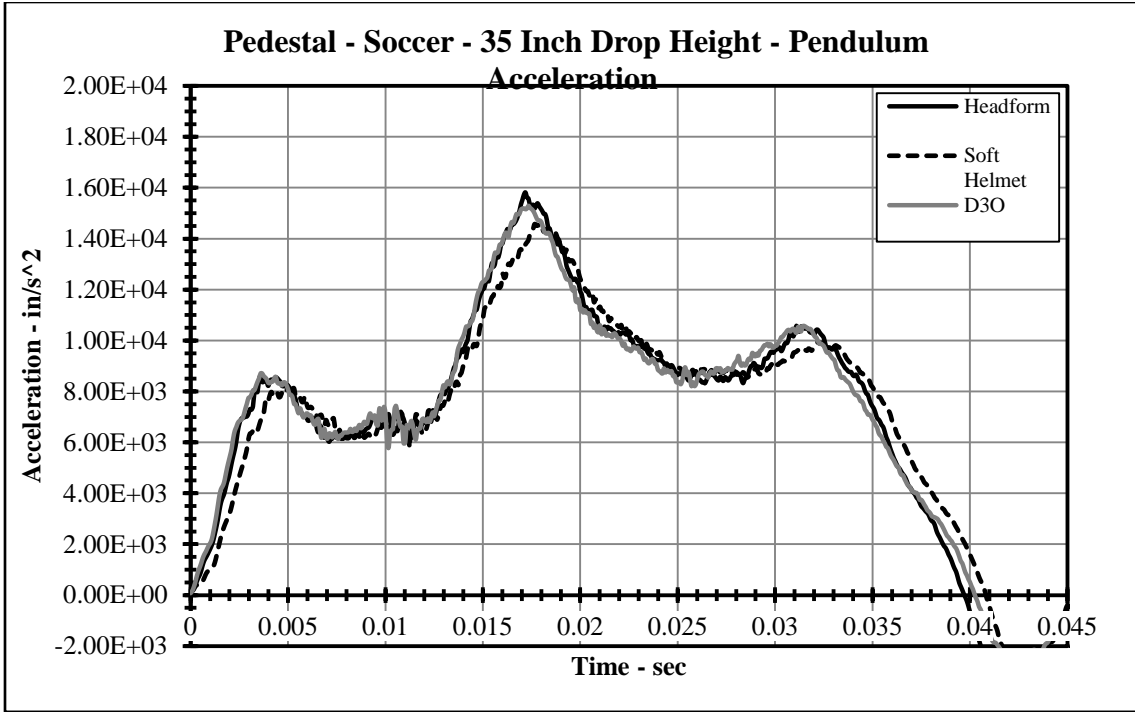


Figure 75: Rigid pedestal soccer helmet testing, 35 inch drop height, pendulum acceleration.

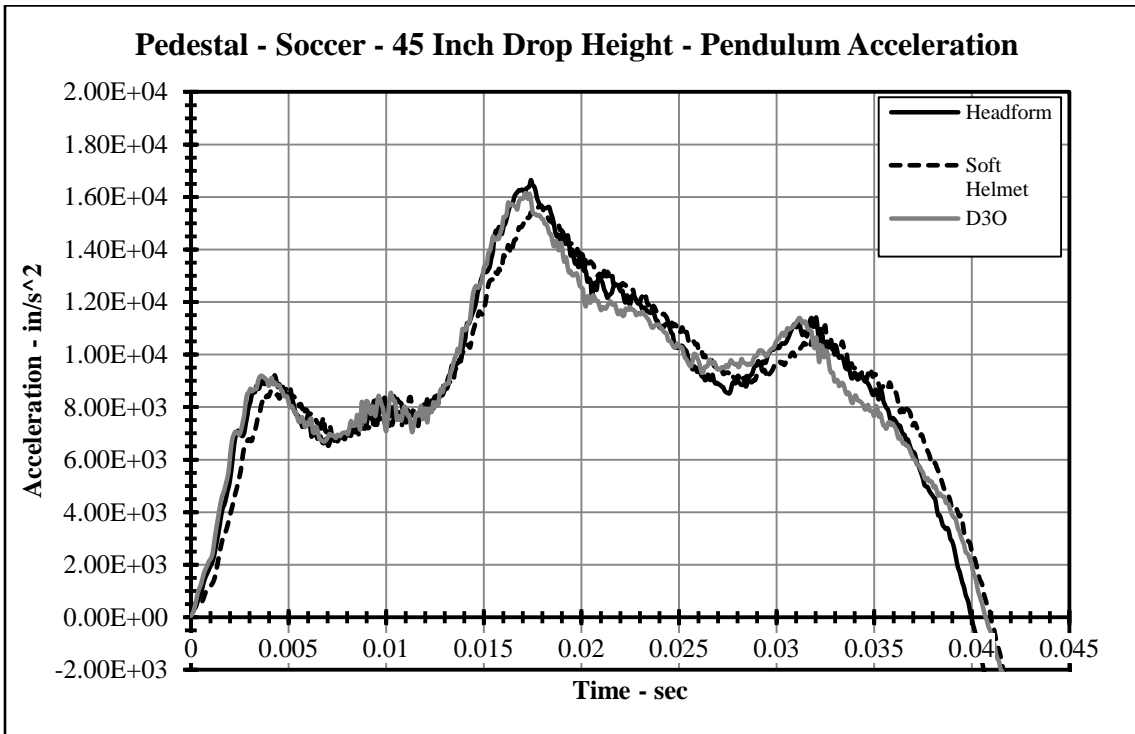


Figure 76: Rigid pedestal soccer helmet testing, 45 inch drop height, pendulum acceleration.

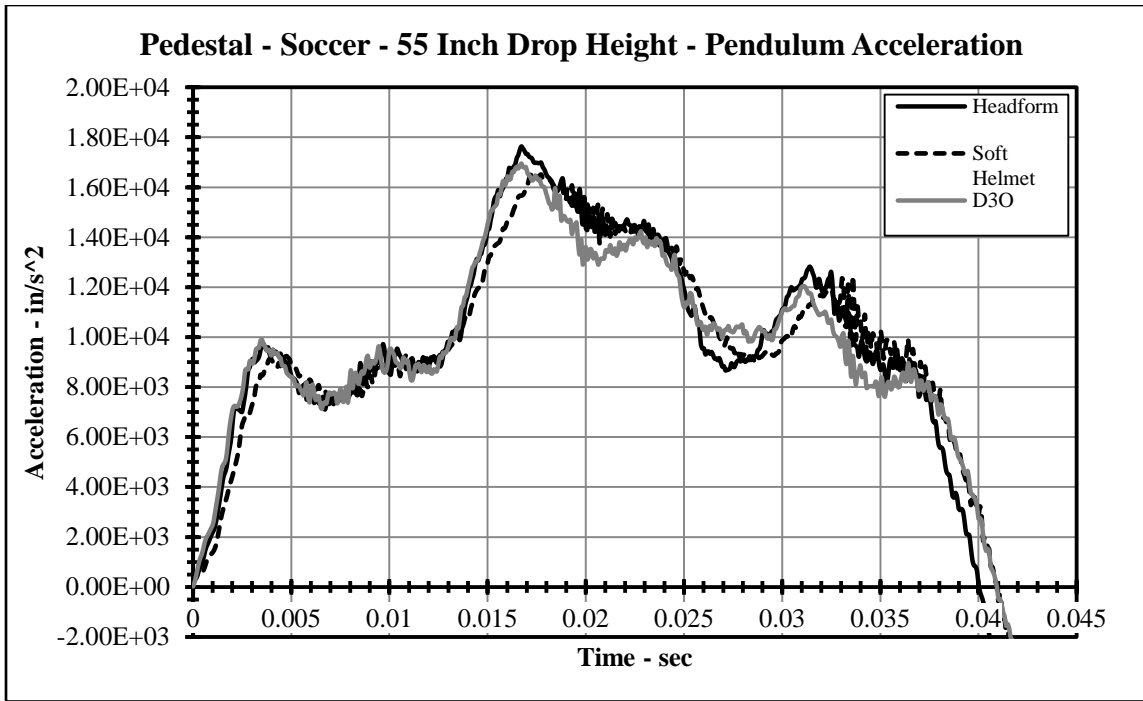


Figure 77: Rigid pedestal soccer helmet testing, 55 inch drop height, pendulum acceleration.

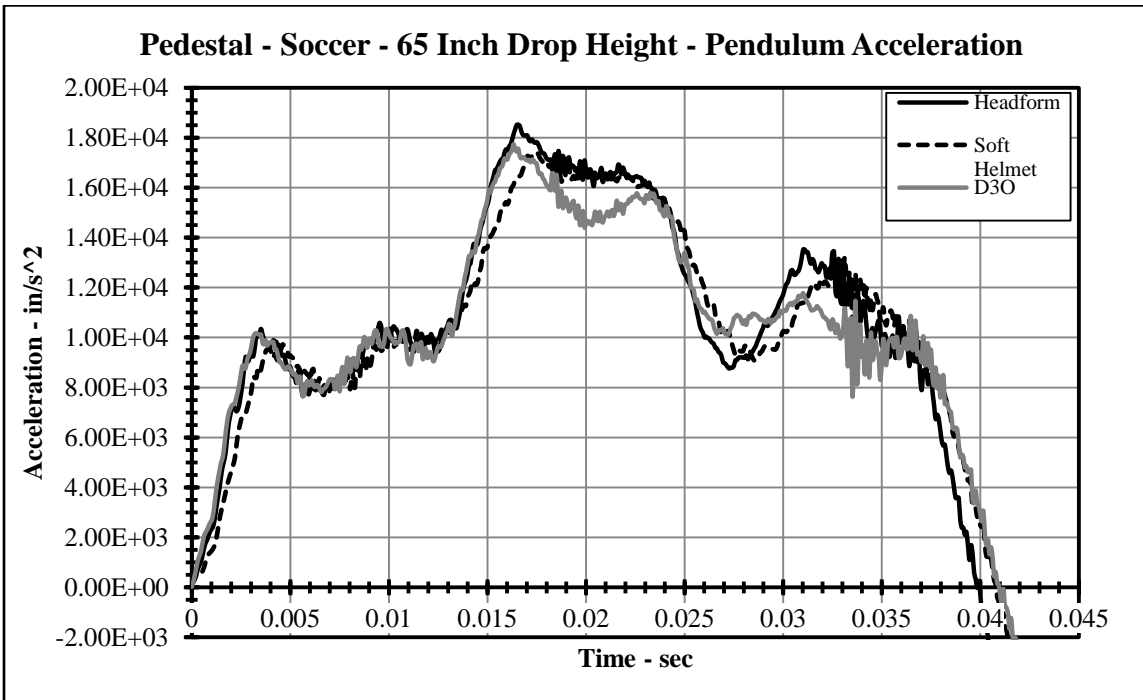


Figure 78: Rigid pedestal soccer helmet testing, 65 inch drop height, pendulum acceleration.

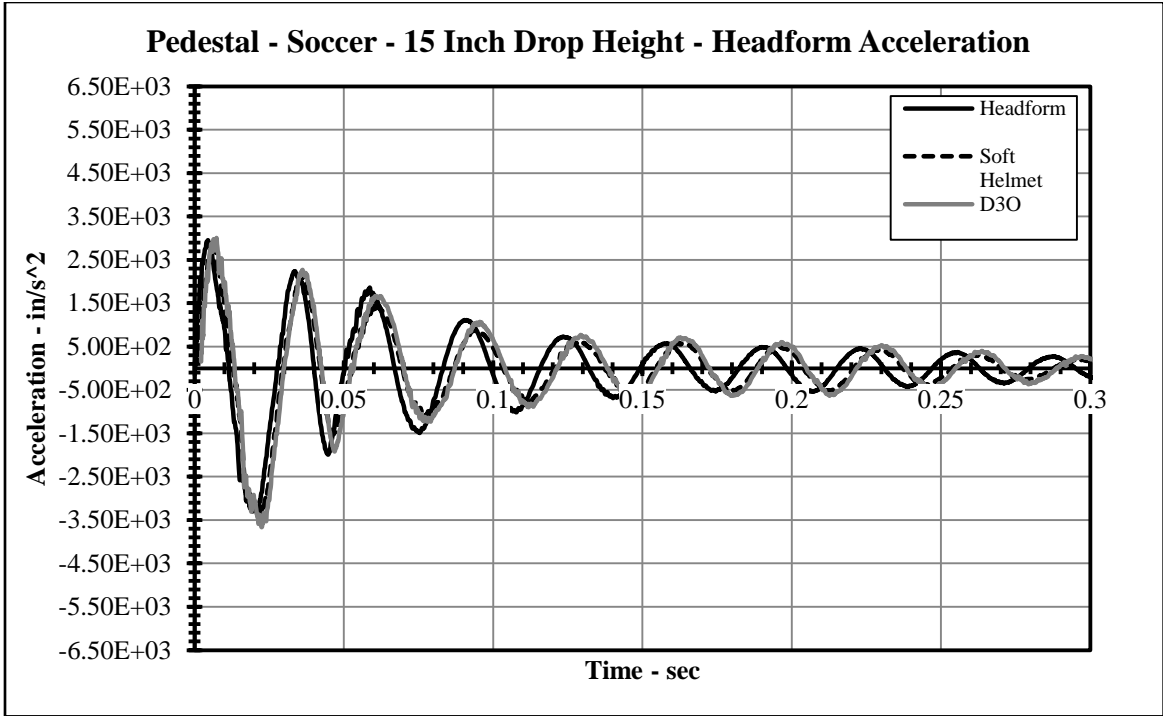


Figure 79: Rigid pedestal soccer helmet testing, 15 inch drop height, headform acceleration.

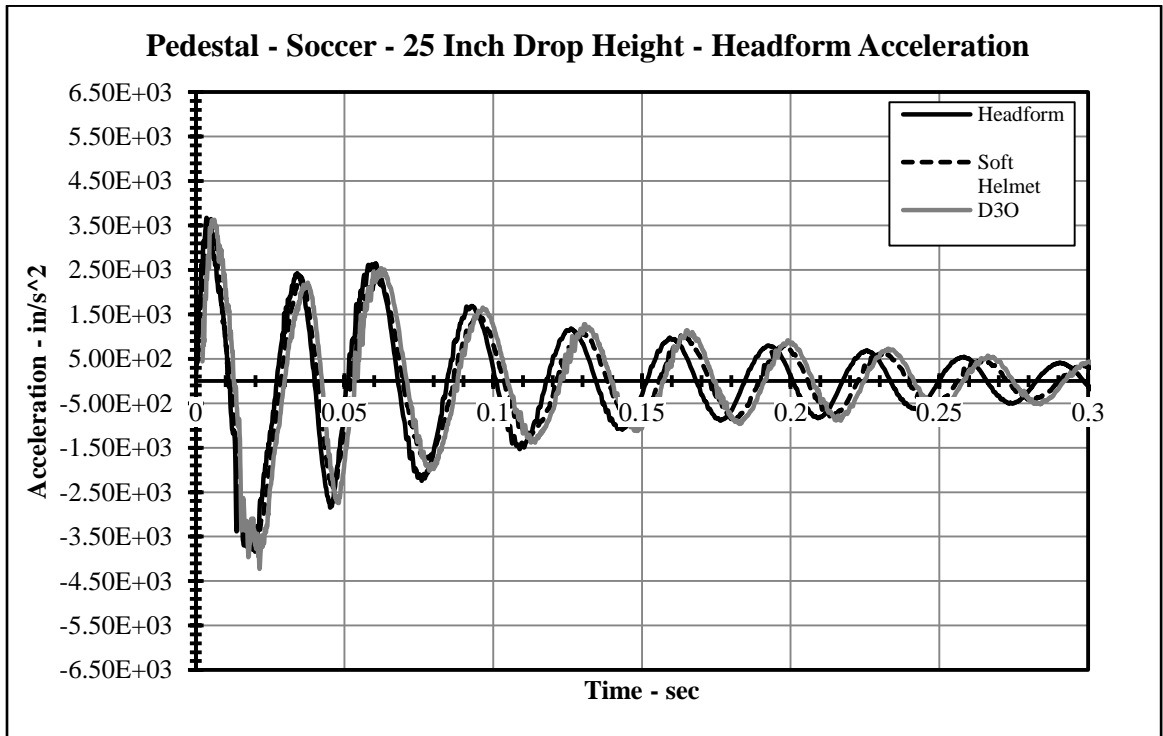


Figure 80: Rigid pedestal soccer helmet testing, 25 inch drop height, headform acceleration.

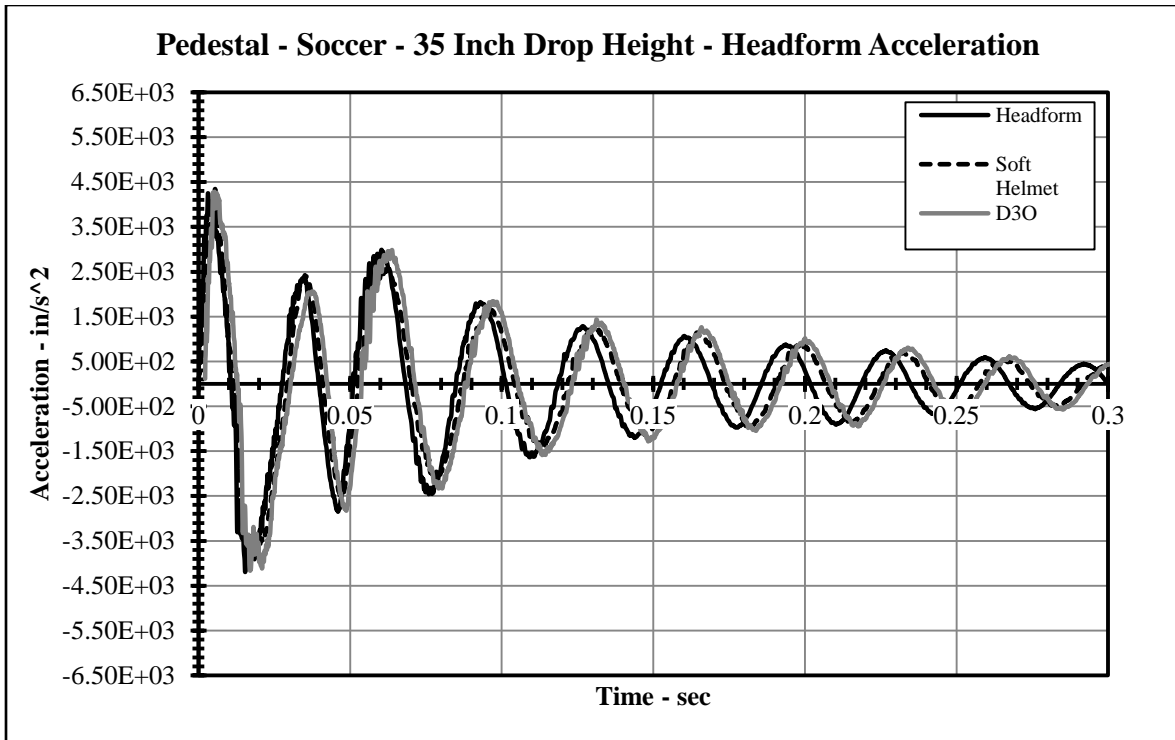


Figure 81: Rigid pedestal soccer helmet testing, 35 inch drop height, headform acceleration.

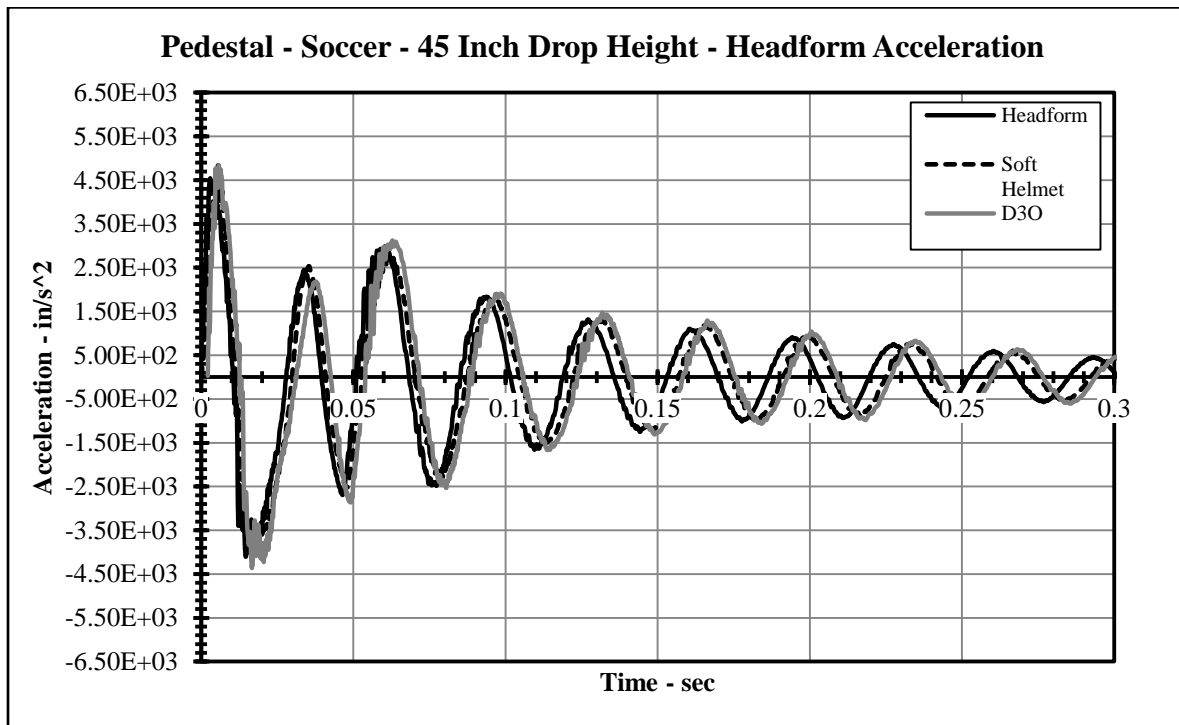


Figure 82: Rigid pedestal soccer helmet testing, 45 inch drop height, headform acceleration.

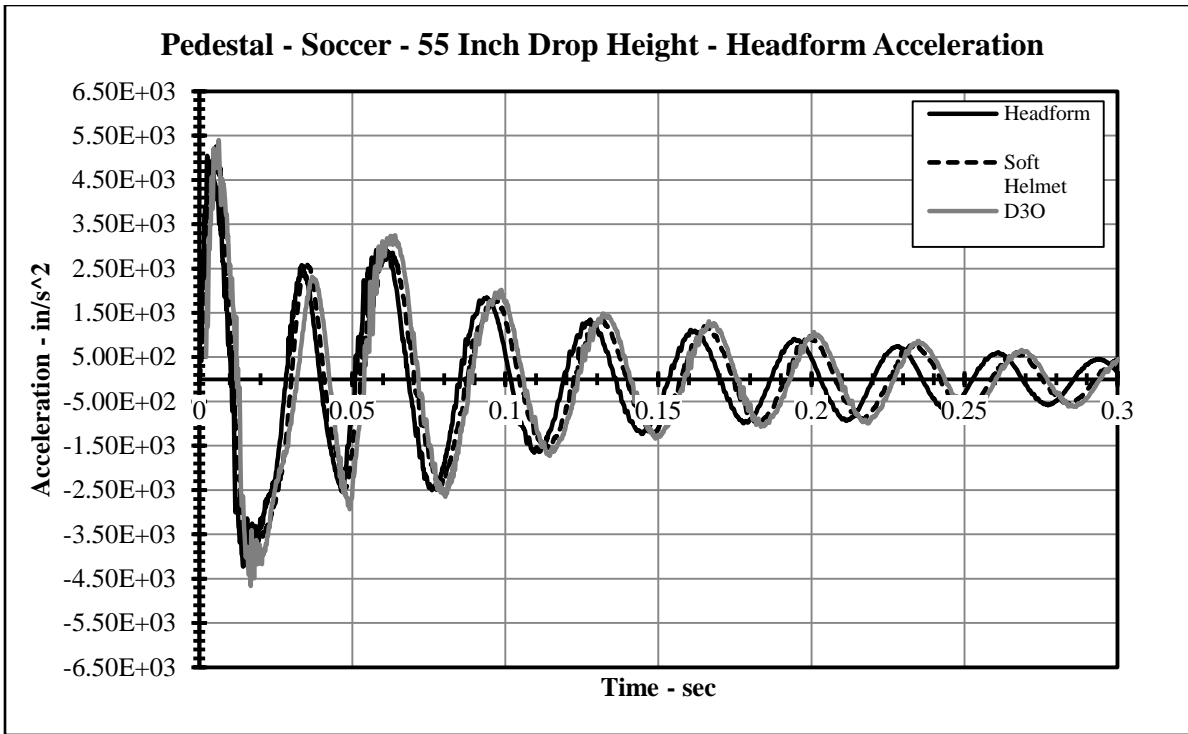


Figure 83: Rigid pedestal soccer helmet testing, 55 inch drop height, headform acceleration.

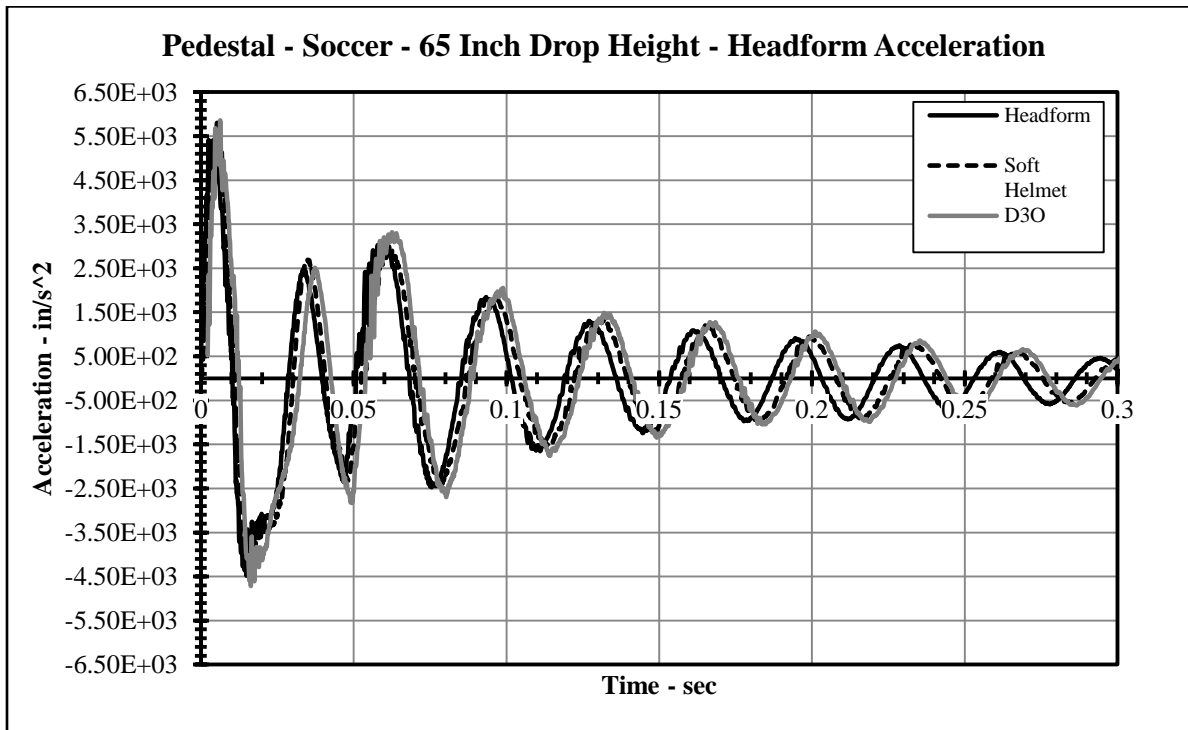


Figure 84: Rigid pedestal soccer helmet testing, 65 inch drop height, headform acceleration.

A-4. Sample MATLAB Code

```
% This program calls the function Vel_SI_HIC.m
% and writes teh velocity, SI and HIC data to
% the assigned spread sheet

clc,clear,close all;
sp = 'Pitcher Hat Baseball SI Mod.xlsx';
ws = '12';
pen_x = 'D3:D182';
pen_y = 'E3:E182';
hed_ix = 'G3:G110';
hed_iy = 'H3:H110';
hed_rx = 'G111:G203';
hed_ry = 'H111:H203';
hed_irx = 'G3:G203';
hed_iry = 'H3:H203';

Vel_SI_HIC(sp,ws,pen_x,pen_y,hed_ix,hed_iy,hed_rx,hed_ry,hed_irx,hed_iry)

ws = '26';
pen_x = 'D3:D182';
pen_y = 'E3:E182';
hed_ix = 'G3:G110';
hed_iy = 'H3:H110';
hed_rx = 'G111:G203';
hed_ry = 'H111:H203';
hed_irx = 'G3:G203';
hed_iry = 'H3:H203';

Vel_SI_HIC(sp,ws,pen_x,pen_y,hed_ix,hed_iy,hed_rx,hed_ry,hed_irx,hed_iry)

ws = '32';
pen_x = 'D3:D182';
pen_y = 'E3:E182';
hed_ix = 'G3:G110';
hed_iy = 'H3:H110';
hed_rx = 'G111:G203';
hed_ry = 'H111:H203';
hed_irx = 'G3:G203';
hed_iry = 'H3:H203';

Vel_SI_HIC(sp,ws,pen_x,pen_y,hed_ix,hed_iy,hed_rx,hed_ry,hed_irx,hed_iry)

ws = '45';
pen_x = 'D3:D182';
pen_y = 'E3:E182';
hed_ix = 'G3:G110';
hed_iy = 'H3:H110';
hed_rx = 'G111:G203';
hed_ry = 'H111:H203';
hed_irx = 'G3:G203';
hed_iry = 'H3:H203';

Vel_SI_HIC(sp,ws,pen_x,pen_y,hed_ix,hed_iy,hed_rx,hed_ry,hed_irx,hed_iry)
```

```

function [] = Vel_SI_HIC(spread, sheet, row, pen_x, pen_y, ...
    head_i_x, head_i_y, head_r_x, head_r_y, head_ir_x, ...
    head_ir_y)

% This function processes impact data and calcs. Vel, SI, HIC

g = 9.8067; %gravity
p = 5/2;    %exponent in SI and HIC

%% Read in Data from Excel-----
-----
% pendulum accelerations
pendulum_x = xlsread(spread,sheet,pen_x);
pendulum_y = xlsread(spread,sheet,pen_y);

% Initial Headform Accelerations-----
-----

headform1_x = xlsread(spread,sheet,head_i_x);
headform1_y = abs(xlsread(spread,sheet,head_i_y));

% Rebound Headform Accelerations-----
-----

headform2_x = xlsread(spread,sheet,head_r_x);
headform2_y = abs(xlsread(spread,sheet,head_r_y));

% Initial+ Rebound Headform Accelerations-----
-----

headform1and2_x = xlsread(spread,sheet,head_ir_x);
headform1and2_y = abs(xlsread(spread,sheet,head_ir_y));

%% Getting time differences
*****
*****

% pendulum-----
-----

pendulum_delta = pendulum_x(end) - pendulum_x(1);

% Headform Initial-----
-----

headform1_delta = headform1_x(end) - headform1_x(1);

% Headform Rebound-----
-----

headform2_delta = headform2_x(end) - headform2_x(1);

```

```

% Headform Inital + Rebound-----
-----
headformland2_delta = headformland2_x(end) - headformland2_x(1);

%% Velocities **-----**-----**-----**-----**-----**-----**-----**-----**-----**-----**
-----**-----**-----**-----**-----**
% Pendulum-----
-----

pen_vel = trapz(pendulum_x,pendulum_y)
xlswrite(spread,pen_vel,'Velocity&SI-HIC',strcat('B',row))
% Headform Inital-----
-----

head_i_vel = trapz(headform1_x,headform1_y)
xlswrite(spread,head_i_vel,'Velocity&SI-HIC',strcat('D',row))
% Headform Rebound-----
-----

head_r_vel = trapz(headform2_x,headform2_y)
xlswrite(spread,head_r_vel,'Velocity&SI-HIC',strcat('F',row))
%% SI Values **-----**-----**-----**-----**-----**-----**-----**-----**-----**
**-----**-----**-----**-----**-----**
% Pendulum-----
-----

pen_SI = trapz(pendulum_x,(abs((pendulum_y))./g).^p)
xlswrite(spread,pen_SI,'Velocity&SI-HIC',strcat('H',row))
% Headform initial-----
-----

head_i_SI = trapz(headform1_x,(abs((headform1_y))./g).^p)
xlswrite(spread,head_i_SI,'Velocity&SI-HIC',strcat('I',row))
% Headform Rebound-----
-----

head_r_SI = trapz(headform2_x,(abs((headform2_y))./g).^p)
xlswrite(spread,head_r_SI,'Velocity&SI-HIC',strcat('J',row))
% Headform Initial + Rebound-----
-----

head_i_and_r_SI = trapz(headformland2_x,...
    (abs((headformland2_y))./g).^p)
xlswrite(spread,head_i_and_r_SI,'Velocity&SI-HIC',strcat('K',row))
%% HIC Values **-----**-----**-----**-----**-----**-----**-----**-----**-----**
**-----**-----**-----**-----**-----**
% Pendulum-----
-----

pen_HIC = pendulum_delta*((1/pendulum_delta)*(trapz(pendulum_x,...
    ((pendulum_y)./g))))^p)

```

```

xlswrite(spread,pen_HIC,'Velocity&SI-HIC',strcat('L',row))
% Headform initial-----
-----

head_i_HIC = headform1_delta*((1/headform1_delta)*(trapz...
    (headform1_x,((headform1_y)./g))))^p)
xlswrite(spread,head_i_HIC,'Velocity&SI-HIC',strcat('M',row))
% Headform rebound-----
-----

head_r_HIC = headform2_delta*((1/headform2_delta)*(trapz...
    (headform2_x,((headform2_y)./g))))^p)
xlswrite(spread,head_r_HIC,'Velocity&SI-HIC',strcat('N',row))
% Headform Initial + rebound-----
-----

head_i_and_r_HIC = headformland2_delta*((1/headformland2_delta)*(trapz...
    (headformland2_x,((headformland2_y)./g))))^p)
xlswrite(spread,head_i_and_r_HIC,'Velocity&SI-HIC',strcat('O',row))
end

```

REFERENCES

- [1] Benn, Darren. "The Design, Build and Validation of a Hybrid Tower Used to Conduct Helmet Impact Tests" (Master's Thesis). 2015. UNLV. Retrieved from Dr. Douglas Reynolds UNLV.
- [2] Comstock, Dawn R. Currie, Dustin W. Pierpoint, Lauren A. "National High School Sports-Related Injury Surveillance Study 2014-2015 School Year" 2015.
<[http://www.ucdenver.edu/academics/colleges/PublicHealth/research/Research Projects/piper/projects/RIO/Documents/Convenience%20Report_2014_15.pdf](http://www.ucdenver.edu/academics/colleges/PublicHealth/research/Research%20Projects/piper/projects/RIO/Documents/Convenience%20Report_2014_15.pdf)>
- [3] El Sayed, Tamer. Mota, Alejandro. Fraternali, Fernando. Ortiz, Michael. "Biomechanics of Traumatic Brain Injury". Computational Methods in Applied Mechanical Engineering. 2008
- [4] Hess, Robert L. Weber, Kathleen. Melvin, John W. "Review of Literature and Regulation Relating to Head Impact Tolerance and Injury Criteria" Highway Safety and Research Institute. 1980.<<https://deepblue.lib.umich.edu/bitstream/handle/2027.42/449/45122.0001.001.pdf?sequence=2>>
- [5] NOCSAE. "Standard Test Method and Equipment Used in Evaluating the Performance Characteristics of Headgear/Equipment, NOCSAE ND 001". 2015.
<<http://nocsae.org/>>

- [6] NOCSAE. “Standard Projectile Impact Test Method and Equipment Used in Evaluating the Performance Characteristics of Protective Headgear, Faceguards or Projectiles, NOCSAE ND-021”. 2015. <<http://nocsae.org/>>
- [7] NOCSAE. “Standard Performance Specifications for Newly Manufactured Baseball/Softball Batters Helmets, NOCSAE ND 022”. 2012. <<http://nocsae.org/>>
- [8] NOCSAE. “Laboratory Procedural Guide for Certifying Newly Manufactured Baseball/Softball Batter’s Helmets, NOCSAE ND 023”. 2014. <<http://nocsae.org/>>
- [9] Pellam, EJ. Viano, DC. Tucker, AM. Casson, IR. Waeckerie, JF. “Concussions in Professional Football: reconstruction of game impacts and injuries”. Neurosurgery. 2003. <<http://www.ncbi.nlm.nih.gov/pubmed/14519212>>
- [10] Smith, David W. Bailes, Julian E. Fisher, Joseph A. Robles, Javier. Turner, Ryan C. Mills, James D. “Internal Jugular Vein Compression Mitigates Traumatic Axonal Injury in a Rat Model by Reducing the Intracranial Slosh Effect” Neurosurgery. 2012.
- [11] Spiotta, Alejandro M. Bartsch, Adam J. Benzel, Edward C. “Heading in Soccer: Dangerous Play?” Neurosurgery. 2012.

CURRICULUM VITAE

EDUCATION

University of Nevada, Las Vegas (ABET) Las Vegas, NV

- *Masters of Science, Mechanical Engineering (will defend September 2016)*
- GPA 3.67.

University of Nevada, Las Vegas (ABET) Las Vegas, NV

- *Bachelor of Science, Mechanical Engineering*
- GPA 3.01.

College of Southern Nevada Las Vegas, NV

- Two Year Transfer Program, Pre-Engineering
- Transfer GPA 3.60.

Mechanical Design Experience

University of Nevada, Las Vegas Las Vegas, NV 08/2008-present

- Design and development of a rear suspension system for a motorcycle including displacement, velocity and force analysis as well 3D printed prototype.
- Development of a manufacturing process for the mass production of a titanium bracket.
- Optimization of a Fe-Co-Ni metal matrix used in high pressure high temperature (HPHT) diamond synthesis.
- Design of mechanical systems for a fully automated 1:20 scale model service elevator including electrical and micro-controller integration.
- Design of a pneumatically operated computer controlled nozzle for a commercial water feature.
- Supervising of design and mechanical component selection for student projects.

Key Accomplishments:

Completed three different engineering projects for use in university curriculum. The projects were taken from concept to working prototype in only seven weeks.

Research & Development Experience

University of Nevada, Las Vegas Las Vegas, NV 08/2008-present

Autonomous Exploration Vehicles Using Multiple Redundant Systems

- Design and development of drive system, suspension and steering for the primary ground vehicle.
- Design and development of a mechanism for securing, loading and unloading secondary autonomous ground vehicles.
- Programming micro -controllers and P.L.C.'s to govern vehicle operation and monitor feedback from a variety of sensors.

Testing of Air Handling Equipment for Noise and Air Distribution

- Acoustically lined ducts were tested for noise attenuation as part of a project for ASHRAE.
- Chill beam style in ceiling heat exchangers were tested for radiated noise.

- Several styles of clean room HVAC diffusers were tested for air distribution.

Teaching Experience

University of Nevada, Las Vegas Las Vegas, NV 1/2014-present

- Taught the following courses as a teaching assistant in mechanical engineering:
ME337L Measurements Lab: Using NI ELVIS and LabVIEW to develop virtual instruments (VI's) and measure 1st and 2nd order circuits and sensor data.

ME319 Intro to Programming for Engineers: Developing applications using MATLAB and Simulink

ME421L Automatic Controls Lab: Developing PID control schemes for dc motors, HVAC, pump station and rotary pendulum using NI ELVIS and Simulink.

Key Accomplishments:

- Initiated development of a technical writing module within the controls lab to improve the quality of student lab reports.

Work Experience

University of Nevada Las Vegas Las Vegas, NV 09/2009–06/2016

Undergraduate Researcher/Research Assistant/Teaching Assistant

- Worked on research projects as an undergraduate in automation and acoustics.
- Worked on research projects as a graduate student in vibrations, acoustics and controls.
- Taught 300-400 level classes and laboratories in mechanical engineering.

Nevada Valve Train Las Vegas, NV 09/2004–05/2009

Engine Builder

- Diagnosis of mechanical failure in a wide variety of internal combustion engines.
- Repair and remanufacturing of internal combustion engines using industry standard procedures.
- Modification of internal combustion engines per customer specifications.

Key Accomplishments:

- Designed a pressured fed lubrication system for antique internal combustion engines.

Ambassador Limousine/Honda West Las Vegas, NV 03/2001–08/2004

Automotive Technician

- Repair and maintenance of limousine fleet and customer cars.
- Installation of lighting, signage, radio's and g.p.s. tracking systems.

Rinker Materials Corporation Las Vegas, NV 03/2000–02/2001

Heavy Duty Repairman

- Repair and maintenance of materiel processing and handling equipment.
- Fabrication of structural and mechanical components from schematics.
- Modification of schematics and designs for a given application.